

POLITECNICO DI TORINO

Master's Degree in Energy and Nuclear Engineering

Life Cycle Assessment of a Hydrogen Valley



Supervisors

Prof. Massimo Santarelli
Eleonora Cordioli (FBK)

Candidate

Zaheer Ali

Academic Year 2024/2025

Abstract

This thesis aims to investigate the environmental impacts associated with the entire life cycle of key components within a Hydrogen Valley, where multiple end-users are fed by green hydrogen. To comprehensively understand the hydrogen valley concept, eight comparative case studies were conducted to investigate different technological pathways, including hydrogen production through water electrolysis and steam methane reforming, transportation via pipeline and tube trailers, storage options, and end-use applications in mobility (fuel cell electric vehicles and heavy-duty trucks) and industry (steelmaking, and ammonia production). The assessment was carried out by applying a cradle-to-gate system boundary in OpenLCA using the Environmental Footprint 3.1 (EF 3.1) method to evaluate key environmental indicators, including climate change, acidification, eutrophication, non-renewable energy use, water use, and the depletion of metals and minerals.

The results reveal that producing hydrogen through electrolysis powered by renewable electricity can reduce greenhouse gas emissions by more than 70% compared to conventional, fossil-based pathways. The hydrogen produced is either utilized on-site or transported to end-users to feed a fleet of fuel cell electric vehicles and heavy-duty trucks, or serves as a key feedstock for industrial decarbonization. The results highlight that the final use of hydrogen for both mobility and industrial applications produces valuable environmental benefits compared to fossil-based options. However, the findings also show that electricity generation for electrolysis and compression stages remains the dominant hotspot across most scenarios. Moreover, the manufacturing of advanced materials such as carbon fiber tanks, fuel cell stacks, and electrolyzer components further contributes to environmental impacts related to acidification and material resource depletion. By assessing each step of the hydrogen value chain separately, this work provides a solid basis for building a full environmental picture of a hydrogen valley.

Keywords: renewable hydrogen, hydrogen valley, life cycle assessment, sustainability, green hydrogen, hydrogen production, hydrogen storage, hydrogen transportation, electrolysis, fuel cell, decarbonization.

Abbreviations

AEM	Anion Exchange Membrane
AEMWE	Anion Exchange Membrane Water Electrolysis
ASU	Air Separation Unit
AWE	Alkaline Water Electrolysis
BEV	Battery Electric Vehicle
BF	Blast Furnace
BOF	Basic Oxygen Furnace
BoP	Balance of Plant
BPP	Bipolar Plate
CCS	Carbon Capture and Storage
CFRP	Carbon Fiber Reinforced Polymer
DRI	Direct Iron Reduction
EAF	Electric Arc Furnace
EEA	European Environment Agency
FCEV	Fuel Cell Electric Vehicle
FCT	Fuel Cell Truck
FU	Functional Unit
GDL	Gas Diffusion Layer
GHGs	Greenhouse Gases
GWP	Global Warming Potential

HRS	Hydrogen Refueling Station
ICEV	Internal Combustion Engine Vehicle
IEA	International Energy Agency
IPCC	Intergovernmental Panel on Climate Change
IRENA	International Renewable Energy Agency
LCA	Life Cycle Assessment
LCI	Life Cycle Inventory
LCIA	Life Cycle Impact Assessment
LOHCs	Liquid Organic Hydrogen Carriers
MEA	Membrane Electrode Assembly
MoFs	Metal-Organic Frameworks
NREL	National Renewable Energy Laboratory
PEM	Proton Exchange Membrane
PEMFC	Proton Exchange Membrane Fuel Cell
PEMWE	Proton Exchange Membrane Water Electrolysis
PSA	Pressure Swing Adsorption
PTL	Porous Transport Layer
SMR	Steam Methane Reforming
SOEC	Solid Oxide Electrolyzer
TRL	Technology Readiness Level

Table of Contents

Abstract	II
List of Figures	IX
List of Tables	XII
1 Introduction	1
1.1 Climate Change, Energy Transition, and Role of Hydrogen	1
1.2 Concept of Hydrogen Valley	2
1.3 Hydrogen Value Chain	4
1.4 Research Gaps and Motivation	5
1.5 Research Scope and Objectives	5
2 Hydrogen Value Chain	7
2.1 Hydrogen Production Methods	9
2.1.1 Steam Methane Reforming (SMR)	9
2.1.2 Water Electrolysis	10
2.1.3 Coal Gasification	14
2.1.4 Other Hydrogen Production pathways	15
2.2 Hydrogen Storage Technologies	16
2.2.1 Compressed Hydrogen Storage System (CH_2)	17
2.2.2 Liquified Hydrogen Storage systems (LH_2)	18
2.2.3 Cryo-Compressed Hydrogen Storage System (CCH_2)	18
2.2.4 Solid Material-Based Hydrogen Storage	18
2.2.5 Liquid Material-Based Hydrogen Storage	18
2.3 Hydrogen Transportation Modes	19
2.3.1 Hydrogen transportation through pipelines	19
2.3.2 Hydrogen Transport Via Tube Trailers	20
2.3.3 Hydrogen Transportation Via Ships	21
2.4 Hydrogen End-Use Applications	21
2.4.1 Gas Turbines	21
2.4.2 Green ammonia production	22
2.4.3 Steel production	23

2.4.4	Fuel Cell Electric Vehicles (FCEVs)	25
3	Life Cycle Assessment (LCA) Background	30
3.1	Principles and Framework for LCA	31
3.1.1	Goal and Scope Definition	31
3.1.2	Life Cycle Inventory (LCI) Analysis	32
3.1.3	Life Cycle Impact Assessment (LCIA)	33
3.1.4	Interpretation	33
3.2	Importance of LCA in Hydrogen Systems	34
3.3	Previous LCA Studies on Hydrogen Systems	34
4	Methodology	36
4.1	Goal and Scope Definition	36
4.2	Functional Units and System Boundary	37
4.3	LCIA Method and Impact Categories	37
4.4	LCA Modelling Software	39
4.5	Modelling Structure in OpenLCA	39
5	Comparative LCA of Different Case Studies	41
5.1	Introduction	41
5.2	Case Study 1: Comparative LCA of Various Hydrogen Production Routes	44
5.2.1	Case Study Description	44
5.2.2	Results of Case Study 1	49
5.3	Case Study 2: Comparative LCA of PEM Electrolysis with Different Electricity Sources	53
5.3.1	Case Study Description	53
5.3.2	Results of Case Study 2	54
5.4	Case Study 3: Comparative LCA of Different Hydrogen Transportation Modes	57
5.4.1	Case Study Description	57
5.4.2	Results of Case Study 3	58
5.5	Case Study 4: Comparative LCA of On-site vs Off-site Hydrogen Production for HRS	62
5.5.1	Case Study Description	62
5.5.2	Results of Case Study 4	63
5.6	Case Study 5: Comparative LCA of Passenger Vehicle Technologies	66
5.6.1	Case Study Description	66
5.6.2	Results of Case Study 5	69
5.7	Case Study 6: Comparative LCA of Heavy-duty Vehicle Technologies	72
5.7.1	Case Study Description	72
5.7.2	Results of Case Study 6	73
5.8	Case Study 7: Comparative LCA of Steel Production Routes	76

5.8.1	Case Study Description	76
5.8.2	Results of Case Study 7	77
5.9	Case Study 8: Comparative LCA of Ammonia Production Routes . .	81
5.9.1	Case Study Description	81
5.9.2	Results of Case Study 8	82
6	Discussion	86
6.1	Main Outcomes and Interpretation	86
6.2	Environmental Hotspots in Hydrogen Value Chain	89
7	Conclusions and Directions for Future Research	90
7.1	Concluding remarks	90
7.2	Insights and Recommendations	91
7.3	Research Limitations	92
7.4	Future Works	93
	Bibliography	95
A	Appendix	108

List of Figures

1.1	Map of European Hydrogen Valleys supported by the Clean Hydrogen Partnership [7]	3
1.2	Hydrogen value chain Scheme [14]	4
2.1	Color taxonomy of hydrogen by production pathway and energy source [16]	7
2.2	Scheme of the steam methane reforming process [19]	10
2.3	Schematic illustration of PEM water electrolysis [23]	11
2.4	Schematic view of PEM water electrolysis cell layers [24]	11
2.5	Flowsheet of the proton exchange water electrolysis (PEMWE) plant [25]	12
2.6	Schematic illustration of Alkaline water electrolysis [28]	13
2.7	Schematic view of an Alkaline water electrolysis cell layers [30]	13
2.8	BoP diagram of alkaline electrolyzer [31]	14
2.9	Gasification-based hydrogen production [34]	15
2.10	Schematic diagram for a two-step metal oxide thermochemical cycle [35]	15
2.11	Overview of existing hydrogen storage technologies [37]	16
2.12	Type IV high-pressure vessel [40]	17
2.13	Key components of a hydrogen pipeline system [50]	19
2.14	Tube trailer for transporting hydrogen [57]	20
2.15	Hydrogen-fueled Combined cycle gas turbine [62]	22
2.16	Ammonia production route adapted from [69]	23
2.17	Schematic diagram of hot-rolled steel production via the BF/BOF route [70]	24
2.18	Schematic diagram of hot rolled coil production via the DRI/EAF route [70]	25
2.19	Off-site (left) and On-site H ₂ production hydrogen gas refueling station's main components [73]	26
2.20	Simplified scheme of a hydrogen-powered fuel cell system in road vehicles [75]	26
2.21	Schematic diagram of the operating principle of PEM fuel cell [75]	27
2.22	Schematic diagram of the components of a single PEMFC [78]	28

2.23	Balance of plant (BoP) of PEM fuel cell [79]	28
3.1	Life Cycle Assessment Framework	31
3.2	System boundaries for hydrogen-related studies [85]	32
3.3	Schematic steps from inventory to category endpoints [86]	33
4.1	PEM electrolysis modelling structure in OpenLCA	40
5.1	Main stages of hydrogen value chain under consideration	41
5.2	Contribution analysis of PEMWE and AWE across four environmental impact categories for producing 1 kg of H ₂ at 30 bar	51
5.3	Material composition of PEM and Alkaline electrolyzer stacks under the material resources category	52
5.4	Normalized environmental impacts of hydrogen production using different electricity sources. The grid mix scenario is used as a baseline (100%), and the relative impact reductions of wind and solar PV are shown.	55
5.5	Contribution of different hydrogen production stages to GWP	56
5.6	Relative environmental impacts of hydrogen delivery via pipeline and tube-trailer systems for the complete supply chain. Pipeline transport is used as the 100% reference baseline	60
5.7	Contribution analysis of life cycle processes to the climate change impact for hydrogen delivery via pipeline (left) and tube-trailer (right)	60
5.8	Comparative environmental impacts of on-site and off-site hydrogen production for HRS (on-site=100%)	64
5.9	Climate change contribution analysis for both on-site (left) and off-site (right) scenarios	65
5.10	Contribution of life cycle stages to environmental impacts of a Fuel Cell Electric Vehicle (FCEV) across four categories (per km)	71
5.11	Contribution of life cycle stages to environmental impacts of a Fuel Cell Truck (per tonne-kilometer)	75
5.12	Comparative environmental impacts of BF/BOF and hydrogen-based DRI/EAF steelmaking routes (BF/BOF = 100%)	79
5.13	Contribution analysis of major life cycle processes in BF/BOF steelmaking process across the impact categories of acidification, climate change, and non-renewable energy resource use	79
5.14	Contribution analysis of major life cycle processes green H ₂ -DRI/EAF, and grey H ₂ -DRI/EAF steelmaking processes across the impact categories of acidification, climate change, and non-renewable energy resource use	80
5.15	Environmental impacts of green ammonia relative to grey ammonia	84
5.16	Contribution of different processes to climate change. Green ammonia (left), Grey ammonia (right)	84

6.1	Summary of main findings across hydrogen supply chain	86
6.2	Summary of main findings across hydrogen end-use applications . . .	87

List of Tables

4.1	Proposed EF impact categories and units	38
5.1	H ₂ production scenarios with different pathways	44
5.2	Construction KPIs of PEMWE stack [25]	45
5.3	Energy and water demand of the PEMWE model [25]	46
5.4	Operational KPIs of PEMWE stack [25]	46
5.5	Material demand for a single 2.5 MW PEMWE stack [25]	47
5.6	LCI of the system construction [25]	47
5.7	Stack specifications for baseline AE [102, 103]	48
5.8	Materials for BoP and PE [29]	48
5.9	Baseline AE stack materials [26]	49
5.10	Life Cycle Impact results of hydrogen production via SMR, PEMWE, and AWE	50
5.11	PEM electrolysis scenarios with different electricity sources	53
5.12	Comparative environmental impacts of hydrogen production via elec- trolysis using grid mix, wind, and solar PV electricity	54
5.13	Hydrogen pipeline specifications [50]	57
5.14	Material composition of storage tank (per 1100 kgH ₂) [58]	58
5.15	Comparative environmental impacts for hydrogen transport via pipeline and tube-trailer	59
5.16	Life Cycle Inventory Data for Fueling Station [107]	62
5.17	Main parameters of HRS [58, 39]	63
5.18	Comparison of environmental impacts between on-site and off-site hydrogen production for HRS	64
5.19	Main technical characteristics of the ICE vehicle [100]	66
5.20	Main technical characteristics of the BEV vehicle [100]	67
5.21	Main technical parameters of the FCEV [110, 111]	67
5.22	Main modelling parameters of PEMFC stack [112]	68
5.23	Environmental impacts of ICEV, BEV, and FCEV (per km driven)	69
5.24	Environmental impacts of BEV and FCEV when powered by wind (per km driven)	70
5.25	Main characteristics of a Euro 6 truck	72

5.26	Main technical characteristics of the FCET	73
5.27	Environmental impacts of diesel and fuel cell heavy-duty trucks (per tonne-kilometer)	74
5.28	Summary of input parameters for steelmaking processes (per tonne of HRC) [70]	77
5.29	Environmental impacts of three steelmaking processes (per tonne of HRC)	78
5.30	Design parameters of the green ammonia production plant [68]	82
5.31	Environmental impacts of two ammonia production processes (per kg of NH_3 produced)	83
A.1	Life cycle inventory (LCI) for hydrogen storage tank system used in FCEVs [112]	108
A.2	LCI for 80 kW Electric Motor for FCEV [116]	108
A.3	LCI for main PEMFC Stack components (per kW) [112]	109
A.4	LCI for Other PEMFC Stack Components per kW [112]	110
A.5	LCI for the balance of plant (per kW) of PEMFC [112]	111
A.6	LCI for a new hydrogen transmission pipeline (per km of pipeline [50])	112
A.7	LCI for production of 1 kg of Green and Grey Ammonia [68]	113
A.8	LCI for Hot Rolled Coil Production (BF/BOF route)	114
A.9	LCI for Slab Cast Steel Production (BF/BOF route)	114
A.10	LCI for Refined Steel Production (BF/BOF route)	114
A.11	LCI for Crude Steel Production (Basic Oxygen Furnace)	115
A.12	LCI for Hot Metal Production (Blast Furnace)	115
A.13	LCI for Hot Rolled Coil Production (DRI/EAF route)	116
A.14	LCI for Slab Cast Steel Production (DRI/EAF route)	116
A.15	LCI for Refined Steel Production (DRI/EAF route)	116
A.16	LCI for Iron Ore Pellet Production (Pelletization, DRI/EAF route) .	117
A.17	LCI for Sponge Iron Production (H_2 -DRI)	117
A.18	LCI for Crude Steel Production (Electric Arc Furnace, H_2 -DRI route)	118

Chapter 1

Introduction

1.1 Climate Change, Energy Transition, and Role of Hydrogen

The Intergovernmental Panel on Climate Change (IPCC) identifies global warming as one of the pressing challenges of the 21st century [1]. Its latest report provides clear evidence that human activities are a dominant driver of climate change. The persistent release of greenhouse gases (GHGs), particularly carbon dioxide (CO₂), has led to rising atmospheric temperatures and significant environmental impacts [1]. As a result, the call for urgent global action has never been stronger. According to the European Environment Agency (EEA), the European Union has made noticeable progress in reducing GHG emissions. 37% reduction of emissions as compared to 1990 levels is reported [2]. However, the Energy and transport sector collectively remains responsible for more than 50% of overall emissions in Europe, primarily due to the use of fossil fuels as the primary energy source. Also, agricultural methane and nitrous oxide have barely declined [2]. Achieving the goals of the Paris Agreement requires a rapid reduction in emissions, and the most efficient way to do that is the deployment of renewable energy technologies and low-carbon energy carriers [3].

Hydrogen is increasingly recognized as a flexible and clean energy carrier. Although it is the smallest molecule, hydrogen has a very high energy content per unit mass (120 MJ/kg) compared to conventional fuels such as methane (50 MJ/kg). Unlike fossil fuels, hydrogen can be produced from renewable energy sources. Moreover, when hydrogen is produced using renewable energy sources, it emits no carbon dioxide during operation, releasing only water. Its adaptability makes it suitable for a wide range of applications, from industrial processes and transportation to power generation and heating [4]. It is because of this versatility that hydrogen is considered a key component of the energy transition, which can help connect renewable energy production with sectors that are not easily decarbonized. Beyond its technical properties, hydrogen also has strong strategic and political relevance. It plays a central role in major policy frameworks, such as the EU Green Deal [5],

which aims to achieve climate neutrality by 2050 and explicitly highlights renewable hydrogen as a key pillar for reducing fossil fuel dependence and accelerating emissions reductions.

Hydrogen’s growing importance is also linked to its ability to bridge the gap between different parts of the energy systems. Hydrogen can be stored for long periods and transported over long distances, making it a crucial component of a flexible and resilient energy network. Furthermore, development can stimulate economic growth and innovation, creating new industries and employment opportunities in renewable energy, infrastructure, and advanced technologies. Governments and international organizations are increasingly investing in hydrogen strategies and projects such as Hydrogen Valleys in Europe to demonstrate their potential at scale [6].

1.2 Concept of Hydrogen Valley

A hydrogen valley is a large-scale, integrated ecosystem that connects the entire hydrogen value chain within a specific region, encompassing production and storage, as well as distribution and final use across multiple sectors. The primary objective is to establish a self-sufficient hydrogen economy that operates efficiently within a specific area, demonstrating how hydrogen can drive both decarbonization and local economic growth. According to the Clean Hydrogen Partnership [7], hydrogen valleys demonstrate how renewable energy can be converted into hydrogen, which can then be used to power transport, industries, and buildings, reducing reliance on fossil fuels while promoting innovation and sustainable development.

In practice, a hydrogen valley connects different sectors to make the most of shared resources. For instance, renewable electricity can be used for hydrogen production through electrolysis, and the produced hydrogen can be stored or distributed to serve different applications such as mobility (fuel cell vehicles and buses), industry (steel, chemicals, refineries), and energy systems (power generation, heating, or grid balancing). Additionally, by-products of the system, such as oxygen or waste heat, can also be captured and repurposed within the local network to improve efficiency.

A leading example of this concept is the HEAVENN (Hydrogen Energy Applications in Valley Environments for Northern Netherlands) project, one of Europe’s most advanced hydrogen valleys, located in the provinces of Groningen and Drenthe [8]. HEAVENN integrates the entire hydrogen value chain from renewable power generation to multiple end-use applications. The project aims to produce approximately 36,500 tonnes of green hydrogen per year using proton exchange membrane (PEM) electrolysis powered by renewable electricity. Hydrogen is stored in compressed form within underground caverns and distributed through pipelines, trucks, and ships to serve mobility, power generation, and industrial sectors. The project’s full-scale operation and integration are expected to continue through 2035 as part of the Netherlands’ long-term hydrogen roadmap [9].

Another prominent example of a large-scale hydrogen valley is the North Adriatic

Hydrogen Valley (NAHV), a cross-border initiative jointly developed by Slovenia, Croatia, and the Friuli Venezia Giulia region of Italy. NAHV aims to build an integrated hydrogen value chain that connects renewable hydrogen production, storage, distribution, and multiple end-use applications across the three regions. The project plans to produce more than 5,000 tonnes of renewable hydrogen per year, mainly through electrolyzers powered by renewable or low-carbon electricity [10]. This hydrogen will be used in transport, industry, and energy systems, while a portion will be exchanged across borders to demonstrate coordinated regional markets. NAHV also includes pilot activities for hydrogen distribution via pipelines and trucks, along with the development of refueling and industrial infrastructure. Operating under the EU Horizon Europe programme from 2023 to 2029, the initiative is intended to serve as a scalable model for hydrogen deployment in Central and Southeastern Europe [11].

Another example of a hydrogen valley is GREEN HYSLAND, a small-scale but fully integrated project on the island of Mallorca, Spain. The project plans to produce about 330 tonnes of green hydrogen per year using PEM electrolysis powered by local solar energy [12]. This hydrogen will be used for mobility, injected into the local gas grid, and supplied to public buildings, demonstrating a wide range of applications within a compact area [13]. It also includes local storage and a refueling station to complete the value chain.

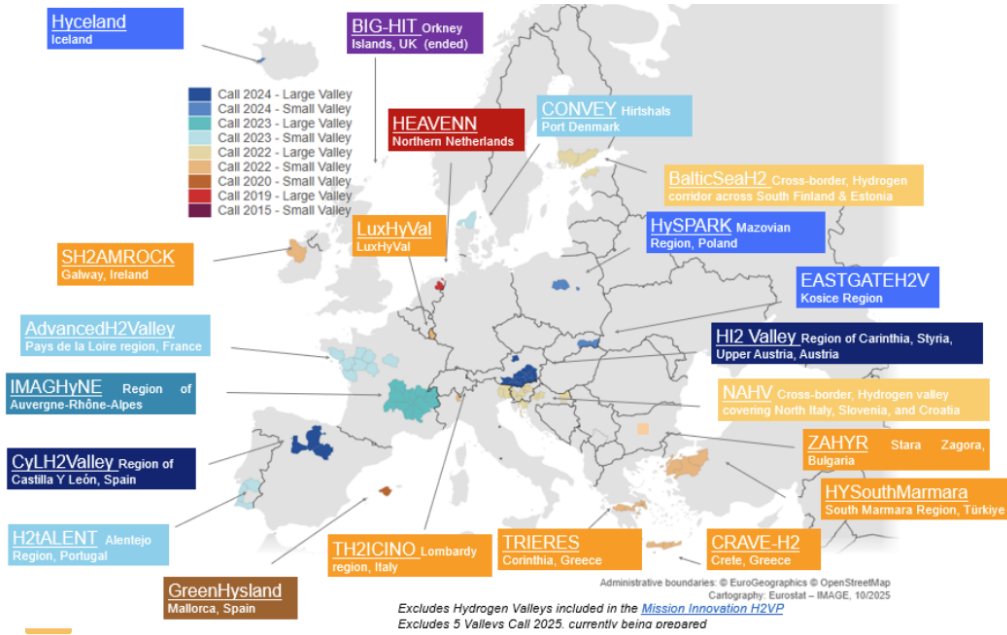


Figure 1.1: Map of European Hydrogen Valleys supported by the Clean Hydrogen Partnership [7]

The map (Figure 1.1) provides an overview of the expanding landscape of Hydrogen

Valleys in Europe, showcasing the regions that have received support from the Clean Hydrogen Partnership to advance integrated hydrogen ecosystems.

1.3 Hydrogen Value Chain

The hydrogen value chain includes all stages involved in producing, storing, transporting, distributing, and utilizing hydrogen as an energy carrier or industrial feedstock. Understanding this chain is essential to evaluating the environmental, economic, and technical implications of hydrogen deployment, as each stage differs in terms of efficiency, emissions, and overall benefits. In general, the hydrogen value chain can be divided into production, storage, transport, and end-use applications (Figure 1.2).

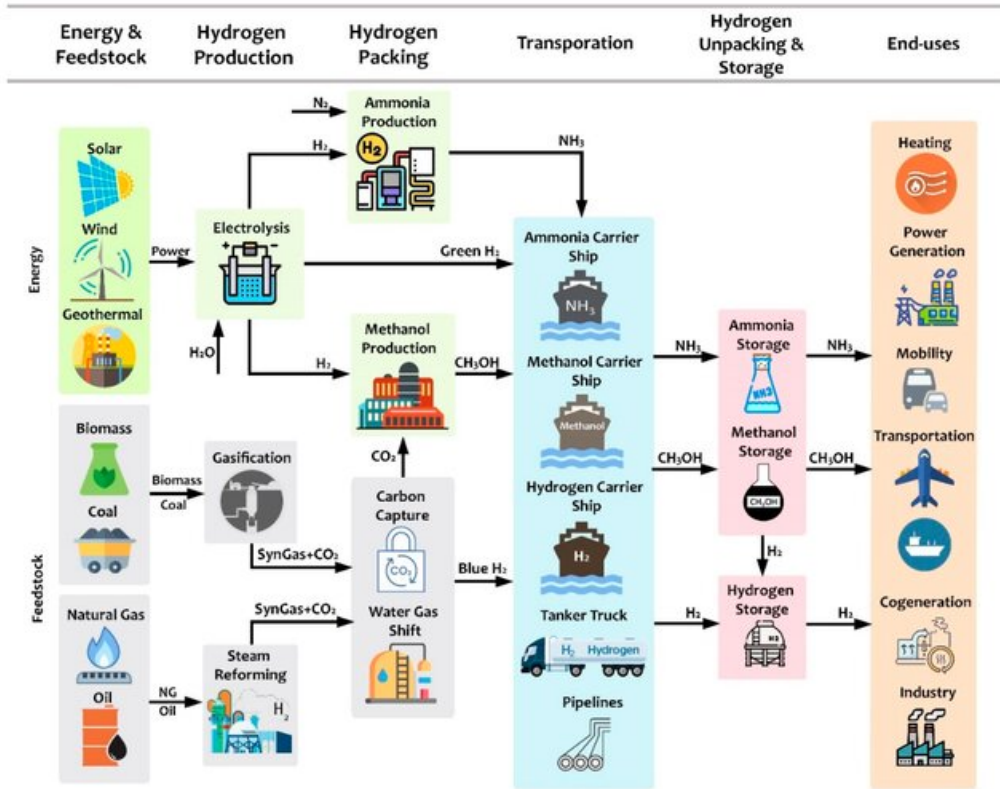


Figure 1.2: Hydrogen value chain Scheme [14]

The detailed processes involved in production, storage, transportation, and end-use are discussed in Chapter 2.

1.4 Research Gaps and Motivation

Despite the growing interest in hydrogen as a key enabler of the low-carbon transition, several critical research gaps remain in understanding its full environmental implications. Most existing LCA studies focus on isolated components of the hydrogen value chain, rather than on the overall integrated system. Consequently, the overall ecological benefits or burdens of deploying hydrogen at a regional scale, such as in a hydrogen valley, remain incompletely assessed.

Most studies also adopt a narrow system boundary, often excluding upstream and downstream processes, which can underrate the impacts of manufacturing and material use. Furthermore, there are limited comparative analyses of different electrolysis technologies, transportation modes, and storage options in terms of life cycle environmental performance. These research gaps and previous studies on LCA of hydrogen systems are explained in detail in Chapter 3.

This research is motivated by the need to bridge these gaps through a comprehensive life cycle assessment of the entire hydrogen value chain, encompassing production, storage, transportation, and end-use in both mobility and industrial applications.

1.5 Research Scope and Objectives

The primary aim of this thesis is to extend the knowledge base on the environmental performance of a Hydrogen Valley through a comprehensive life cycle assessment (LCA) approach. The study examines each step of the hydrogen value chain individually: production, storage, transportation, and end-use, while accounting for all relevant upstream and downstream processes. This step-by-step analysis allows for a transparent comparison of alternative technologies and configurations at each stage. The results of this thesis will serve as a methodological foundation for future studies aimed at evaluating real-world Hydrogen Valley implementations.

Life Cycle Assessment (LCA) is applied to fulfill the following objectives of the thesis:

1. Quantify and compare the environmental impacts of green hydrogen production pathways with conventional fossil-based hydrogen production routes.
2. Identify environmentally optimal solutions among different hydrogen storage and transportation options.
3. Assess the performance of multiple end-use applications when supplied with green hydrogen.
4. Identify critical environmental hotspots along the hydrogen value chain and identify stages where efficiency improvements can lead to significant environmental gains.

5. Provide key insights and recommendations for policy makers, researchers, and industry stakeholders to support the sustainable deployment of hydrogen infrastructure.

Chapter 2

Hydrogen Value Chain

Hydrogen, the smallest but most abundant element in the universe, is receiving increasing attention as a way to promote a low-carbon economy due to its versatility in integrating into multiple sectors. However, the environmental impact of hydrogen is strongly influenced by its production method. A color-coding system called the ‘hydrogen rainbow’ is used by the hydrogen industry to categorize hydrogen according to its production method and the carbon emissions associated with it [15].

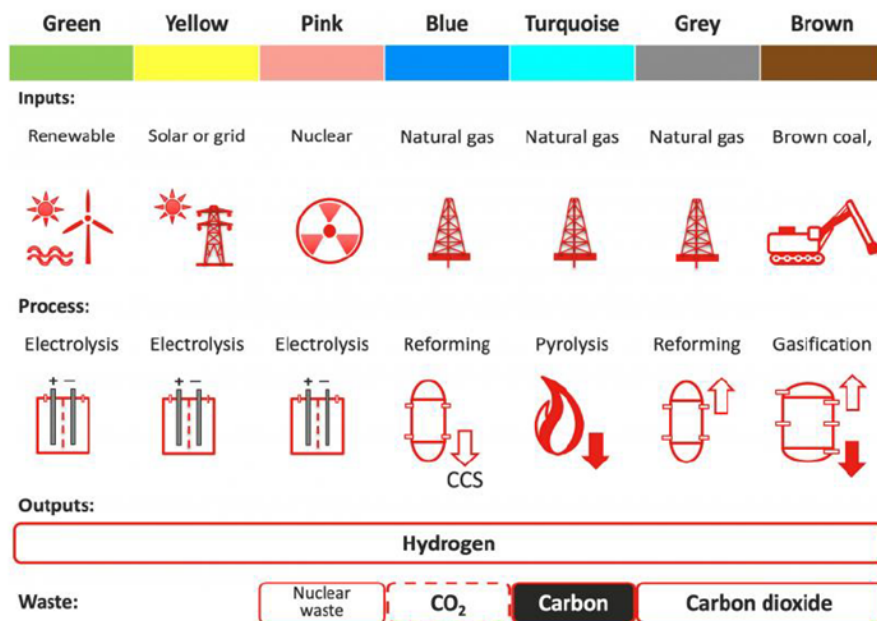


Figure 2.1: Color taxonomy of hydrogen by production pathway and energy source [16]

As shown in Figure 2.1, the most commonly recognized categories include:

- **Green hydrogen:** Generated via electrolysis powered by a renewable energy

source.

- **Yellow hydrogen:** Similar to green but produced typically from solar or sometimes from a grid mix.
- **Grey hydrogen:** Produced from natural gas through steam methane reforming (SMR) without carbon capture.
- **Blue hydrogen:** Same as grey with the addition of carbon capture and storage (CCS).
- **Pink hydrogen:** Produced through electrolysis using nuclear energy.
- **Brown hydrogen:** Produced from coal gasification.

In this study, three methods of hydrogen production are considered for the Life Cycle Analyses, i.e., SMR (grey hydrogen), PEM electrolysis (green hydrogen), and Alkaline Electrolysis (green hydrogen). Since SMR is the most used method of hydrogen production globally, it serves best as a baseline for the comparison. Green hydrogen production via water electrolysis is now a major focus of research, largely because it offers a promising pathway to reduce dependence on fossil fuels. In addition, PEM and AWE electrolysis are the technologies most commonly used in the concept of hydrogen valleys [17].

AWE technology is considered to be the most mature technology, with Technology Readiness Level (TRL) 9 commercially used at the MW scale, while PEM is a rapidly scaling technology, with TRL 8-9. Other technologies like SOEC and thermochemical methods are still at low TRL levels (4-5) and have not yet been deployed commercially at the MW scale [18].

For hydrogen storage, since compressed gaseous hydrogen storage is the most widely used and mature technology, this study focuses on a compressed hydrogen storage system with Type IV tanks for mobility applications. Although several other storage solutions exist, such as liquid hydrogen, metal hydrides, and underground storage in salt caverns, these are either less mature or more energy-intensive. Moreover, this study focuses on regional distribution, where the distances are relatively small to medium; therefore, only pipelines and tube trailers were considered as hydrogen transportation modes.

As for the end uses of hydrogen, this study focuses on two major application sectors that are currently at the forefront of hydrogen research i.e. mobility and industry. In the mobility sector, hydrogen use is examined through fuel cell electric vehicles (FCEVs) and hydrogen-powered heavy-duty trucks, while in the industrial sector, attention is given to ammonia and steel production. While hydrogen can also serve other applications—such as power generation, heating, synthetic fuels, and seasonal energy storage—these are beyond the scope of this work. The selected end uses, therefore, represent the most mature, impactful, and widely discussed pathways for near-term hydrogen deployment.

2.1 Hydrogen Production Methods

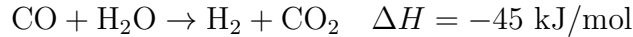
2.1.1 Steam Methane Reforming (SMR)

The most conventional method of producing hydrogen involves the reaction of methane with steam to produce hydrogen and carbon dioxide [19]. Hydrogen is then separated from CO_2 , typically through a PSA (Pressure Swing Adsorption) unit, and the CO_2 is vented to the atmosphere. Without CCS technology, this process produces grey hydrogen; however, when integrated with CCS technology, which allows for the capture of the CO_2 generated in the reforming process, it produces blue hydrogen.

In the Steam methane reforming process, the feedstock (natural gas or methane) first undergoes a desulfurization process to prevent the production of sulfur oxides using adsorption beds that remove sulfur compounds. Clean natural gas is sent to the Steam reforming reactor (burner), where it is mixed with steam and passed over a nickel-based catalyst to produce H_2 and CO. The operating temperature and pressure in the reformer are 700-1000°C and 15-30 bar, respectively [19]. The reaction is endothermic, which requires an external heat supply, typically provided by burning additional natural gas.



Produced gas mainly contains H_2 , CO, CO_2 , H_2O , and trace CH_4 . In produced gas, the percentage of CO is quite significant (7%). To decrease the content of CO produced, CO is further reacted with water in two Water gas shift reactors to produce hydrogen and carbon dioxide.



Along with H_2 , produced gas also contains residual gases, CO, CO_2 , and H_2O , which require purification and separation of H_2 . Pressure swing adsorption (PSA) is commonly used for purifying hydrogen to a purity of more than 99.9%. Separated CO_2 is typically vented or captured.

Without CCS technology, CO_2 emissions per kg of H_2 are around 8-12 kg, and the SMR process has a 60%-85% efficiency [20].

The overall SMR process flow is illustrated in Figure 2.2.

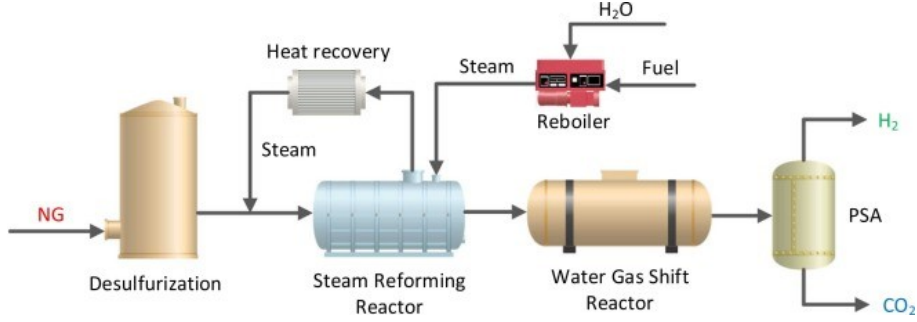


Figure 2.2: Scheme of the steam methane reforming process [19]

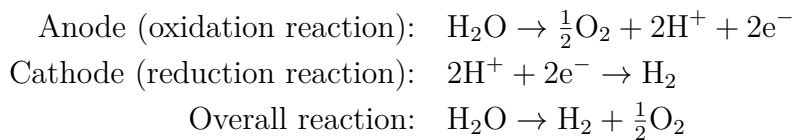
2.1.2 Water Electrolysis

This process splits water into hydrogen and oxygen using electricity. The environmental impact of this process is heavily influenced by the source of electricity used. The main electrolysis technologies include Proton Exchange Membrane (PEM) electrolysis, Alkaline Electrolysis (AWE), Solid Oxide Electrolyzers (SOECs), and Anion Exchange Membrane (AEM) [21]. PEM, AWE, and AEM are characterized by low operation temperature in the order of 40-80°C. The SOEC technology operates at temperatures above 700°C. Only 0.04% of the overall production was covered by water electrolysis in 2021 [22].

Proton Exchange Membrane Water Electrolysis (PEMWE)

In the PEM electrolysis process, an electrolyzer is used to undergo a chemical reaction to split water into hydrogen and oxygen using electricity. The PEM electrolyzer consists of an anode, a cathode, and a proton-conducting solid membrane [23].

Deionized water is supplied (as shown in Figure 2.3) to the anode side of the electrolyzer. When a DC electric current is applied, water is split into hydrogen and oxygen through the following reactions:



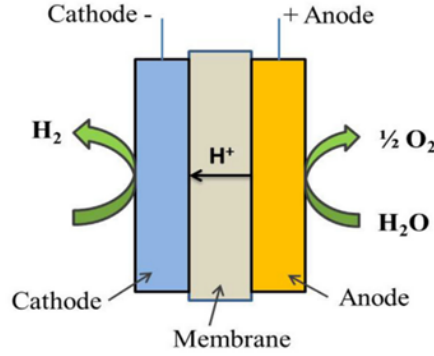


Figure 2.3: Schematic illustration of PEM water electrolysis [23]

At the anode, the water molecules are oxidized to form oxygen gas, protons (H^+), and electrons. The protons conducted flows through the solid polymer membrane (e.g., Nafion), which supports the flow of protons while blocking gases to ensure high-purity hydrogen. Also, the electrons conducted at the anode travel through the external circuit, providing the electric current needed for the reduction reaction. At the cathode, protons combine with electrons to form hydrogen gas.

Besides the membrane, electrodes, and catalysts, a PEM electrolyzer stack contains several supporting parts (as shown in Figure 2.4. Bipolar plates guide water and gases while carrying current through the stack. The Porous Transport Layer (PTL) positioned between the catalyst and the bipolar plate helps water reach the catalyst and facilitates the smooth escape of oxygen and hydrogen. To improve the contact between the electrode and bipolar plate and to ensure the flow of electricity, current collectors are used. Gaskets keep the cell sealed and prevent leakage. Finally, the end plates hold everything together under pressure.

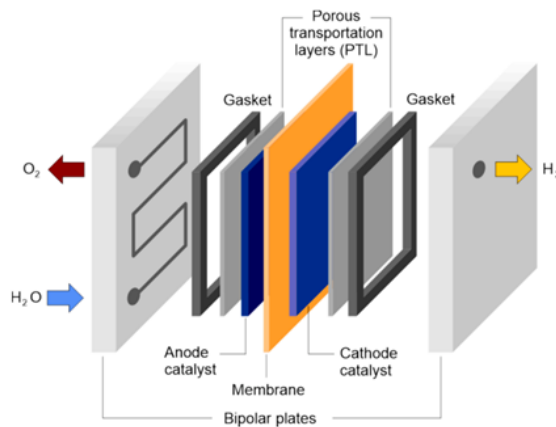


Figure 2.4: Schematic view of PEM water electrolysis cell layers [24]

In addition to the electrolyzer stack, a complete PEM system includes the Balance

through the following reactions:

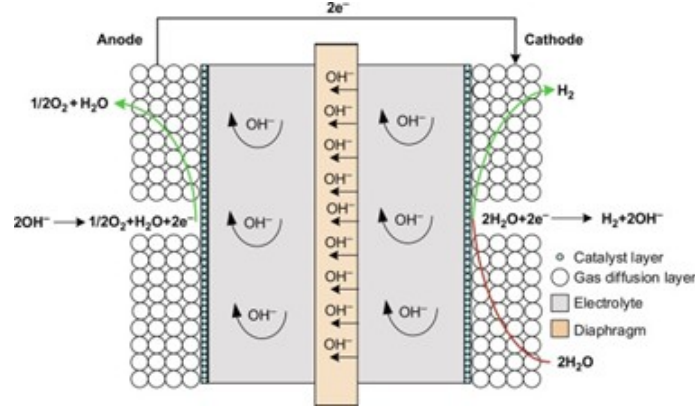
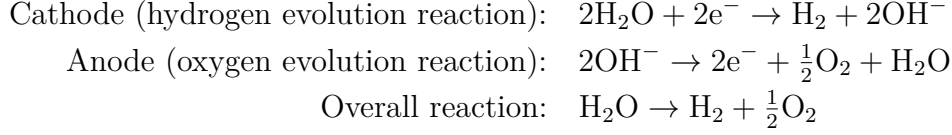


Figure 2.6: Schematic illustration of Alkaline water electrolysis [28]

At the cathode, water is reduced to hydrogen gas and hydroxide ion (OH^-). OH^- ions migrate through the electrolytic solution towards the anode. At the anode, hydroxide ions are oxidized to form oxygen and water. Electrons travel from the external circuit from the anode to the cathode. To avoid the mixing of hydrogen and oxygen gas, a separator (diaphragm) is used. The separator is typically made of a porous inorganic material such as Zirfon (made of zirconia and polysulfone) [29].

Just like the PEM stack, the AWE stack also contains bipolar plates, current collectors, gaskets, and endplates as a supporting structure. Porous transport layers (PTLs) are usually not used because the aqueous electrolyte already provides high ionic conductivity (Figure 2.7). Nickel is typically used as a catalyst in AWE.

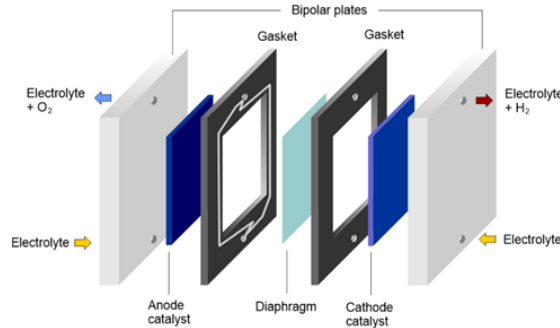


Figure 2.7: Schematic view of an Alkaline water electrolysis cell layers [30]

The balance of plant (BoP) of AWE is quite similar to that of PEMWE, as shown in Figure 2.8. The main difference lies in the type of electrolyte used. Since AWE uses a basic solution of KOH, a lye tank is used. Lye (KOH solution) must be pumped through both the anode and the cathode and must be recirculated.

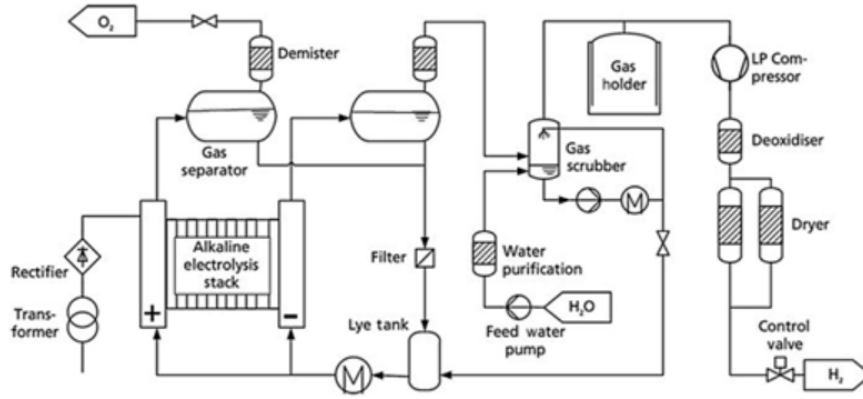


Figure 2.8: BoP diagram of alkaline electrolyzer [31]

The operating temperature ranges from 60 to 80°C, and the pressure is ambient up to a few bars.

AWE technology is the least expensive but has some shortcomings in comparison to PEMWE. The efficiency and purity of hydrogen produced in this process are lower than those of the PEMWE process. The hydrogen produced has a purity of 99.5–99.9% and an efficiency range between 60–70% [32].

2.1.3 Coal Gasification

This process involves converting coal into hydrogen and carbon monoxide (Syngas). In this process, we inject feedstock (coal) into the gasifier (operating at 1400 °C, 30 bar), and you introduce oxygen and steam as shown in Figure 2.9. The gasifier's exhaust produces syngas, which is primarily composed of hydrogen and carbon monoxide, with a small amount of carbon dioxide, methane and water. The produced syngas undergoes additional cleaning and separation processes to separate hydrogen from other impurities [33].

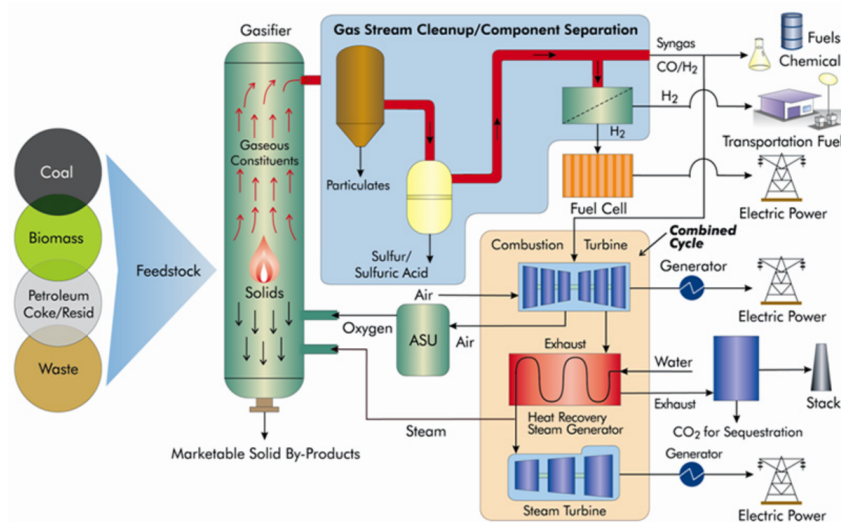


Figure 2.9: Gasification-based hydrogen production [34]

2.1.4 Other Hydrogen Production pathways

Thermochemical water splitting

An emerging technology that uses a temperature direct heat source to drive a chemical cycle (e.g., metal oxide 2-step loop) that splits water into water and hydrogen, as shown in the Figure 2.10. Although this method has high efficiency, it remains at a pilot scale due to material and cost challenges [35].

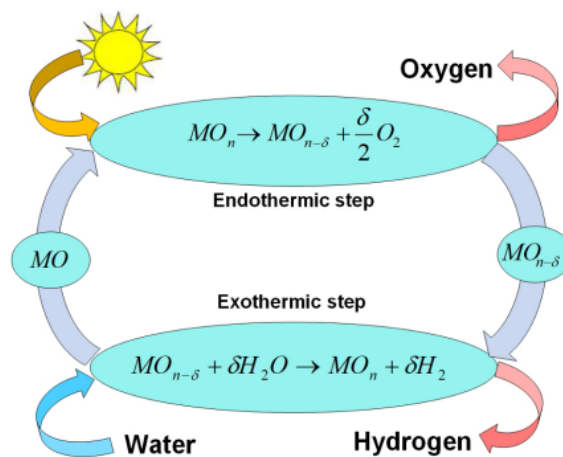


Figure 2.10: Schematic diagram for a two-step metal oxide thermochemical cycle [35]

Biomass gasification

Biomass gasification is a thermochemical process that converts organic materials such as wood, agricultural residues, and waste into hydrogen-rich syngas through partial oxidation at high temperatures (typically above 700°C) in the presence of limited oxygen and/or steam [36]. This process produces a mixture of gases, primarily hydrogen (H_2), carbon monoxide (CO), and carbon dioxide (CO_2). The produced syngas further undergoes a water-gas shift reaction, where CO reacts with water vapor to produce additional hydrogen and carbon dioxide. Hydrogen is then separated from CO_2 , typically through a PSA (Pressure Swing Adsorption) unit, and CO_2 is either captured or vented to the atmosphere.

2.2 Hydrogen Storage Technologies

Hydrogen storage is a critical step in the hydrogen value chain as it enables the coupling and decoupling of production from the end-use applications. Hydrogen storage is one of the biggest challenges today. Gaseous hydrogen storage at ambient pressure is highly inefficient because hydrogen gas is very light and has a volumetric density (0.089 kg/m^3) lower than air. Therefore, its density must be increased significantly. The density of hydrogen can be increased in various ways, including compression, liquification, or chemical binding for storage and transportation. The selection of storage depends on several factors, including cost, energy demand, material availability, safety, and life cycle impacts.

Figure 2.11 provides a schematic overview of different possible hydrogen storage methods.

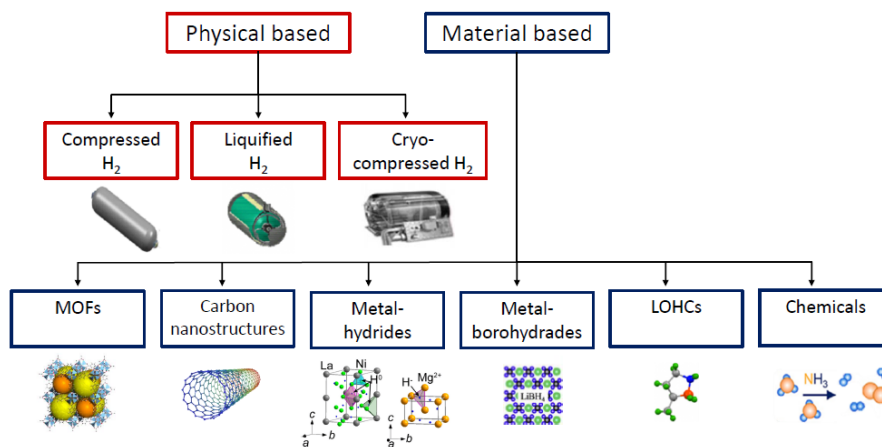


Figure 2.11: Overview of existing hydrogen storage technologies [37]

2.2.1 Compressed Hydrogen Storage System (CH_2)

CH_2 is the most widely used and most mature technology, where hydrogen gas is compressed to high pressures and stored in cylinders or tanks. The tanks can be classified into different types (I, II, III, and IV). Metallic pressure vessels are known as type I. Type II vessels are created with a metal liner reinforced with composite fiber (CFRP) attached to the cylinder hoop. The metallic liner in the Type III vessel is fully wrapped in CFRP, while the Type IV vessel has a polymer liner that is fully wrapped in CFRP [38].

Type IV storage tanks are the latest generation of storing compressed hydrogen. They are designed to store hydrogen at very high pressures. They are lighter than all other tank types, which makes them ideal for use in mobility applications. They are standard technologies used in Fuel Cell Electric Vehicles (FCEVs) and also deployed in tube trailers and Hydrogen Refueling Stations (HRS). The stored pressure depends on the usage. In HRS, these tanks are capable of storing compressed hydrogen at a pressure as high as 900 bar. In mobility applications, it stores compressed hydrogen at 700 bar for light-duty vehicles, 350 bar for heavy-duty vehicles, and around 500 to 540 bar in trailer transport [39].

The structure and materials are illustrated in Figure 2.12. The liner is made of high-density polyethylene (HDPE), so hydrogen embrittlement is not an issue, unlike in Type 1. To provide mechanical strength to withstand high pressures, carbon fiber-reinforced polymer (CFRP) is wrapped all around the liner. The tank is connected to the hydrogen supply lines with auxiliary components such as a boss and a valve (typically made of aluminum or stainless steel) [40].

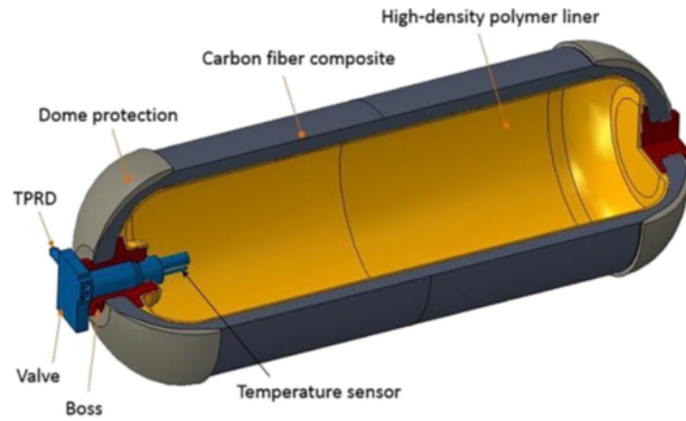


Figure 2.12: Type IV high-pressure vessel [40]

At 700 bar, a Type IV tank can hold 5-6 wt.% of hydrogen, and a hydrogen density of 57 kg/m^3 can be reached [41].

2.2.2 Liquified Hydrogen Storage systems (LH_2)

The LH_2 system stores hydrogen in liquid form instead of gaseous form. It requires hydrogen cryogenic cooling until -253°C (20K) [42]. This process is highly energy-intensive [43]. It also has a higher energy density ($71 \text{ kg}/\text{m}^3$), nearly twice that of compressed gas. Despite the insulation, boil-off (a small amount of H_2 evaporates) loss occurs during storage.

2.2.3 Cryo-Compressed Hydrogen Storage System (CCH_2)

CCH_2 is a hybrid storage technology that combines the features of compressed hydrogen storage systems and liquified hydrogen storage systems. In these tanks, the hydrogen is stored in gaseous form at cryogenic temperatures but under high pressure (200-250 bar) [44]. CCH_2 tanks have higher storage capacity than CH_2 tanks and lower boil-off losses than LH_2 tanks.

2.2.4 Solid Material-Based Hydrogen Storage

Solid material-based hydrogen storage involves storing hydrogen within solid materials, rather than as a compressed gas or in liquid form. In solid material storage, hydrogen can be absorbed into the lattice of metals/alloys (e.g., Metal hydrides) [45], or physically adsorbed in porous materials such as metal-organic frameworks (MOFs) [46] and carbon nanotubes.

Metal hydrides store hydrogen through a chemical reaction between hydrogen gas and a metal or an alloy. Under suitable conditions, it reacts with the host metal to form a metal hydride compound, embedding hydrogen atoms within the lattice (absorption). When heat is applied, the reaction is reversed and hydrogen is released (desorption). The metal hydride hydrogen storage tank has a higher volumetric density than the technologies mentioned above. Magnesium hydride-based storage tanks reach a volumetric density of up to approximately $180 \text{ kg}/\text{m}^3$ under optimal conditions [47].

On the other hand, adsorbent materials such as carbon nanotubes and metal-organic frameworks store hydrogen through a physisorption process in which hydrogen molecules adsorb to the surface of the solid due to weak van der Waals forces.

2.2.5 Liquid Material-Based Hydrogen Storage

Liquid material-based hydrogen storage involves the use of liquid compounds that can chemically or physically store hydrogen. Unlike gaseous or solid-state storage methods, this approach allows hydrogen to be stored, transported, and handled in liquid form under ambient or near-ambient conditions. The two most prominent categories within this approach are Liquid Organic Hydrogen Carriers (LOHCs) and inorganic chemical liquid carriers (e.g., ammonia).

LOHCs are organic compounds that can reversibly absorb and release hydrogen through hydrogenation and dehydrogenation reactions. In the hydrogenated form, they act as the storage medium, and in the dehydrogenated form, they can be reused for multiple cycles. Hydrogen can also be stored by reacting chemically with inorganic molecules that are easier to store and transport under standard conditions, such as ammonia (NH_3) and methanol (CH_3OH).

2.3 Hydrogen Transportation Modes

Three main modes of transporting hydrogen are pipelines, tube trailers, and ships. The choice of transportation is strongly influenced by factors such as distance, volume, infrastructure, and end-use requirements.

2.3.1 Hydrogen transportation through pipelines

For small to medium distances, large-scale gaseous hydrogen transport via pipeline has resulted in low operating costs [48]. Globally, hydrogen pipeline networks extend over 4,500 km, with around 1,600 km located in Europe [49].

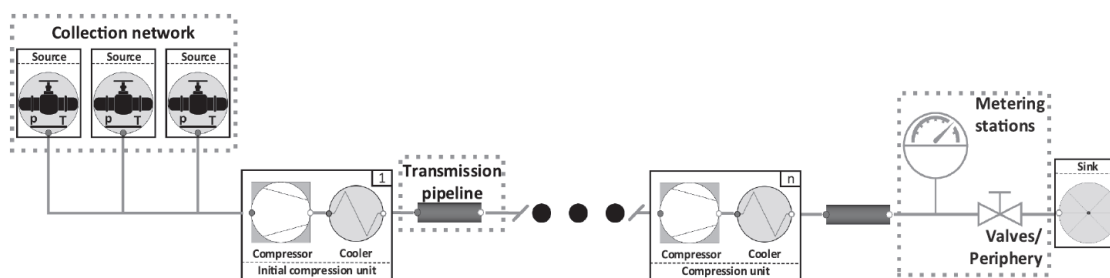


Figure 2.13: Key components of a hydrogen pipeline system [50]

Figure 2.13 illustrates a hydrogen pipeline network where pipelines carry pressurized hydrogen gas from feed-in stations to substations, where the gas is expanded and delivered to distribution pipelines. The operating pressure ranges between 20 and 100 bar (typically 70 bar). The diameter of a hydrogen pipeline ranges between 400 and 1,400 mm, higher than that of natural gas pipelines [51]. The flow velocity varies between 10 and 20 m/s, depending on the pipe design [52]. To compensate for pressure losses in the pipelines, compression stations are placed. Recompression is carried out every 100 km to 600 km. Metering stations as well as valves are placed at 8-30 km intervals [51]. For high-pressure, large-scale hydrogen transmission, high-strength, low-alloyed steel is used. API 5L steel grades X40-X70 are considered to be suitable for hydrogen transmission [53].

One of the major concerns in hydrogen pipeline transport is hydrogen embrittlement. Hydrogen molecules are tiny and can penetrate steel pipes, making them

brittle. To avoid this problem, the pipeline is typically coated internally using Galvalume alloy, which is composed of aluminum (55 wt%), zinc (43.4 wt%), and silicon (1.6 wt%) [54].

In comparison to natural gas, hydrogen escapes more easily from joints such as valves, seals, gaskets, and fittings [55]. Also, leak detection is challenging since hydrogen is a colorless and odorless gas. One way to detect leakage is by blending odorants; however, this approach is difficult because the odorant must disperse at the same rate as hydrogen gas to escape with it [56]. It also compromises the purity of hydrogen being transported. That is why hydrogen needs to be monitored and handled carefully.

In recent years, there has been growing interest in repurposing existing natural gas pipelines for hydrogen transport. Much of today's gas network could potentially be adapted to carry either pure hydrogen or hydrogen–natural gas blends, which would greatly reduce the cost and time required to build entirely new infrastructure. Using pipelines that are already in place also makes it easier to connect production sites with industrial clusters and demand centers. However, converting these pipelines is not straightforward. Materials and components must be carefully assessed to ensure they can safely handle hydrogen, since issues like embrittlement, pressure limitations, and the suitability of existing compressors and valves can significantly affect performance and safety.

2.3.2 Hydrogen Transport Via Tube Trailers

Tube trailers are one of the most common and flexible options for short-distance hydrogen distribution. In this method, hydrogen is compressed to high pressures (typically 200-500 bar) and stored in multiple cylindrical tanks (tubes) mounted on a truck trailer (as shown in Figure 2.14).



Figure 2.14: Tube trailer for transporting hydrogen [57]

The storage capacity of the tank depends on the pressure, cylinder type, and trailer design. Composite tanks can store more than 1000 kg of hydrogen per trip when stored at 500 bar [58]. At 200 bar pressure, the storage capacity is around 250 kg [59]. The fuel for the trailer is typically diesel, but in the future, hydrogen in combination with fuel cells might be an option.

2.3.3 Hydrogen Transportation Via Ships

For very long distances across borders, transportation via ships is used. Shipping compressed hydrogen over long distances is not practical due to its low volumetric density, which would necessitate a large fleet of vessels. Hydrogen is more efficiently moved either as liquid hydrogen (LH_2) or after being converted into ammonia (NH_3). The process of producing ammonia from hydrogen is explained in detail in Section 2.4.2. Liquid ammonia is often preferred over liquid hydrogen for maritime transport because NH_3 contains 17.6 wt.% hydrogen; its volumetric hydrogen density ($108 \text{ kgH}_2/\text{m}^3$) is actually higher than that of liquid hydrogen ($71 \text{ kg}/\text{m}^3$) [60].

2.4 Hydrogen End-Use Applications

Hydrogen is a versatile energy carrier that can decarbonize multiple sectors. According to the International Renewable Energy Agency (IRENA), hydrogen can have the following applications: industrial, energy, power-to-fuel, heating, and mobility [61]. In the energy system, hydrogen can replace natural gas in conventional cogeneration power plants. It also enables power-to-fuel pathways, where it is converted into synthetic fuels such as e-methanol or e-ammonia. Hydrogen can furthermore contribute to low-carbon heating in buildings and industrial processes, either through direct combustion or combined heat and power systems. In the mobility sector, hydrogen powers fuel cell vehicles and is particularly relevant for applications where batteries are less practical, including heavy-duty trucks, buses, maritime transport, and potentially aviation. Moreover, hydrogen is increasingly being explored as a key solution for decarbonizing highly CO_2 intensive industries, particularly steel and cement. The following sections provide details about its most important applications.

2.4.1 Gas Turbines

One possible application of hydrogen in the power sector is to use it as a fuel in gas turbines of conventional combined cycle power plants for electricity generation (as shown in Figure 2.15). Hydrogen can replace natural gas or can be blended with it and combusted in modified gas turbines, reducing CO_2 emissions from power plants [62]. Several manufacturers, such as Siemens, are developing turbines capable of firing 100% hydrogen [63].

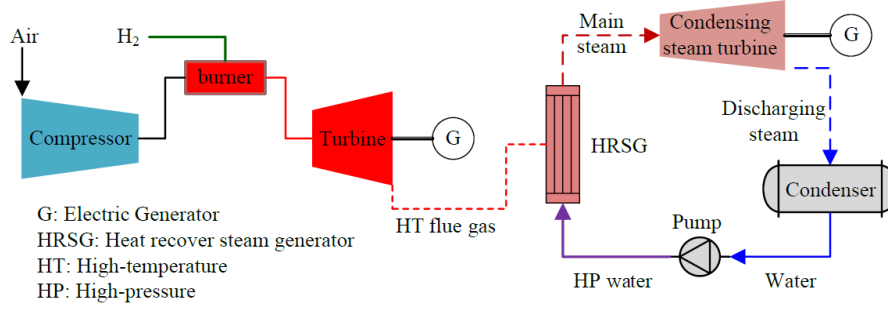


Figure 2.15: Hydrogen-fueled Combined cycle gas turbine [62]

2.4.2 Green ammonia production

Ammonia has emerged as a promising low-carbon energy carrier due to its high energy density and ease of storage and transport [64]. Fertilizer production is the major consumer of ammonia, accounting for about 85% of the total ammonia production [65].

The most common methods of ammonia production are the Haber-Bosch process and solid-state ammonia synthesis. Currently, around 90% of the global ammonia production is obtained through the Haber-Bosch process, which reacts hydrogen (H_2) with nitrogen (N_2) under high pressure and temperature in the presence of an iron-based catalyst [66].



Nitrogen is commonly obtained from air using a cryogenic distillation process in an air separation unit (ASU). Hydrogen, on the other hand, can be obtained from various feedstocks. Steam methane reforming of natural gas is the conventional way of producing hydrogen for ammonia synthesis [67]. CO_2 emissions can be significantly reduced by using hydrogen produced through water electrolysis using renewable electricity [68]. Figure 2.16 illustrates potential pathways for NH_3 production.

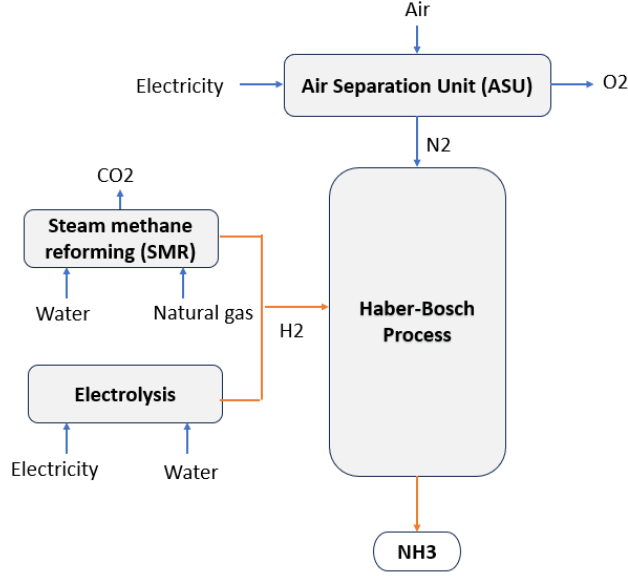


Figure 2.16: Ammonia production route adapted from [69]

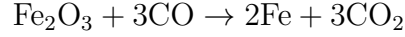
The operating temperature of the Haber-Bosch process is around 400-500 °C, while the pressure ranges between 150 and 300 bar. Typically, an iron-based catalyst is used.

2.4.3 Steel production

The steel industry is highly energy and emissions-intensive. The steel industry ranks first in CO_2 emissions and second in energy consumption among industrial sectors [70]. Steel is primarily produced through two main routes: the Blast Furnace/Basic Oxygen Furnace (BF/BOF) route and the Electric Arc Furnace (EAF) route. The EAF route relies on scrap steel or direct iron reduction (DRI) and accounts for 29% of global steel production. Hydrogen becomes increasingly relevant in this context because it can replace fossil fuels, particularly natural gas, in the DRI process, enabling the production of “green steel.” When hydrogen produced from renewable electricity is used as the reducing agent, the DRI–EAF pathway can substantially reduce CO_2 emissions, offering a promising route for deep decarbonization of the steel sector.

Globally, around 71% of steel is produced using the conventional Blast Furnace/Basic Oxygen Furnace (BF/BOF) process. It requires significant raw materials, including coal, limestone, and iron ore. Coal is transformed into coke in coke ovens, and limestone is converted to lime in lime kilns. The processed materials, including iron ore (Fe_2O_3), are introduced into a blast furnace operating between 1500 and 2300 °C for primary ironmaking. Coke (C) serves as a fuel and a reducing agent. Hot air is blasted into the furnace, which reacts with coke to produce CO and CO_2 .

CO further reduces iron ore to molten iron (pig iron). The following reaction occurs inside the furnace:



Molten pig iron (from BF) is sent to the Basic Oxygen Furnace (BOF) to convert molten iron into steel. BOF operates by blowing high-purity oxygen produced on-site in the Air Separation Unit (ASU) onto molten iron. The temperature inside BOF is around 1600-1700 °C. Finally, the molten steel is transferred to the continuous casting stage for solidification and the hot rolling process for shaping into a finished product. The complete BF/BOF process is explained in Figure 2.17.

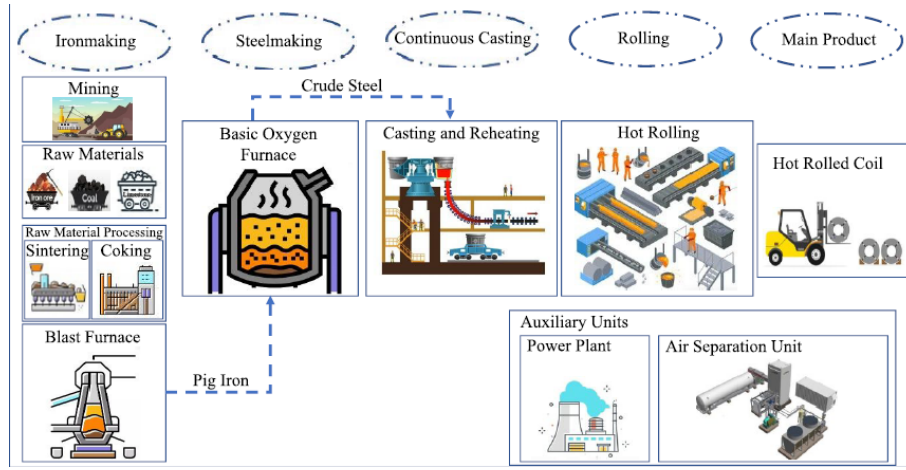
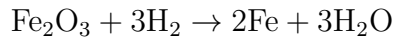


Figure 2.17: Schematic diagram of hot-rolled steel production via the BF/BOF route [70]

Alternatively, hydrogen can replace coal to reduce iron ore (Fe_2O_3) in the Direct Reduced Iron/Electric Arc Furnace (DRI/EAF) process. In this process, iron ore must be transformed into pellets first and then introduced into the DRI shaft. The reducing gas (hydrogen) at high temperature, around 800-1050 °C, is injected into the shaft. It removes oxygen from iron ore pellets to produce solid sponge iron known as DRI and water, following the reaction:



The sponge iron is then charged into the EAF, where it is heated between 1500 and 1700 °C, which melts the DRI to produce molten steel. If hydrogen is produced using renewable electricity, it reduces emissions since it produces H_2O as a byproduct instead of CO_2 . The complete H2-DRI/EAF process is explained in Figure 2.18.

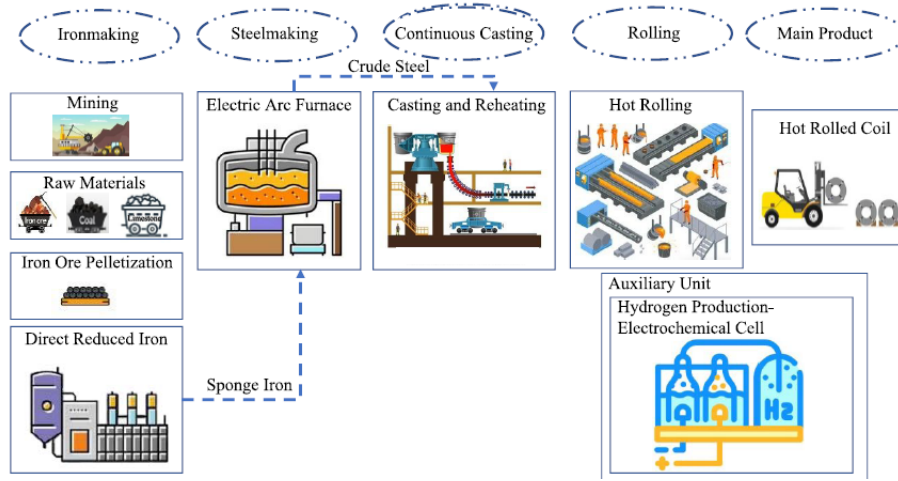


Figure 2.18: Schematic diagram of hot rolled coil production via the DRI/EAF route [70]

2.4.4 Fuel Cell Electric Vehicles (FCEVs)

Fuel cell electric vehicles are a type of vehicle that uses hydrogen as a fuel to generate electricity on board through a fuel cell system. Unlike Battery Electric Vehicles (BEVs), which store energy in batteries, FCEVs continuously produce electricity by reacting hydrogen with oxygen from the air. The only byproduct of this reaction is water, which makes this technology emission-free. There are several variants of fuel cells, which differ in the fuel and the electrolyte used. Proton Exchange Fuel Cell (PEMFC), fueled by compressed gaseous hydrogen, is the technology of choice [71]. They are characterized by a low weight, short startup time, and lower operating temperature (approximately 60-80°C). This technology is used not only in light-duty applications such as passenger cars, but also increasingly in heavy-duty applications, including trucks, buses, and long-haul transport.

According to the International Energy Agency (IEA), approximately 57,300 passenger FCEVs were registered worldwide in 2022. The majority of these vehicles were located in South Korea (51%), followed by the United States (26%) and Japan (13%) [72].

For the operation of FCEV, hydrogen is supplied via a Hydrogen Refueling Station (HRS). HRS serves as the interface between the hydrogen supply and the end-user of mobility. Hydrogen is usually delivered to HRS via tube trailers, pipelines, or is produced on-site. Figure 2.19 illustrates the process of hydrogen refueling.

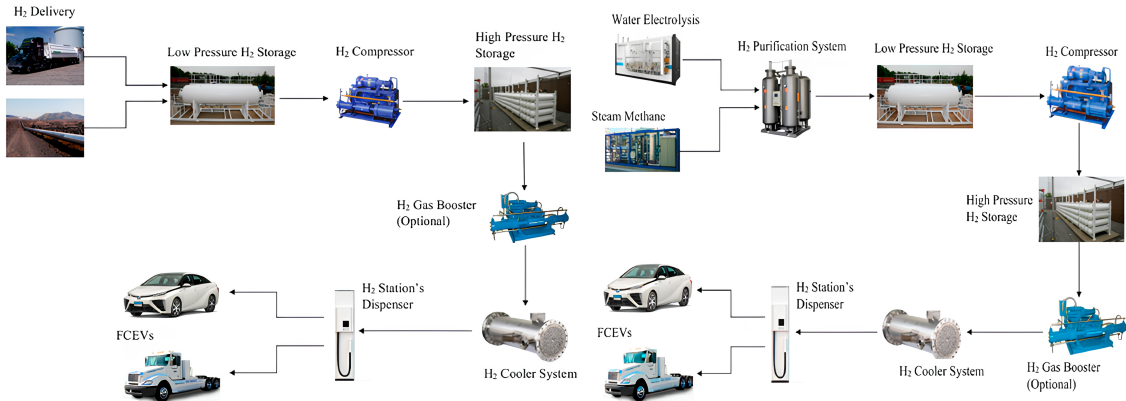


Figure 2.19: Off-site (left) and On-site H₂ production hydrogen gas refueling station's main components [73]

The Hydrogen Refueling Station consists of a compressor, cooler, onsite storage, and dispenser. It may also include a hydrogen production unit if it is produced on-site. Initially, hydrogen delivered to HRS is compressed to high pressure (up to 900 bar) with required cooling and stored in carbon fiber storage tanks. The storage capacity of the tanks exceeds 350 kg. The dispenser further transfers the hydrogen into the vehicle's tanks at different pressures (700 bar for passenger cars and 350 bar for heavy-duty trucks). The lifetime of all the components is usually 20 years [74].

Key components of an FCEV are shown in Figure 2.20, which include the fuel cell stack, hydrogen storage tanks, electric motor, glider (vehicle without powertrain), and battery. In BEVs, electrical energy provided by the battery (typically a Li-ion battery) powers the electric motor; however, this energy is supplemented in FCEVs by a fuel cell and an additional battery.

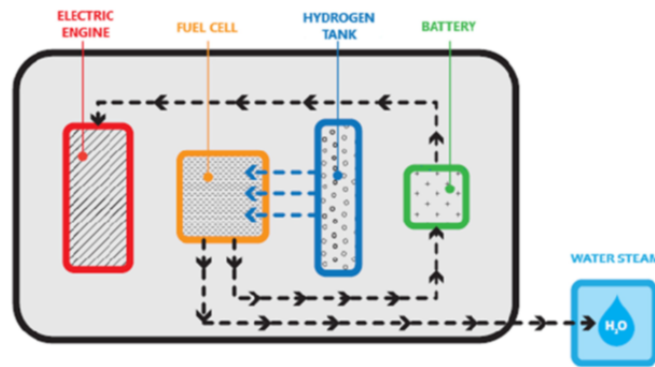


Figure 2.20: Simplified scheme of a hydrogen-powered fuel cell system in road vehicles [75]

A Type IV storage tank is used to store hydrogen at high pressure, which is

continuously supplied to a fuel cell for operation. The number of tanks required, pressure, and capacity of the storage tank vary depending on the vehicle size. In a FCEV passenger car, it has the capacity to store 5-6 kg of H₂ at a pressure of around 700 bar [76], whereas in heavy-duty trucks, up to 40 kg of hydrogen can be stored at 350 bar pressure.

The heart of an FCEV is the Proton Exchange Membrane Fuel Cell (PEMFC) system. The core components of a PEM fuel cell include the Membrane Electrode Assembly (MEA), comprising catalyst layers and two electrodes (anode and cathode) separated by a proton-conducting polymer membrane, which serves as an electrolyte. For the catalyst, platinum deposited on a porous carbon layer is the technology of choice for PEMFCs in FCEVs [77]. The membrane typically used is Nafion. The operating principle of a PEM fuel cell is illustrated in Figure 2.21.

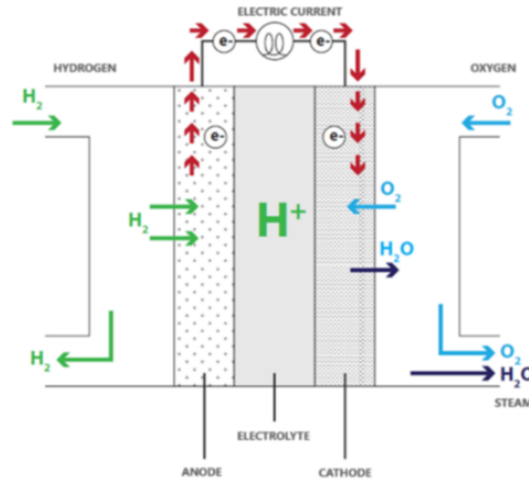
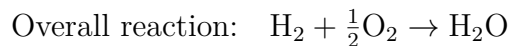
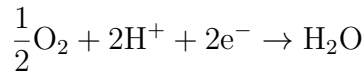


Figure 2.21: Schematic diagram of the operating principle of PEM fuel cell [75]

Hydrogen from the storage tank is supplied to the anode of the fuel cell, where, in the presence of a catalyst, it is split into protons and electrons by the following reaction:



Electrons travel through the external circuit, generating an electric current to power the motor. Protons, on the other hand, pass through the membrane to the cathode, where they combine with oxygen to produce water as a by-product:



Other main components of the PEMFC stack are the gas diffusion layers (GDLs), bipolar plates (BPPs), gaskets, and end plates (as shown in Figure 2.22). GDLs

are porous carbon-based layers placed on both sides of the MEA, allowing the gas reactants to reach the catalyst layers and provide permeability for water removal. It also provides electrical conductivity between the catalyst layers and bipolar plates. Bipolar plates (made of graphite) have several functions within the fuel cell: they help distribute the fuel and oxidant within the cell; they facilitate water and heat management; they separate different cells in the stack; and they carry electrical current from the cell. The gaskets seal the MEA to the bipolar plates. End plates clamp the fuel cells together to form a stack.

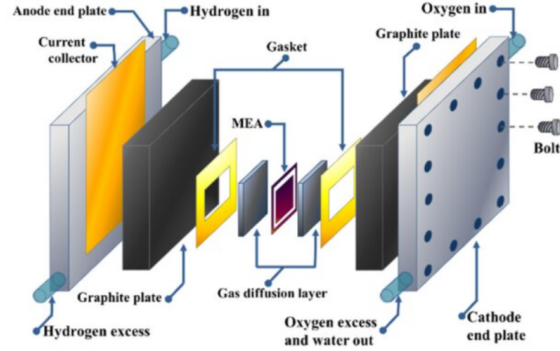


Figure 2.22: Schematic diagram of the components of a single PEMFC [78]

In addition to the stack itself, the PEMFC system has Balance of Plant (BoP), which includes all the supporting components that help the fuel cell operate efficiently and safely. BoP can be divided into four main components: heat management, fuel management, air management, and water management. All the components involved in managing the BoP of the PEM fuel cell are illustrated in Figure 2.23.

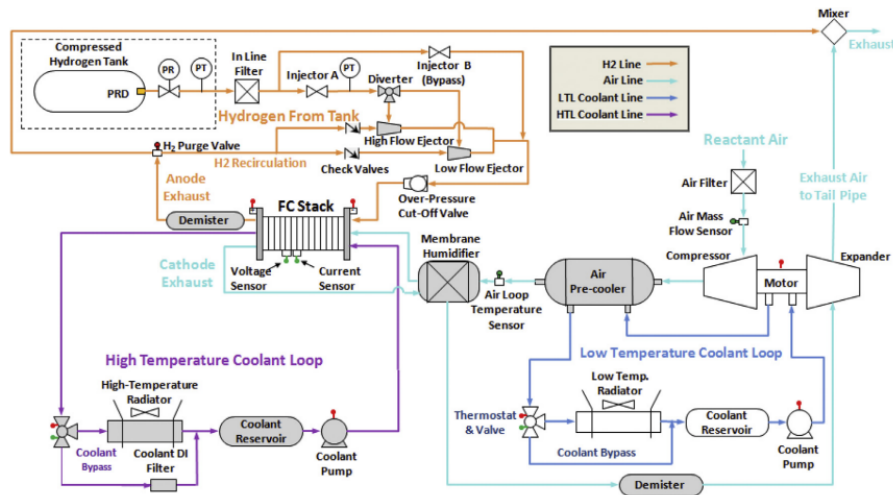


Figure 2.23: Balance of plant (BoP) of PEM fuel cell [79]

The air management system delivers oxygen to the cathode using a compressor, an air filter, air ducts, and flow sensors to maintain the required airflow and pressure. The fuel management system supplies hydrogen to the anode through blowers, ejectors, and pipes, managing its flow and recirculation to improve efficiency. The water management system controls moisture levels to keep the membrane hydrated without causing flooding. Lastly, the thermal management system keeps the stack temperature within the optimal range for performance and durability. Together, these systems ensure smooth, efficient, and reliable operation of the PEM fuel cell under different conditions.

Chapter 3

Life Cycle Assessment (LCA) Background

Life Cycle Assessment (LCA) is a standardized method that is used to assess the environmental impacts of a product or service throughout its entire life cycle, including raw material extraction, manufacturing, distribution, use, and end-of-life management. LCA can be applied for broad understanding as well as for decision-support purposes, benefiting policymakers, companies, and consumers. LCA is conducted following the ISO 14040 and ISO 14044 standards, which together establish the internationally accepted framework for producing transparent and reliable assessments. ISO 14040 provides principles of LCA, the general framework, and the main phases of LCA [80]. ISO 14044 complements this by offering more detailed requirements and procedures, including rules for data quality, allocation, system boundaries, reporting, critical review, and methodological choices [81].

At the European level, the Joint Research Centre (JRC) provides further operational guidance through the ILCD Handbook [82], which elaborates practical modelling rules, data quality indicators, and documentation requirements. The JRC quality checklist supports LCA practitioners by providing a structured way to evaluate the transparency, consistency, and overall methodological quality of a study. For emerging hydrogen systems, the SH2E (Sustainability Assessment of Hydrogen Energy Systems) guidelines offer additional sector-specific methodological advice, proposing harmonized rules for electricity attribution, system boundaries, and multi-output processes across hydrogen production, storage, transport, and end-use stages [83]. Before SH2E, the FC-HyGuide (or HYGuide) guidance document served as a pioneering sector-specific manual for conducting LCAs on hydrogen production pathways and fuel cell technologies [84].

3.1 Principles and Framework for LCA

The LCA framework is illustrated in Figure 3.1.

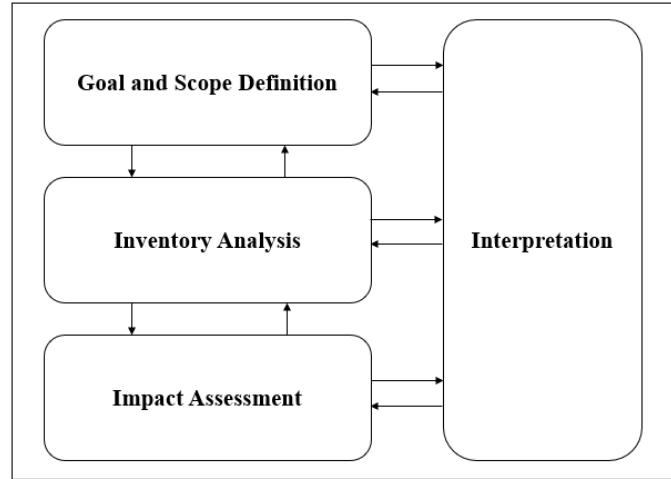


Figure 3.1: Life Cycle Assessment Framework

According to ISO 14040 and ISO 14044 standards, an LCA study has the following phases:

1. Goal and scope definition
2. Life cycle inventory (LCI) analysis
3. Life cycle impact assessment (LCIA)
4. Interpretation

3.1.1 Goal and Scope Definition

The goal defines the objective of a study. The goal definition answers the following questions: What? Why? And for whom? The answers describe the intended application, reasons for conducting the research, and the intended audience.

The scope determines the width and depth with which the LCA is conducted. The scope describes the limits of the study in terms of the analyzed system, its functional unit, and the system boundary.

Functional unit

Serves as a reference baseline for all input and output data within a study. It provides a quantitative measure of the service delivered by a product system, ensuring that results are comparable across different technologies or scenarios. In simple terms, it

defines “what” is being assessed and “how much” of it. For example, in a hydrogen production scenario, the functional unit could be “1 kg of hydrogen produced”.

System boundaries

The system boundaries define which processes and life cycle stages are included and excluded from an LCA study. Figure 3.2 presents possible system boundaries in the context of LCA.

Depending on the study objectives, the system boundary can take different forms. A cradle-to-gate system boundary incorporates all processes from resource extraction (“cradle”) to the factory gate, excluding use and disposal phases. A cradle-to-grave boundary covers the complete life cycle, from raw materials to end-of-life treatment or recycling. Meanwhile, a gate-to-gate approach focuses only on specific production stages within a broader system.

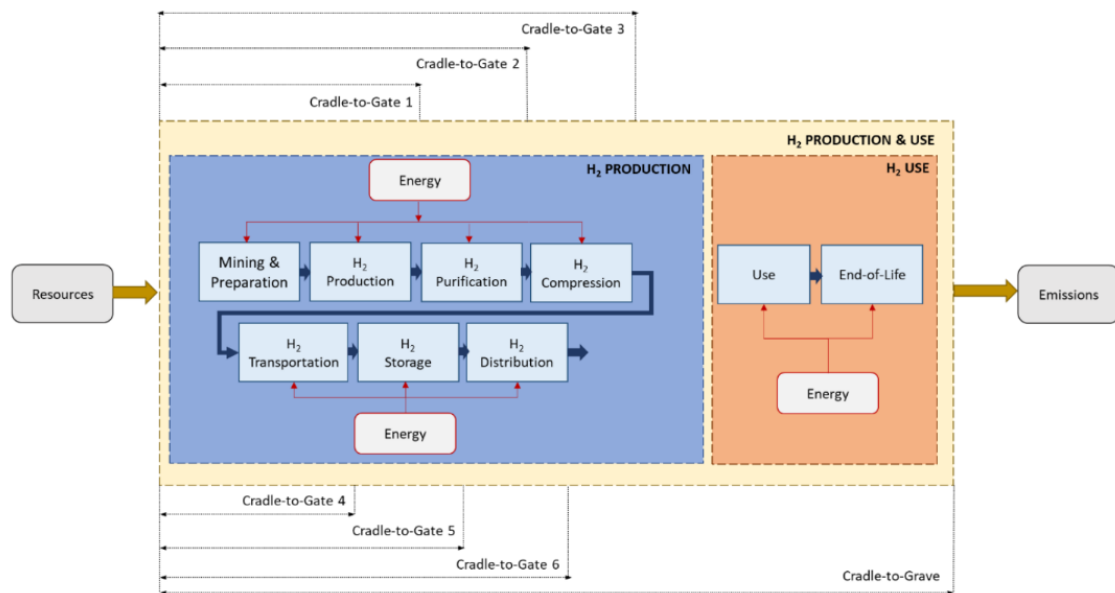


Figure 3.2: System boundaries for hydrogen-related studies [85]

3.1.2 Life Cycle Inventory (LCI) Analysis

LCI analysis is the phase of LCA where all relevant inputs and outputs associated with a product are systematically quantified, including resources consumed, as well as emissions to air, water, and soil throughout the product’s life cycle. Foreground and background data are researched in an iterative process. Data can be obtained from primary sources (e.g., manufacturers, industry reports, and literature) or secondary sources, such as LCA databases like Ecoinvent.

3.1.3 Life Cycle Impact Assessment (LCIA)

LCIA is the phase where LCI data is translated to potential environmental impacts (e.g., acidification, climate change, eutrophication, water and land use, resource depletion, etc.), providing a clear understanding of how a product or process affects environmental outcomes.

In this stage, impact categories can be reported at the “midpoint” or “endpoint” level. Figure 3.3 illustrates the relationship between midpoint and endpoint indicators.

Midpoint indicators explain the potential impacts at an intermediate stage, before actual damage occurs. They focus on specific environmental problems like climate change, acidification, eutrophication, ozone depletion, etc. Endpoint indicators, on the other hand, describe the final consequences or damages on key protection areas, including human health, ecosystem quality, and resource availability.

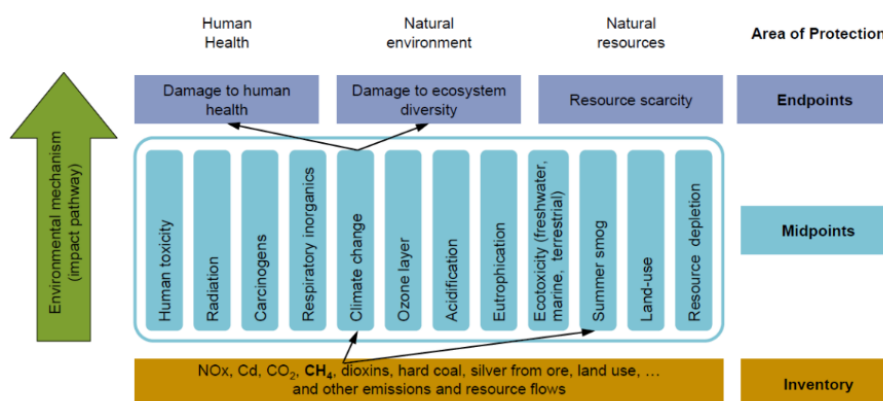


Figure 3.3: Schematic steps from inventory to category endpoints [86]

To quantify the environmental impacts of a product, several impact assessment methods exist. Commonly used midpoint-oriented methods include “Environmental footprint (EF)”, “CML”, and “ReCiPe”, which quantify environmental impacts at an intermediate point. On the other hand, endpoint-oriented methods such as Eco-Indicator 99 and ReCiPe endpoint translate the impacts measured at the midpoint level into overall damage categories, including effects on human health, ecosystems, and resource availability. Each assessment method includes slightly different types of impact categories. Selecting an LCIA method depends on the objectives, scope, and available data for the LCA study.

3.1.4 Interpretation

This phase evaluates the results from the previous phases to draw meaningful conclusions. In this stage, the consistency and completeness of results are ensured to identify which elementary flows or impact categories contribute the most to the environmental impact.

3.2 Importance of LCA in Hydrogen Systems

Hydrogen is widely considered a key energy carrier for achieving deep decarbonization across multiple sectors. It is often considered a “clean fuel,” but that’s only true if its entire life cycle is clean. While hydrogen produces no emissions during use, its production, storage, and distribution can still generate significant environmental burdens. This is where life cycle assessment (LCA) plays a vital role.

Different hydrogen production routes have vastly different environmental impact profiles. LCA provides a comprehensive cradle-to-grave framework that enables a fair comparison between various hydrogen production pathways, including grey hydrogen from natural gas, blue hydrogen with carbon capture, and green hydrogen powered by renewables, to determine which option is most sustainable. Similarly, multiple storage and transportation methods exist for hydrogen, each with its own specific demands for energy and materials. Through LCA, these options can be systematically evaluated to identify which technologies have the lowest environmental burdens and which contribute most to overall impacts across the supply chain.

By revealing these impacts, LCA helps make sure that hydrogen technologies genuinely contribute to decarbonization rather than shifting emissions to other parts of the value chain. Ultimately, incorporating LCA into hydrogen development ensures that the growing hydrogen economy evolves progresses sustainably and supports long-term climate objectives.

3.3 Previous LCA Studies on Hydrogen Systems

Life Cycle Assessment (LCA) has been extensively applied to evaluate the environmental impacts of hydrogen production and its supply chains. One of the earliest detailed assessments was carried out by the National Renewable Energy Laboratory (NREL), which analyzed hydrogen production through steam methane reforming (SMR). That study showed quite significant GHG emissions of about 9–12 kg CO_2 -eq per kg of hydrogen produced when no carbon capture was applied [87]. Carbon capture and storage technologies contribute significantly to the reduction of GHG emissions. Most recent reviews confirm that the conventional way of producing hydrogen is carbon-intensive unless combined with CCS technologies [88].

Over the past few years, the focus on hydrogen production through water electrolysis has received considerable attention. A systematic review by Puig-Samper et al. [89] found wide variability in reported results, mainly due to methodological choices (functional unit, system boundaries, electricity source, electrolyzer efficiency, etc.).

The type of technology used to produce green hydrogen affects the LCA results. Wei et al. [90] examined four types of electrolyzers, i.e., Proton exchange membrane (PEM), Alkaline (AWE), Solid oxide (SOEC), and Anion exchange membrane (AEMWE), showing that stack lifetime, material requirements, efficiency, and operating conditions strongly impact the results. A targeted review by Shaya and

Glöser-Chahoud [91] reported that PEM and AWE perform quite similarly when powered by renewables, while the global warming potential (GWP) of electrolysis often exceeds SMR when supplied by the grid.

The source of electricity plays the most important role in assessing the environmental impacts. Depending on boundary assumptions and electricity carbon intensity, global warming impacts of PV-electrolysis range from 0.7-6.6 kg CO_2 -eq/kg H_2 [92]. Another investigation on green hydrogen via electrolysis confirmed that wind-powered systems outperform solar-powered systems with PEM technology, achieving the lowest GWP among electrolyzers [93].

Beyond production, recent LCA studies are increasingly focusing on integrating production with other stages of a hydrogen value chain, including storage, transportation, and refueling stages. Osman et al. [94] highlights that distribution and hydrogen refueling stations (HRS) can add significant burdens, while pipelines are more favorable for high-volume delivery as compared to tube trailers.

Although there are very few LCA studies on hydrogen end uses in mobility, industry, and the power sector, recently, there has been an advancement in incorporating hydrogen end-use applications into the LCA framework. For instance, a substantial reduction in GHG emissions has been observed using green hydrogen-based fuel cell electric vehicles, compared with battery electric vehicles and conventional internal combustion engine vehicles [95, 96]. The steelmaking process accounts for the majority share of global CO_2 emissions in the industry sector. Recent studies, including one by Vogl et al. [97], suggest that integrating green hydrogen into the steelmaking process can result in decarbonization. Similarly, Lee et al. [98] reveals that hydrogen can substantially reduce emissions when replacing natural gas in the conventional Haber-Bosch ammonia production process.

Moreover, there are only a few studies that provide guidelines for conducting LCA on hydrogen and fuel cell (FCH) systems. SH2E (Sustainability Assessment of Harmonised Hydrogen Energy Systems) project, for instance, is working to harmonize methodologies by issuing guidelines that integrate environmental (LCA), economic (LCC), and social (SLCA) assessments specifically for fuel cell and hydrogen (FCH) technologies [85]. Before SH2E, the FC-HyGuide (or HYGuide) guidance document served as a pioneering sector-specific manual for conducting LCAs on hydrogen production and fuel cell systems [84].

Chapter 4

Methodology

This chapter is dedicated to describing the methodological framework used to conduct this study. A life cycle assessment (LCA) approach, based on ISO 14040 and 14044 standards, was applied to quantify the potential environmental impacts associated with a Hydrogen Valley system. LCA is a widely used and standardized method for evaluating environmental impacts across all stages of a product or process. Although other approaches, such as Material Flow Analysis, Carbon Footprinting, or Energy Analysis, can also be applied, LCA is preferred here because it provides a comprehensive, system-wide view, making it well-suited for comparing different technological pathways.

4.1 Goal and Scope Definition

The primary goal of this study is to explore and compare the environmental impacts of various hydrogen technological pathways within the context of the Hydrogen Valley concept. The technological steps of the hydrogen value chain include its production, storage, transportation, and end-use across multiple sectors. The study aims to identify the most sustainable technological pathways for the deployment of hydrogen within each stage of its value chain.

To achieve this goal, the study addresses the following key research questions:

1. *What are the environmental impacts associated with each stage of the hydrogen value chain from production to end-use?*
2. *How do the environmental impacts of emerging hydrogen-based systems compare to those of conventional fossil-based energy systems?*
3. *Which processes or components contribute significantly to the overall environmental impacts in a hydrogen valley system?*
4. *Which technology offers the highest potential for emission reduction when powered by green hydrogen?*

The LCA study aims to guide policymakers, researchers, and industry stakeholders in designing environmentally sustainable hydrogen systems and in identifying priority areas for technology development to support low-carbon transitions.

The scope of this work includes all life cycle stages, ranging from raw material extraction to the use phase of various hydrogen value chain scenarios. The functional units are defined according to the specific case studies. The use phases for all stages of the hydrogen value chain are restricted to Italy. Production and other upstream processes are referenced to the location of activities by the original equipment manufacturers and their suppliers, respectively.

4.2 Functional Units and System Boundary

In this study, the functional unit is selected according to the specific hydrogen applications under investigation. For instance, for hydrogen production, the functional unit (FU) is “1 kg of hydrogen produced and stored at 30 bar”. For hydrogen transport, FU is “1 kg of hydrogen transported over a distance of 100 km”. For end-use applications, the functional unit varies according to the sector. For example, “1 km driven by a passenger car or 1 tonne-kilometre (tkm) of freight transported by a heavy-duty truck” for transportation, and “1 tonne of steel or 1 kg of ammonia produced” for industrial processes. Defining the functional unit for each process makes sure that all impacts are assessed and compared using the same scale. However, because each step of the hydrogen value chain operates under a different functional unit, the results cannot be directly compared across stages. This means that hydrogen production, transport, and end-use must be assessed separately, and the outcomes interpreted within the context of each specific functional unit rather than as part of a single, unified comparison.

The system boundaries establish which processes are included or excluded in the life cycle assessment. This study adopts a “cradle-to-gate” system boundary for all processes under consideration, encompassing all stages, from raw material extraction and manufacturing of key components to system operation. For mobility and industrial applications, the boundaries also include hydrogen consumption during operation. End-of-life treatment, recycling, and disposal are excluded due to data limitations.

4.3 LCIA Method and Impact Categories

The life cycle impact assessment (LCIA) in this study is conducted using the “mid-point Environmental Footprint 3.1 (EF v3.1)” method, as recommended by the European Commission [99]. Midpoint analysis explains the potential impacts on specific environmental problems such as global warming, acidification, eutrophication, or ozone depletion. The EF3.1 provides a harmonized framework for evaluating the

environmental impacts of products, processes, or systems across a wide range of impact categories.

The specific environmental indicators under study, based on the recommendations of HyGuide [84], are: climate change (GWP), acidification, eutrophication (terrestrial/freshwater/marine), Resource use (minerals and metals), and Resource use (energy carriers). Moreover, Water use is also evaluated, but only for the hydrogen production case, where its relevance is significantly higher. Land use could be a useful indicator, but it is strongly dependent on local geographical conditions. Because the hydrogen value chain in this study is defined in a general, non-site-specific way, land use results would not provide meaningful insights, so this category was not included.

It should be noted that other indicators within the EF3.1 method (ionizing radiation, ozone depletion, particulate matter, etc.) could also be considered.

Additional description of EF3.1 impact indicators is presented in Table 4.1.

Table 4.1: Proposed EF impact categories and units

EF Impact Category	Unit
Climate change	kg CO ₂ eq
Acidification	mol H ⁺ eq
Eutrophication, terrestrial	mol N eq
Eutrophication, freshwater	kg P eq
Eutrophication, marine	kg N eq
Resource use, energy carriers	MJ
Resource use, minerals, and metals	kg Sb eq

Climate change refers to the overall contribution of greenhouse gas (GHG) emissions to global warming over a time span of 100 years. Emissions such as carbon dioxide (CO₂), methane (CH₄), and nitrous oxide (N₂O) are expressed as carbon dioxide equivalents (CO₂-eq) based on their respective global warming potentials. The acidification category measures the potential release of acidifying substances, mainly sulfur dioxide (SO₂), nitrogen oxides (NO_x), and ammonia (NH₃), which can lead to acid rain and soil degradation. These impacts are quantified in moles of hydrogen ion equivalents (mol H⁺-eq).

Terrestrial eutrophication (expressed in mol N eq) reflects the accumulation of nitrogen-based pollutants primarily from ammonia and nitrogen oxide emissions, which stimulate excessive plant growth. Freshwater eutrophication (expressed in kg P eq) arises from the discharge of phosphorus compounds, such as phosphates, into freshwater systems. Marine eutrophication, on the other hand, assesses nitrogen enrichment in marine environments, which can disrupt aquatic life and water quality, and is expressed in kilograms of nitrogen equivalent (kg N eq).

Energy resource use (expressed in MJ) measures the total consumption of non-renewable energy sources throughout the entire life cycle, and mineral and metal resource use evaluates the depletion of finite raw materials essential for producing

hydrogen-related technologies, including electrolyzers, fuel cells, and storage tanks. This category is expressed in kilograms of antimony equivalents (kg Sb-eq), indicating the relative scarcity and extraction potential of these resources compared to antimony. Key contributors to this impact include platinum, iridium, nickel, and titanium used in electrolyzers, as well as structural materials such as steel, aluminum, and carbon fiber in storage tanks and vehicle components. These materials require energy-intensive mining and refining processes, which significantly influence the mineral and metal resource use category.

4.4 LCA Modelling Software

Several software tools, both commercial and open-source, are available to support LCA studies. Among the most widely used are OpenLCA, SimaPro, and GaBi, which are well-established platforms in both academic research and industrial applications for modeling, calculating, and interpreting environmental impacts.

This study utilizes OpenLCA, which is open source and free software. OpenLCA requires the integration of an external database for inventory and impact assessment data. The Ecoinvent v3.11 cutoff database was used in this study. Ecoinvent is one of the most widely used and trusted life cycle inventory (LCI) databases, providing detailed environmental information for a broad range of products, materials, and industrial processes. It covers many important sectors, including energy, transport, manufacturing, agriculture, and chemical production, making it a reliable foundation for building consistent and realistic LCA models. The database accounts for the use of secondary raw materials in the production phase of the product system.

The OpenLCA allows creating new processes or using those processes in the imported database. Additionally, Microsoft Excel and Python v3.12.12 were employed for data processing, visualization, and graph generation. Excel was primarily used for organizing LCI data, performing scenario analysis, and calculating summary tables, while Python (version 3.12.12) was used to create high-quality graphs and charts to illustrate trends, contribution analyses, and comparative results clearly and effectively.

4.5 Modelling Structure in OpenLCA










To ensure transparency, consistency, and reproducibility, each stage of the hydrogen value chain was modeled in OpenLCA using a structured and modular approach.

For each process, all relevant input and output flows were identified and created or selected from the Ecoinvent database, which includes electricity supply, raw materials, transportation services, and emissions. These flows were then linked within dedicated processes, such as PEM electrolysis, hydrogen compression, pipeline transport, or fuel cell stack manufacturing, where input requirements and emissions were specified. Each hydrogen value chain step was modeled as an independent unit process. Once

the unit processes were defined, they were linked together to form a complete product system that corresponds to the functional unit of each case study. Once the product system was created, the EF 3.1 impact assessment method was finally applied to get the results.

To illustrate the modelling structure, Figure 4.1 shows the PEM electrolysis process as implemented in OpenLCA as an example.

▼ Inputs

Flow	Category	Amount	Unit	Costs/Re...	Uncertain...	Avoided ...	Provider
 electricity, high voltage	D:Electricity, gas, ste...	56.30000	 kWh		none		 electri...
 PEM Electrolyzer System	T: PEMWE activities	1/16253...	 Item(s)		none		 PEM ...
 water, ultrapure	E:Water supply; sew...	9.28000	 kg		none		 mark...

▼ Outputs



Flow	Category	Amount	Unit	Costs/Re...	Uncertain...	Avoided ...	Provider
 H2, gaseous, 30bar (...)	T: PEMWE activities	1.00000	 kg		none		

Figure 4.1: PEM electrolysis modelling structure in OpenLCA

In the PEM electrolysis model, the main inputs include electricity supply, ultrapure water, and the manufacturing of the PEM electrolyzer system, which provides both the stack and BoP manufacturing. These inputs collectively generate 1 kg of hydrogen at 30 bar. In the OpenLCA process structure, electricity inputs are linked directly to the specific energy source used, whether wind, solar, or grid mix. Likewise, the electrolyzer system manufacturing stage is connected to detailed upstream BoP components and material flows, such as titanium plates, platinum catalyst, the polymer membrane, etc.

Chapter 5

Comparative LCA of Different Case Studies

5.1 Introduction

This chapter provides a comparative LCA across various stages of hydrogen value. The complete hydrogen value chain is modeled using OpenLCA software. The analysis aims to assess the environmental impacts associated with hydrogen production, storage, transportation, and utilization. By examining different technological routes and system configurations, this study identifies the most sustainable pathways for hydrogen deployment within a Hydrogen Valley framework. Figure 5.1 presents a breakdown of the main stages in the hydrogen supply chain.

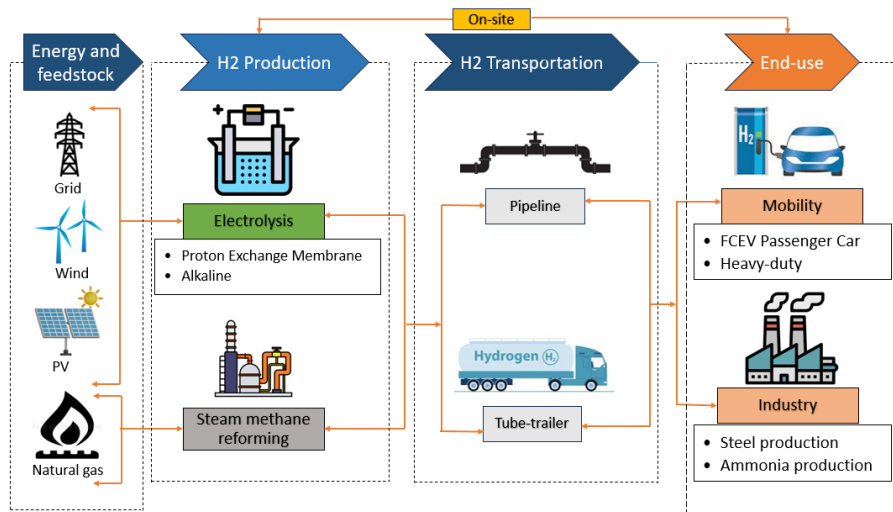


Figure 5.1: Main stages of hydrogen value chain under consideration

The assessment follows the guidelines outlined in ISO 14040 and ISO 14044

standards for conducting LCA studies. The analysis is conducted using the Ecoinvent v3.11 database. As recommended, the Environmental Footprint (EF 3.1) method is used for impact assessment [99], which quantifies key impact categories including climate change (GWP), acidification, eutrophication, and the use of energy and raw materials.

Because of the limited availability of open-access data and inventories from industries, foreground system data are sourced from the literature, whereas the data for the background system are sourced from the Ecoinvent v3.11 database [100].

To evaluate different configurations of the hydrogen value chain, this study comprises several case studies, which include:

- Case study 1: Comparative LCA of various hydrogen production routes
- Case study 2: Comparative LCA of PEM Electrolysis with different electricity sources
- Case study 3: Comparative LCA of different hydrogen transportation modes
- Case study 4: Comparative LCA of on-site vs off-site hydrogen production for Hydrogen refueling Station (HRS)
- Case study 5: Comparative LCA of passenger vehicle technologies
- Case study 6: Comparative LCA of heavy-duty trucks
- Case study 7: Comparative LCA of steel production routes
- Case study 8: Comparative LCA of ammonia production routes

For hydrogen production, the choice of PEMWE, AWE, and SMR for hydrogen production in this study allows for a fair comparison across different technologies. SMR is currently the most widely used method for hydrogen production, whereas PEMWE and AWE, on the other hand, represent the most mature technologies for producing green hydrogen, powered by renewable electricity. Among the different forms of hydrogen assessed, gaseous hydrogen was considered for storage and transport because it is the standard form currently used in real-world systems, especially in Europe, and remains the most practical option for pipelines and tube trailers. Light and heavy-duty mobility were included because they are among the largest potential markets for hydrogen, and they illustrate how hydrogen competes differently with battery-electric alternatives depending on vehicle size, duty cycle, and range requirements. Steel and ammonia were added as industrial case studies because they are two of the most promising and large-scale applications for clean hydrogen: steelmaking as a major emissions hotspot seeking low-carbon reduction routes, and ammonia as both a key chemical product and an energy carrier with growing relevance.

The comparative life cycle assessment conducted in this chapter provides a clear understanding of the environmental implications associated with various hydrogen value chain pathways. By integrating production, transportation, and end-use perspectives, the study enables the identification of critical hotspots and trade-offs across different technologies. The insights gained from this analysis help define optimized configurations for a low-carbon hydrogen economy within the Hydrogen Valley concept.

5.2 Case Study 1: Comparative LCA of Various Hydrogen Production Routes

5.2.1 Case Study Description

The first case study compares the environmental performance of three hydrogen production technologies, i.e., Proton Exchange Membrane Water Electrolysis (PEMWE), Alkaline Water Electrolysis (AWE), and Steam Methane Reforming (SMR). The reason for choosing these three technologies for comparison is already explained in Chapter 2. The goal is to assess which hydrogen production route offers the lowest environmental impacts, comparing SMR and electrolysis-based routes while ensuring that all electrolysis options rely on the same low-carbon electricity source. The geographical scope of our study is Italy. On-shore Wind power is considered an electricity source for electrolysis since it is widely used for green hydrogen production.

The functional unit is “1 kg of hydrogen produced and stored at 30 bar”. A cradle-to-gate approach is used. The system boundary covers the entire life cycle, from raw material extraction to hydrogen production. It includes all stages of component manufacturing, material and component transportation, electricity generation, and hydrogen production, followed by compression (if needed), and temporary storage at 30 bar in storage tanks. Table 5.1 provides three configurations analyzed in this study.

Table 5.1: H₂ production scenarios with different pathways

Scenario	Electricity source	Production Technology	System boundary
1A	Wind power	SMR	Cradle-to-gate
1B	Wind power	PEMWE	Cradle-to-gate
1C	–	AWE	Cradle-to-gate

The production of hydrogen through the SMR process (Scenario 1A) is taken from the Ecoinvent v3.11 database. 1 kilogram of gaseous hydrogen is produced through steam methane reforming (without carbon dioxide capture) of natural gas at 25 bar. The Ecoinvent v3.11 SMR process includes hydrogen purification in a Pressure Swing Absorption (PSA) unit, but does not include hydrogen storage after production; therefore, storage at 30 bar is modeled separately after its compression from 25 bar to 30 bar. The entire process of hydrogen production through SMR is already explained in Chapter 2.

Regarding the scenarios 1B and 1C, a 5MW PEMWE and a state-of-the-art 2.2 MW AWE are analyzed for the production of hydrogen in this study, respectively. The PEMWE plant comprises two stacks of 2.5MW each along with its Balance of Plant (BoP). Detailed descriptions of the individual components of both the stack and the BoP are provided in Chapter 2. The KPIs of the PEMWE technology are

subdivided into operational KPIs and construction KPIs. AWE system consists of a stack, BoP, power electronics (PE), and an electricity source. The baseline Alkaline Electrolyzer (AE) design is state-of-the-art stacks based on the Norwegian company NEL's design [101]. Hydrogen is generated at ambient pressure and must be compressed to 30 bar before storage. Each component of the AWE stack and BoP is explained in Chapter 2.

Table 5.2 presents the key construction-related KPIs of a state-of-the-art electrolyzer used as an input to the PEMWE model, and Table 5.3 summarizes the energy demand for the construction and operation stage, as well as water demand for the operation of PEMWE. The operational KPIs for the PEMWE stack are given in Table 5.4.

The temporal system boundary corresponds to a plant life of 20 years. However, since some components have shorter useful life, replacement of equipment is also considered. In addition, construction and operation are assumed to take place in Italy.

It should be noted that two stacks are used for the initial operation, while the other two are allocated for replacement throughout the life of the system. In addition, highly pure hydrogen is produced with a purity of 99.999%.

Table 5.2: Construction KPIs of PEMWE stack [25]

Parameter	Unit	State-of-the-art plant
Active cell area	cm ²	1500
Membrane material	–	Nafion 117
Cathode catalyst	–	Platinum supported on carbon black
Cathode catalyst loading	mg cm ⁻²	0.2
Anode catalyst	–	Iridium oxide (IrO ₂) on titanium dioxide support
Anode catalyst loading	mg cm ⁻²	2
Porous transport layer material (anode)	–	Titanium, 30% porosity
Porous transport layer thickness (anode)	mm	1
Porous transport layer coating (anode)	mg cm ⁻²	0.1 iridium
Bipolar plate material	–	Titanium
Bipolar plate thickness	mm	2.5
Bipolar plate coating material (anode side)	–	Platinum
Bipolar plate coating amount	mg cm ⁻²	0.04

Table 5.3: Energy and water demand of the PEMWE model [25]

Parameter	Unit	State-of-the-art
Lifetime hydrogen production	t	16,253
Specific energy demand for electrolysis	kWh/kgH ₂	53.60
Energy demand for BoP	kWh/kgH ₂	2.73
Total energy demand	kWh/kgH ₂	56.33
Water demand	kg/kgH ₂	9.3

Table 5.4: Operational KPIs of PEMWE stack [25]

Parameter	Unit	State-of-the-art plant
Stack scaling	MW	2.5
Mean cell voltage	V	1.96
Current density	A cm ⁻²	2
Stack operating temperature	°C	65
Stack operating pressure	bar	30
Active cell area	cm ²	1500
Active stack area	m ²	69.45
Cells per stack	–	463
Stack lifetime	h	80,000
Pump efficiency	%	26.27
Power electronics efficiency	%	98
System lifetime	yr	20

Table 5.5 represents the material demand for a single 2.5 MW PEMWE stack. Table 5.6 provides a detailed LCI for the construction of the PEMWE system. A schematic overview of all essential components of the plant stack and BoP is already presented in Figures 2.4 and 2.5.

Table 5.5: Material demand for a single 2.5 MW PEMWE stack [25]

Material	SoA amount [kg]
Titanium	996.71
Carbon paper	8.75
Nafion	30.25
Platinum	0.188
Iridium	2.465
Activated carbon	0.24
Synthetic rubber	80.56
Copper	17.06
Stainless steel	156.20

Table 5.6: LCI of the system construction [25]

Component	Unit	SoA value
Stack	pieces	4
Anode gas water separator	kg	660.3
Cathode gas water separator	kg	356.3
Feed pump	pieces	2
Circulating pump	pieces	2
Stack cooling heat exchanger	kg	1340.4
Condenser	kg	1157.7
Dry cooler	pieces	1
Cooling water circulating pump	pieces	2
Power cables	m	50
Data cables	m	2000
Control unit	pieces	1
Power electronics	pieces	22
Foundation	m ³	4.5
Housing	pieces	2

Note that the construction phase of the water purification system is not considered in this study due to a lack of available data. As the ecoinvent v3.11 database does not include a specific dataset for iridium, the platinum dataset is used as a proxy.

Table 5.7 provides the stack specifications for the baseline AWE designs. Table 5.8 lists the materials required for BoP components, and Table 5.9 details the material composition of the AE stack.

Table 5.7: Stack specifications for baseline AE [102, 103]

Parameter	Unit	Baseline value
Stack size	MW	2.2
No. of cells	–	230
Active surface area	m ²	2.1
Power density	W/cm ²	0.5
Current density	A/cm ²	0.245
Pressure	bar	ambient
Temperature	°C	80
Voltage	V	1.85
Lifetime	years	8
Specific energy	kWh/kgH ₂	49
Deionized water	kg/kgH ₂	11.20
Potassium hydroxide	kg/kgH ₂	8.5×10 ⁻⁴
Operating hours at full load	h/yr	4000
Yearly H ₂ production	tons/yr	82448

Table 5.8: Materials for BoP and PE [29]

Materials	Material weight (kg/kgH ₂)
Low alloy steel	1.46×10 ⁻³
High-alloyed steel	5.77×10 ⁻⁴
Aluminum	3.04×10 ⁻⁵
Copper	3.04×10 ⁻⁵
Plastic	9.12×10 ⁻⁵
Electronic material	3.34×10 ⁻⁴
Process material	6.08×10 ⁻⁵
Concrete	1.70×10 ⁻³

Table 5.9: Baseline AE stack materials [26]

Component	Material	Weight (kg/kgH ₂)
Separator	Zirfon UTP 500	1.66×10^{-4}
Cathode	Perforated Carbon Steel	0.02
	Ni plated (156 μm)	3.33×10^{-4}
Anode	Perforated Carbon Steel	0.02
	Ni plated (156 μm)	9.25×10^{-4}
Frames	Carbon Steel	1.60×10^{-3}
Gasket	Synthetic rubber	2.1×10^{-5}
Bipolar plate	Carbon Steel	0.04
	Ni coating (200 μm)	1.47×10^{-3}
End plates	Carbon Steel	5.21×10^{-3}

Zirfon is a zirconia-reinforced polysulfone (ZrO₂-PSU) composite membrane designed for use as a separator in alkaline electrolytic cells [104].

5.2.2 Results of Case Study 1

Table 5.10 compares the key environmental impacts of hydrogen production via SMR, PEMWE, and AWE. SMR serves as a baseline because it is currently the conventional hydrogen production pathway.

The climate change impact of SMR is 11.35 kg CO₂-eq/kgH₂, which is significantly higher than both electrolytic pathways. PEMWE and AWE, with impacts of 2.38 kg CO₂-eq/kgH₂ and 3.433 kg CO₂-eq/kgH₂, achieve reductions of nearly 80% and 70%, respectively. This is due to the replacement of fossil natural gas with renewable electricity as an energy source for hydrogen production. Between the two electrolysis technologies, PEMWE performs better than AWE primarily due to its higher electrical efficiency and lower overall energy demand, as it can directly produce hydrogen at around 30 bar without requiring additional compression before storage. Similarly, non-renewable energy use decreases sharply from 184.12 MJ/kgH₂ in SMR to 28.04 MJ/kgH₂ and 41.31 MJ/kgH₂ for PEMWE and AWE, respectively. This reduction confirms that renewable-powered electrolysis significantly decreases the dependence on fossil fuels.

Unlike climate change and non-renewable energy resources, acidification and eutrophication potentials are higher for the electrolysis systems. This increase is mainly driven by the electricity required for hydrogen production, as the environmental burdens associated with renewable energy generation, particularly wind and solar in this case, dominate the overall impact. Material extraction and component manufacturing, such as the use of nickel, platinum, and steel in electrolyzer production, contribute as well, but to a much smaller extent. Emissions of sulfur and nitrogen oxides generated during these upstream processes contribute significantly to both

acidification and eutrophication impacts. Although these differences are small, they highlight that electrolysis introduces additional material-related burdens, which are less significant in SMR due to its simpler material requirements.

Table 5.10: Life Cycle Impact results of hydrogen production via SMR, PEMWE, and AWE

Impact category	Reference unit	SMR	PEMWE	AWE
Acidification	mol H ⁺ eq	0.0123	0.0265	0.0392
Climate change	kg CO ₂ eq	11.346	2.384	3.433
Energy resources:	MJ	184.118	28.043	41.313
non-renewable				
Eutrophication: freshwater	kg P eq	0.00036	0.00230	0.00221
Eutrophication: marine	kg N eq	0.0028	0.0033	0.0038
Eutrophication: terrestrial	mol N eq	0.029	0.035	0.041
Material resources: metals/minerals	kg Sb eq	0.00002	0.00022	0.00022
Water use	m ³	1.834	1.077	2.403

In terms of material resource depletion, PEMWE and AWE show values roughly 10 times higher than SMR. This reflects the material-intensive nature of electrolysis technologies, which require precious metals such as platinum, iridium, nickel, and titanium. Moreover, AWE requires slightly higher water as compared to PEMWE and SMR, mainly due to the electrolyte solution.

Overall, SMR remains the most carbon- and energy-intensive, but not material-intensive. PEMWE demonstrates the best overall environmental performance, achieving the lowest emissions and energy use despite slightly higher material-related impacts.

On the other hand, the relative contributions of key life cycle processes to four impact categories for PEMWE and AWE hydrogen production systems are illustrated in Figure 5.2. Impact categories include climate change, non-renewable energy use, water consumption, and material resource depletion.

The contribution analysis indicates that electricity for electrolysis (sourced from wind) is the dominant driver of overall environmental impacts in both PEMWE and AWE systems. For global warming potential (GWP) and non-renewable energy use, it

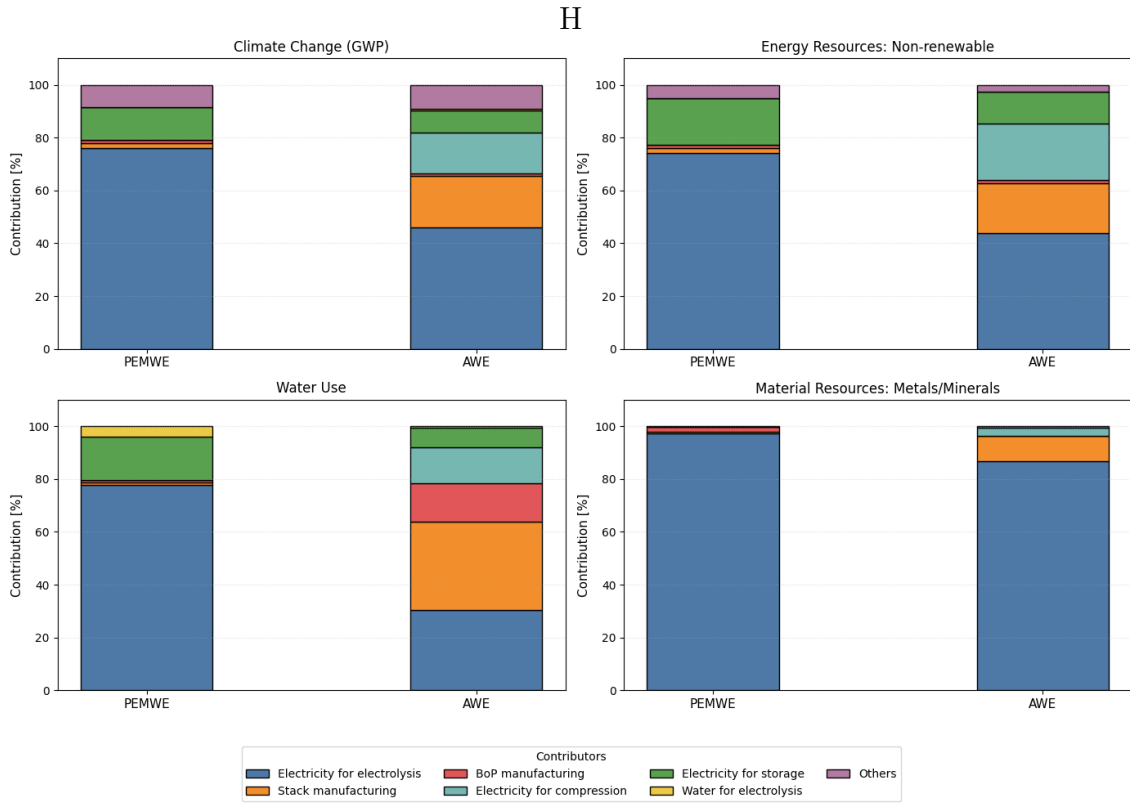


Figure 5.2: Contribution analysis of PEMWE and AWE across four environmental impact categories for producing 1 kg of H₂ at 30 bar

accounts for over 75% in the PEMWE system and around 45% in AWE. In PEMWE, the electricity for compression is negligible since hydrogen is produced directly at the storage pressure of 30 bar, while in AWE, the contribution of electricity for hydrogen compression after its production is significant (15-21%). Stack manufacturing is a minor contributor in PEMWE (< 2%) but represents a notable share of impacts in AWE. It contributes around 19-20% to both GWP and non-renewable energy resource use, primarily due to the steel and nickel required for the stack. The contribution of BoP manufacturing is small in both PEMWE and AWE for both GWP and energy resources.

For water use, the trend is slightly different. PEMWE's water consumption is strongly influenced by the electricity for electrolysis (77%), followed by the electricity for storage manufacturing and operation (16%). In AWE, stack and BoP manufacturing are major contributors, with combined contributions of around 50%, alongside electricity for electrolysis, compression, and storage (30%, 14%, and 7% respectively). For material resources, electricity for electrolysis remains the dominant contributor, accounting for over 97% of the total impacts in PEMWE and approximately 87% in AWE.

Overall, the analysis shows that in PEMWE, the impacts are largely driven by electricity consumption, with other contributions remaining relatively small. In contrast, AWE impacts are influenced not only by electricity, but also significantly by stack and BoP manufacturing, reflecting the higher material intensity.

To better understand the material intensity of both the Alkaline and PEM stacks, Figure 5.3 presents a contribution analysis illustrating the relative share of different materials within the Material Resources impact category.

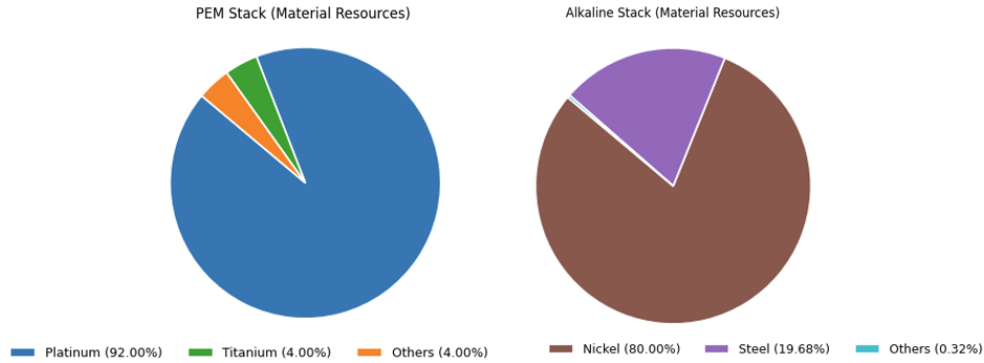


Figure 5.3: Material composition of PEM and Alkaline electrolyzer stacks under the material resources category

Under the Material Resources impact category, the composition of materials used in stack manufacturing differs significantly between Alkaline Electrolyzers and PEM Electrolyzers (PEMWE). In AWE stacks, nickel is the predominant material, contributing around 80% of the total, followed by steel at approximately 20%. This reflects the reliance of alkaline systems on readily available base metals for their electrodes and structural parts. In contrast, PEMWE stacks are dominated by platinum, which represents about 92% of the material contribution due to its role as a catalyst, while titanium and other materials make up roughly 4% each. Consequently, PEMWE manufacturing is more resource-intensive because of its dependence on scarce and high-impact materials, whereas AWE technology relies mainly on more common metals, leading to a comparatively lower burden on material resources.

5.3 Case Study 2: Comparative LCA of PEM Electrolysis with Different Electricity Sources

5.3.1 Case Study Description

The second case study focuses on the hydrogen production stage, specifically evaluating the environmental performance of Proton Exchange Membrane (PEM) electrolysis when powered by three different electricity sources: Wind, Solar Photovoltaic (PV), and Grid mix. The goal of this study is to understand how the source of electricity affects the overall environmental footprint of the process.

In this study, the functional unit is defined as “1 kg of hydrogen produced via PEM electrolysis, at 30 bar, with 99.999% purity”. The cradle-to-gate system boundary includes all upstream processes from raw material extraction to the point of hydrogen production, ready for storage or distribution, while excluding downstream stages related to its use, distribution, and disposal. Table 5.11 provides three configurations analyzed in this study.

Table 5.11: PEM electrolysis scenarios with different electricity sources

Scenario	Electricity source	Production technology	System boundary
2A	Wind power	PEM Electrolysis	Cradle-to-gate
2B	Solar PV	PEM Electrolysis	Cradle-to-gate
2C	Grid mix	PEM Electrolysis	Cradle-to-gate

For consistency, the same PEMWE configuration used in Case Study 1 is applied here, maintaining identical parameters for the PEM stack, capacity, BoP, and LCI inputs.

The LCI data for wind power is taken from the ecoinvent database. The dataset represents the production of electricity at onshore grid-connected wind power plants with a capacity higher than 3 MW in Italy. It includes operation and maintenance expenditures as well as infrastructure inputs. The LCI data for the grid mix is also sourced from the Ecoinvent v3.11 database. The shares were calculated based on statistics from 2021, including voltage transformation and grid losses in Italy. The Italian electricity mix considered in this study includes approximately 41% renewable energy, with the largest share coming from hydropower, followed by solar and wind energy [105]. The LCI data for photovoltaics are taken from the IEA report (2020) [106]. A 570 kWp ground-mounted PV plant based on multi-crystalline silicon modules is considered.

5.3.2 Results of Case Study 2

The comparative results of LCA for hydrogen production by electrolysis using wind, grid mix, and solar PV electricity sources are presented in Table 5.12.

Table 5.12: Comparative environmental impacts of hydrogen production via electrolysis using grid mix, wind, and solar PV electricity

Impact category	Reference unit	Grid mix	Wind	Solar PV
Acidification	mol H ⁺ eq	0.0711	0.0242	0.0208
Climate change	kg CO ₂ -eq	20.971	1.907	2.773
Energy resources:	MJ	351.491	22.154	34.927
non-renewable				
Eutrophication:	kg P eq	0.0054	0.0022	0.0019
freshwater				
Eutrophication:	kg N eq	0.0130	0.0029	0.0034
marine				
Eutrophication:	mol N eq	0.1351	0.0314	0.0390
terrestrial				
Material resources:	kg Sb eq	0.00005	0.00022	0.00012
metals/minerals				
Water use	m ³	12.444	0.908	22.264

The results reveal a clear dependence of environmental performance on the source of electricity used for hydrogen generation. Hydrogen produced via grid electricity shows the highest impacts across nearly all impact categories. The climate change impact reaches about 20.97 kg CO₂-eq, and the non-renewable energy use is 351.49 MJ, which are significantly higher than those for wind and solar-based systems. This is mainly due to the reliance of the electricity grid on fossil fuels. Similarly, higher impacts in acidification and eutrophication categories are also observed. It also results in high water consumption (12.44 m³), mainly due to upstream high-to-medium voltage transformation.

In contrast, wind-based electrolysis demonstrates the lowest environmental impacts across most categories. The climate change potential (1.91 kg CO₂-eq) and energy resource use (22.15 MJ) are notably lower than those of the grid mix, highlighting the benefits of using renewable electricity. The results also show reductions in acidification, eutrophication, water consumption, and material resource use, indicating the overall sustainability advantage of wind power.

Solar PV-powered electrolysis also performs significantly better than grid-based

hydrogen production, with moderate impacts in most categories. However, it shows the highest water consumption (22.26 m³) compared to wind (0.91 m³) and grid mix (12.44 m³), primarily due to the water-intensive production of PV modules. Also, its results are slightly higher than those of wind power primarily due to the energy- and material-intensive manufacturing of photovoltaic panels, which increases the burdens in acidification (0.021 mol H^+ -eq) and material resource use (0.00012 kg Sb-eq).

To better understand the relative environmental performance, Figure 5.4 presents the normalized impacts of hydrogen production through PEM water electrolysis using different electrical sources. The grid mix scenario is used as a baseline, set at 100%, while the impacts of the wind and solar scenarios are expressed relative to this reference. The absolute values on top refer to the impact results in each case. The impact assessment analysis focuses on key impact categories, including Climate Change, acidification, and non-renewable energy resource depletion. All impact categories are expressed per kg of hydrogen produced.

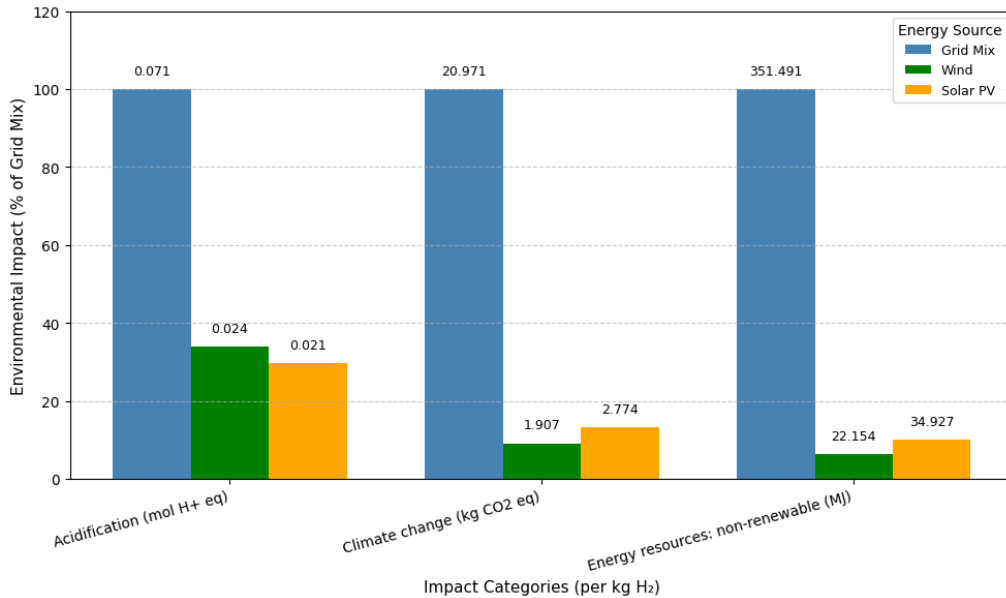


Figure 5.4: Normalized environmental impacts of hydrogen production using different electricity sources. The grid mix scenario is used as a baseline (100%), and the relative impact reductions of wind and solar PV are shown.

The grid mix scenario exhibits the highest contribution to global warming (approximately 21 kg CO_2 -eq/kg H_2) primarily due to the large share of fossil-based electricity within the grid composition. In contrast, a wind-powered electrolysis system achieves the largest reduction, lowering CO_2 emissions by roughly 90-95% relative to the grid mix. The solar PV-based system shows an 80-85% reduction compared to the grid mix, though its impacts are slightly higher than those of the wind-based system due to the energy and material-intensive production of PV modules. Similarly, the

grid mix scenario shows a strong dependence on non-renewable energy resources, as evident from the trend observed in the graph. Moreover, acidification potential also decreases under renewable electricity scenarios, although the impacts are less significant. This is because acidification is influenced not only by fuel combustion in electricity generation, but also by upstream processes related to material extraction and component manufacturing.

However, it should be noted that the grid mix data used in this study is based on Italy's 2021 electricity mix. With the increasing share of renewables in recent years, the associated CO_2 emissions are expected to decrease.

A GWP contribution analysis of different stages in hydrogen production is presented in Figure 5.5. For all scenarios, electricity consumption during the operation is by far the dominant contributor to GHG emissions. This accounts for more than 95% of the total impact, depending on the source of electricity.

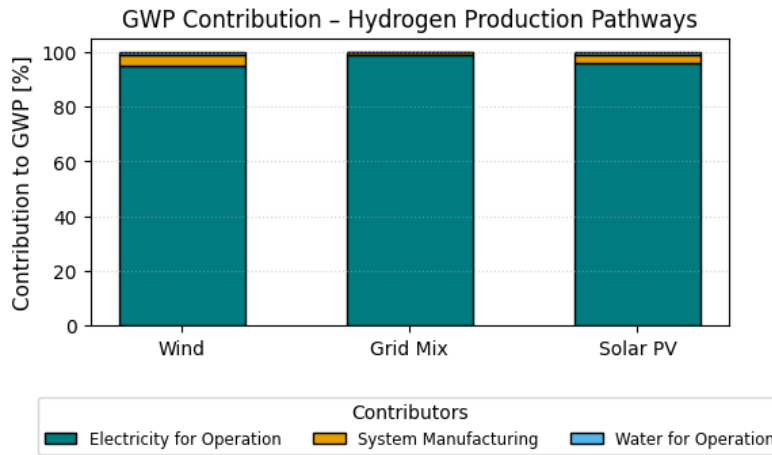


Figure 5.5: Contribution of different hydrogen production stages to GWP

The comparative analysis clearly shows that the source of electricity is the dominant factor influencing the environmental performance of PEM electrolysis. Wind-powered electrolysis shows the lowest impacts, while grid-based electrolysis has the highest. Solar PV performs moderately, with slightly higher impacts than wind. Overall, the results emphasize that coupling PEM electrolysis with renewable electricity is essential for achieving low-carbon and resource-efficient hydrogen production.

5.4 Case Study 3: Comparative LCA of Different Hydrogen Transportation Modes

5.4.1 Case Study Description

This case study compares the environmental performance of two practical hydrogen transportation modes, i.e., gaseous pipeline and compressed gas tube trailer, for distribution to Hydrogen Refueling Stations (HRS). The goal of this study is to identify the most sustainable way between the two in terms of emissions, energy used, and other life cycle impacts per unit of hydrogen delivered.

The distance from the production site to the Hydrogen Refueling Station (HRS) is assumed to be 100 km. Therefore, the functional unit is “1 kg of hydrogen transport over a distance of 100 km (100 kg*km)”. The Cradle-to-Gate approach system boundary encompasses all stages from raw material extraction to transportation infrastructure and operations, including upstream processes related to hydrogen production via PEM electrolysis powered by wind energy and compression required for transportation, which is identified in previous analyses as the most sustainable pathway. The downstream process related to HRS manufacturing and operation is not included. It is important to note that the delivery pressure differs significantly between the two systems. Hydrogen from the pipeline reaches the HRS at approximately 70 bar, whereas hydrogen from the tube-trailer arrives at a much higher pressure of around 500 bar.

For the pipeline transportation, a 100 km transmission pipeline is considered. The operating pressure of the pipeline is 70 bar. Initially, hydrogen is compressed from a storage pressure of 30 bar to 70 bar for transmission. To overcome pressure losses within the pipeline, a compression station is usually installed every 100-150 km, which includes compression with required intercooling, along with other auxiliary components. Since the transport distance in this study is limited to 100 km, no compression station is considered. The Life Cycle Inventory (LCI) of the pipeline, therefore, includes only the manufacturing and operation of the pipeline itself. The main characteristics of a hydrogen pipeline are shown in Table 5.13.

Table 5.13: Hydrogen pipeline specifications [50]

Parameters	Unit	Value
Pipeline lifetime	yr	40
Operating pressure	bar	70
Operating hours	h/yr	8000
Lifetime hydrogen transport	tons	1.2481×10^8

A detailed pipeline inventory is taken from the Ecoinvent v3.11 natural gas pipeline

dataset and modified for hydrogen transport based on data from [58, 50].

In the hydrogen transportation via tube trailers process, the round trip is considered. Hydrogen initially stored at 30 bar is compressed to 500 bar for loading into trailer trucks. The required compression energy is 2.1 kWh/kg [58]. The data for diesel truck manufacturing and operation are sourced from the Ecoinvent v3.11 database, using the dataset for the EURO 6 truck with a payload capacity exceeding 32 tons. Additionally, a high-pressure Type IV composite-based storage tank is considered with a capacity of 1100 kg of hydrogen that can be transported per trip. The overall weight of the truck is 40 t. Table 5.14 provides a detailed LCI for a high-pressure tank per 1100 kg of hydrogen.

Table 5.14: Material composition of storage tank (per 1100 kgH₂) [58]

Material	Unit	Value
Aluminum	kg	660
Rolling aluminum sheets	kg	660
Chromium steel	kg	990
Rolling of chromium steel sheets	kg	990
Carbon fiber	kg	7854
Epoxy resin	kg	3360
Electricity	kWh	495
Steel, low-alloyed	kg	990
Rolling steel sheets	kg	990

5.4.2 Results of Case Study 3

As stated above, to primarily assess the environmental impacts of transportation, only the transport infrastructure and operation are considered. Because the modeled pipeline is short, no compression station is considered; therefore, for pipeline transport, only the construction and operation of the pipeline itself are included. The tube-trailer inventory specifically covers the manufacture and maintenance of a lorry (truck), truck operation (diesel consumption), and the manufacture and use of an on-board storage tank.

Table 5.15 presents the comparative Life Cycle Impact Assessments (LCIA) for hydrogen transport via pipeline and tube-trailer, including the hydrogen supply chain for the operation. The results are presented per 1 kg of hydrogen transported over 100 km.

Hydrogen transportation via pipeline (at 70 bar) shows lower environmental impacts across all impact categories compared to the tube-trailer mode (at 500 bar). The lower climate change potential of pipeline transport (2.66 kg CO₂-eq)

Table 5.15: Comparative environmental impacts for hydrogen transport via pipeline and tube-trailer

Impact category	Reference unit	Pipeline (70 bar)	Pipeline (500 bar)	Tube-trailer (500 bar)
Acidification	mol H ⁺ eq	0.0286	0.0310	0.0315
Climate change	kg CO ₂ -eq	2.663	3.261	3.361
Energy resources: non-renewable	MJ	30.658	40.570	41.963
Eutrophication: freshwater	kg P eq	0.0024	0.0025	0.0026
Eutrophication: marine	kg N eq	0.0035	0.0038	0.0039
Eutrophication: terrestrial	mol N eq	0.0367	0.0408	0.0418
Material resources: metals/minerals	kg Sb eq	0.00023	0.00024	0.00024

as compared to tube-trailer transport (3.36 kg CO₂-eq) is primarily due to the low energy requirement for hydrogen compression. Similar trends are observed in non-renewable energy use, where pipeline transport requires approximately 30 MJ of fossil energy as compared to 42 MJ for a trailer.

Although both systems have relatively low impacts in acidification, material use, and eutrophication categories, the tube-trailer option performs slightly worse, primarily due to the additional diesel fuel use for long-distance truck transport and higher material requirements for storage tanks.

To better visualize the comparative performance of both hydrogen delivery pathways, a normalized comparison was developed, setting the pipeline scenario as the baseline (100%). The impacts of the trailer tube transport system were then expressed relative to this baseline (Figure 5.6).

Among all categories, climate change and non-renewable energy resources dominate the overall environmental profile. The tube trailer option indicates roughly 26% higher greenhouse gas emissions and approximately 37% higher fossil energy demand than the pipeline. These increases are mainly attributed to the energy required for compression to high pressures.

Although the differences in acidification, eutrophication (freshwater, marine, and terrestrial), and material resource use are comparatively smaller, generally within 10-15%, they still indicate that the trailer transportation results in slightly higher impacts. Such categories are strongly influenced by the upstream material extraction and component manufacturing, which are less affected by the transport distance.

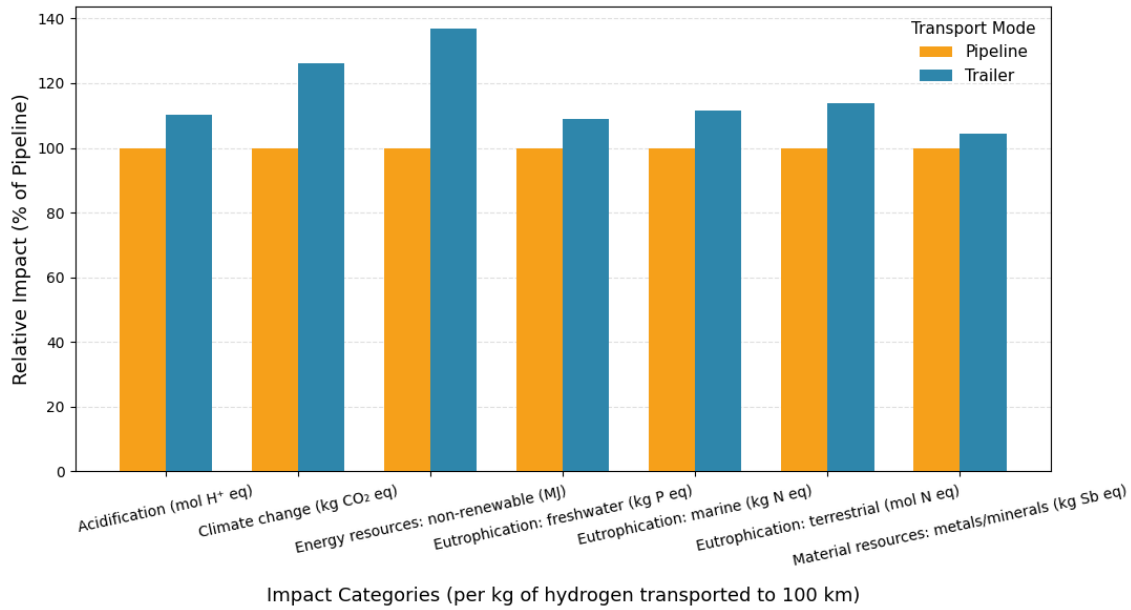


Figure 5.6: Relative environmental impacts of hydrogen delivery via pipeline and tube-trailer systems for the complete supply chain. Pipeline transport is used as the 100% reference baseline

Moreover, Figure 5.7 illustrates the contribution of different life cycle processes to the climate change impact (GWP) for hydrogen delivered via pipeline and trailer-tube systems. Contributions are presented as the percentage of the total GWP for each transport pathway. The contribution analysis shows that electricity production for

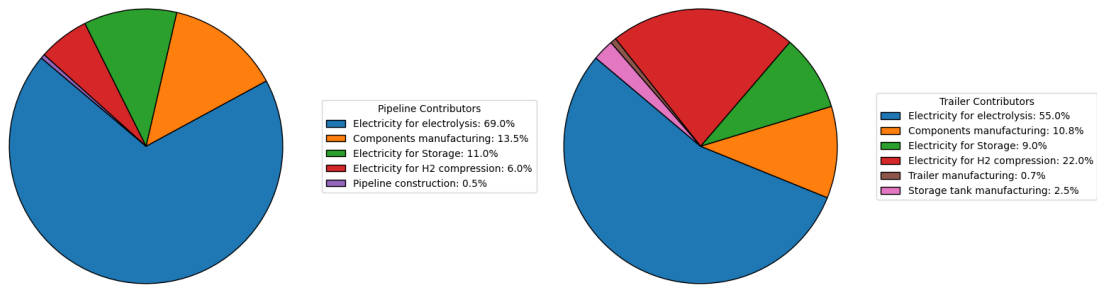


Figure 5.7: Contribution analysis of life cycle processes to the climate change impact for hydrogen delivery via pipeline (left) and tube-trailer (right)

the operation of the hydrogen supply chain is by far the main contributor to GHG emissions. In the case of pipeline transport, 69% of the total CO₂ emissions come from producing the electricity used to split water in the electrolysis process, and 55% in the case of trailer-tube transport, reflecting the energy-intensive nature of electrolysis process. For pipeline transport, electricity required to store and compress hydrogen

accounts for 11% and 6% of the overall emissions, respectively. An interesting result is observed for the construction of the pipeline, which is responsible for only 0.5% emissions in its entire lifetime.

In contrast, for the tube-trailer system, electricity for hydrogen compression plays a more prominent role (22%), because trailer transport requires high compression, which consumes more electricity. The combined effect of trailer and storage tank manufacturing accounts for a small portion (approximately 3.2%).

Overall, the analysis highlights that while the electricity for the electrolysis process dominates the climate change impacts in both systems, the trailer transport shows additional burden from compression, making it environmentally less favorable than the pipeline.

When hydrogen transported by pipeline is compared fairly to tube-trailer transport, meaning both streams are evaluated at the same delivery pressure, the difference in environmental performance narrows substantially. After compressing the pipeline hydrogen from 70 bar to 500 bar, its life cycle impacts become much closer to those of tube trailers. The climate change impact reaches 3.26 kg CO_2 -eq, which is slightly better than the tube-trailer case, and the associated energy-resource use is 40.57 MJ. In other words, once the additional compression step required to equalize delivery pressure is included, pipeline transport no longer shows a clear advantage; its impacts become comparable to tube-trailer transport with electricity for electrolysis and compression being the dominant contributor to climate change.

Transportation distance can significantly influence the environmental performance of pipeline transport. Over longer distances, pipeline systems require additional compression stations to compensate for pressure losses, which introduce further infrastructure needs and electricity consumption for hydrogen re-compression. These processes would increase the overall life cycle impacts of pipeline transport, and at high distances, even higher than tube-trailers. In summary, pipeline transport presents a clear advantage over trailer transport, primarily due to the low compression requirement for transport (70 bar). However, if the hydrogen from the pipeline is compressed to the same pressure as the tube-trailer, it no longer shows a clear advantage.

Another key point to consider is the reuse of existing natural gas pipelines for hydrogen transport. Repurposing current infrastructure can lower environmental impacts, as it eliminates the need for manufacturing and installing entirely new pipelines. Since most of the manufacturing burdens in the hydrogen pipeline scenario originate from steel production, utilizing the existing natural gas network could substantially reduce material demand and construction-related emissions, making hydrogen transport through pipelines a more sustainable option.

5.5 Case Study 4: Comparative LCA of On-site vs Off-site Hydrogen Production for HRS

5.5.1 Case Study Description

This case study examines whether hydrogen for the refueling station should be produced on-site or off-site. In the on-site configuration, a hydrogen production electrolyzer is installed directly at the Hydrogen Refueling Station (HRS). In contrast, the off-site configuration involves producing hydrogen at a central plant and transporting it to the station for compression, storage, and dispensing. The main objective of this assessment is to quantify the additional burden introduced by hydrogen transportation in the off-site scenario. Specifically, the study aims to determine whether the environmental impact of the transport stage is negligible or significant when compared to other phases of the hydrogen value chain.

The functional unit is “1 kg of hydrogen dispensed at the HRS nozzle at 700 bar”. The system boundary includes a cradle-to-gate approach. In the case of on-site production, the system boundary includes upstream hydrogen production to HRS manufacturing and operation. Whereas the system boundary for off-site production also incorporates the hydrogen transportation phase.

As explained in Chapter 2, HRS consists of a compressor, high-pressure storage, a cooler system, and a dispenser. Table 5.16 presents the inventory details of a standard hydrogen refueling station, while Table 5.17 summarizes the key operational parameters considered in this study. The inventory data is taken from [107, 108, 58].

Table 5.16: Life Cycle Inventory Data for Fueling Station [107]

Materials	Mass (kg/kgH ₂)
Low alloy steel	0.07889
High alloy steel	0.0081
Cast iron	0.0023
Copper	0.000910
Aluminum	0.000384
Polymer	0.00028
Carbon fibers	0.00135

Table 5.17: Main parameters of HRS [58, 39]

Parameters	Unit	Value
Capacity	kg/day	850
Utilization factor	%	70
Storage pressure	bar	880
Electricity consumption	kWh/kgH ₂	4.25
Dispense pressure	bar	700

For both on-site and off-site supply scenarios, hydrogen is produced by a PEM electrolyzer powered by wind energy and then stored in a buffer storage tank at 30 bar. Moreover, pipeline transport is considered for transporting hydrogen for off-site configuration. The specifications of the PEMWE system and the pipeline are consistent with those described in earlier case studies.

In the on-site scenario, hydrogen is compressed from 30 bar to 880 bar, whereas in the off-site scenario, it is compressed from 70 bar to 880 bar before being stored in Type IV storage tanks. The compression process, including the required cooling before dispensing, consumes approximately 4.65 kWh per kg of H_2 for on-site production and 4.25 kWh per kg of H_2 for off-site delivery [39].

5.5.2 Results of Case Study 4

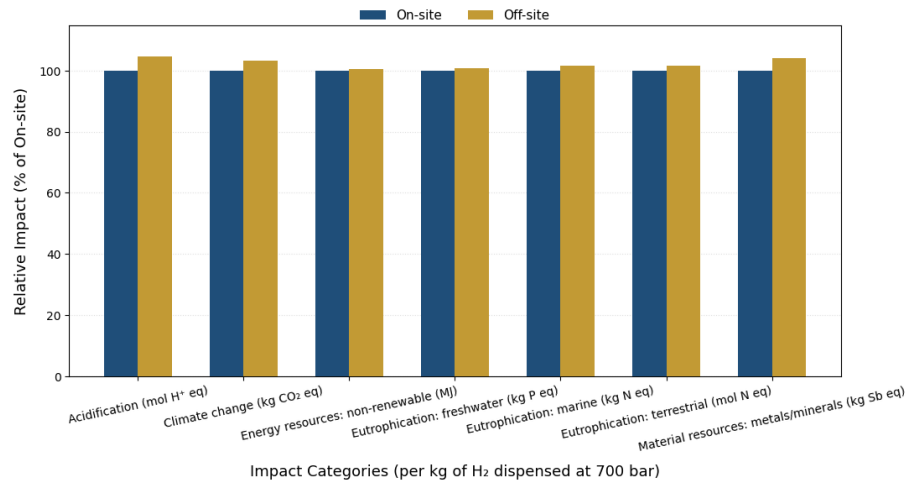
The comparison of life cycle impact assessment between on-site and off-site hydrogen production for a Hydrogen Refueling Station (HRS) is presented in Table 5.18.

Overall, the results indicate that both scenarios show very similar environmental performance, with only minor differences across most impact categories. The on-site production option shows slightly better environmental performance in all impact categories.

Table 5.18: Comparison of environmental impacts between on-site and off-site hydrogen production for HRS

Impact category	Reference unit	On-site	Off-site
Acidification	mol H ⁺ eq	0.0349	0.0365
Climate change	kg CO ₂ -eq	4.293	4.431
Energy resources: non-renewable	MJ	58.229	58.514
Eutrophication: freshwater	kg P eq	0.003	0.003
Eutrophication: marine	kg N eq	0.0047	0.0047
Eutrophication: terrestrial	mol N eq	0.0494	0.0502
Material resources: metals/minerals	kg Sb eq	0.00025	0.00026

To better understand the relative environmental performance, Figure 5.8 presents a comparative analysis of the on-site and off-site hydrogen production scenarios. The on-site scenario is used as a baseline (100%), and the impacts of the off-site system are expressed relative to it. The off-site configuration shows slightly higher impacts,

**Figure 5.8:** Comparative environmental impacts of on-site and off-site hydrogen production for HRS (on-site=100%)

ranging from 2 to 4% higher for most categories, due to the additional process related to hydrogen transportation.

As highlighted in a previous study (5.4), the transportation distance through

pipeline has a significant influence on overall environmental impacts. Longer transport distances require additional recompression stations, which in turn increase electricity consumption and the associated environmental impacts. Expanding the transport distance to 500 km results in GHG emissions of around 4.6 kg CO₂-eq, approximately 7.23% more than the on-site scenario.

The contribution analysis for climate change, shown in Figure 5.9, further supports the overall comparison. In both scenarios, electricity for operation (mainly for

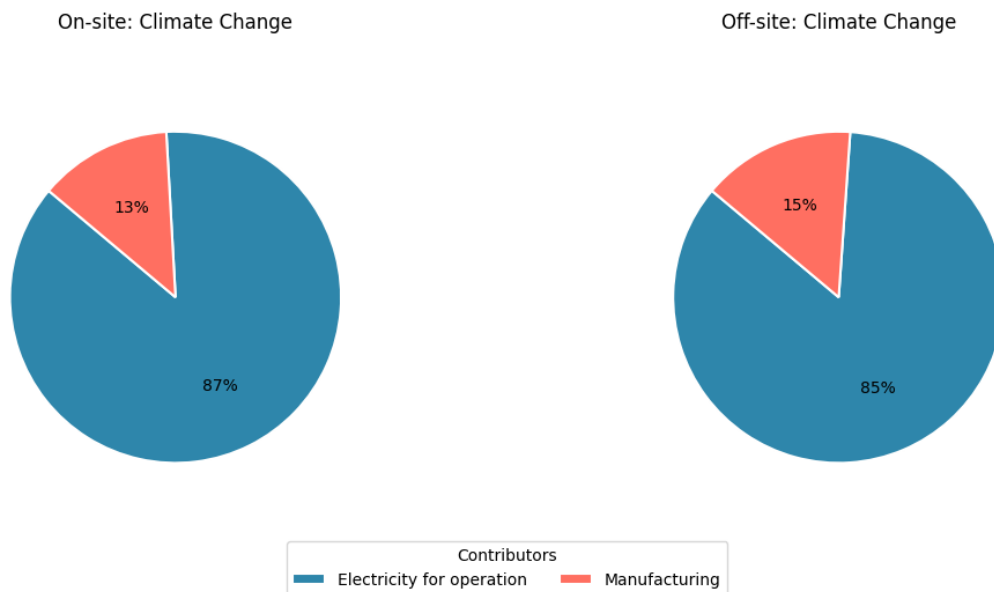


Figure 5.9: Climate change contribution analysis for both on-site (left) and off-site (right) scenarios

electrolysis and compression) is by far the dominant contributor. It accounts for around 85-87% of the overall GHG emissions, while the manufacturing phase is responsible for only 13-15%. Integrating recompression of hydrogen via pipeline transport will further increase GHG emissions. This highlights that the carbon footprint of hydrogen production is primarily influenced by the electricity supply, even when renewable energy sources are used.

Overall, the analysis shows that on-site hydrogen production has lower environmental impacts, particularly for scenarios involving longer transport distances.

5.6 Case Study 5: Comparative LCA of Passenger Vehicle Technologies

5.6.1 Case Study Description

This case study focuses on a comparative Life Cycle Assessment (LCA) of three passenger vehicle technologies, i.e., the Fuel Cell Electric Vehicle (FCEV), the Battery Electric Vehicle (BEV), and the conventional fossil fuel-based Internal Combustion Engine Vehicle (ICEV). The analysis aims to assess whether hydrogen-powered mobility can provide a more sustainable alternative to conventional and battery-based mobility options.

The functional unit is defined as “1 km driven by one passenger car”. The system boundary follows a cradle-to-gate approach, encompassing all stages from raw material extraction to vehicle operation. End-of-life treatment is not considered. For the FCEV, the system boundary also includes the Hydrogen Refueling Station (HRS) infrastructure and operation, as it links the hydrogen supply chain. Based on the results from the previous case study, on-site hydrogen production at HRS is considered, and therefore, the need for hydrogen transportation is eliminated.

The data for the Internal Combustion Engine Vehicle (ICEV) and the Battery Electric Vehicle (BEV) are obtained from the Ecoinvent v3.11 database, using the process “market for transport, passenger, car with internal combustion engine, fleet average” and “market for transport, passenger, car, electric” for ICEV and BEV, respectively. For ICEV, the dataset reflects an average European vehicle fleet composition and includes a representative mix of different car classes (EURO 3, EURO 4, and EURO 5). The vehicle is an average of the various car sizes (small, medium, and large) and fuel types (petrol, diesel, and natural gas) for each EURO category. For the BEV case, the electricity used for battery charging is assumed to be supplied by the grid mix unless otherwise specified in scenario-based comparisons. Tables 5.19 and 5.20 provide the main technical characteristics of the ICE and BEV vehicles.

Parameter	Unit	ICEV
Dry vehicle weight	kg	1200
Average passenger load factor	kg	97.2
Vehicle lifetime	km	150000

Table 5.19: Main technical characteristics of the ICE vehicle [100]

Parameter	Unit	BEV
Dry vehicle weight	kg	918.22
Mass of battery	kg	262
Vehicle lifetime	km	150000
Battery lifetime	km	100000

Table 5.20: Main technical characteristics of the BEV vehicle [100]

The FCEV system modelled is based on a mid-size passenger vehicle comparable to the Toyota Mirai, which includes two hydrogen storage tanks, the battery, the electric motor, the fuel cell system, and the glider (the vehicle without a powertrain). The glider includes: the body of the car, the steering, braking, suspension system, tyres, and electronics [109]. The inventory of the glider is the same for all three vehicles. For the operation of the FCEV, hydrogen produced on-site (through PEMWE) at the HRS is compressed and dispensed at 700 bar for use as vehicle fuel. The main technical characteristics of the FCEV considered in this study are provided in Table 5.21.

Parameter	Unit	FCEV
H ₂ consumption	kg/100 km	0.76
Weight	kg	1800
Glider	kg	800
Vehicle lifetime	km	190000
Electric motor power	kW	80
Driving range	km	600
Storage pressure	bar	700
Tank volume	l	120
Hydrogen stored	kg	5
Li-ion battery	kWh	1.80
PEMFC system	kW	80

Table 5.21: Main technical parameters of the FCEV [110, 111]

To store hydrogen at high pressures, a Type IV 700-bar two-tank storage system yielding a capacity of 5 kg of hydrogen is modelled. The composite material used in these tanks is modelled using 60% wt. T700 carbon fiber and 40% wt. epoxy resin. The auxiliary components of the tank consist of bosses, the plastic tank liner, valves, and a regulator. The main materials for these components are foam, glass

fiber, high-density polyethylene, aluminum, and chromium steel. The main modelling parameters of the PEMFC stack are provided in Table 5.22.

Parameter	Unit	FCEV
Net power	kW	80
Stack power density	mW/cm ²	1095
Active area	m ²	7.31
Total area	m ²	11.7
Pt loading	mg/cm ² _{active}	0.32
Nafion membrane thickness	μm	25.4

Table 5.22: Main modelling parameters of PEMFC stack [112]

The proton exchange membrane fuel cell (PEMFC) system includes the FC stack and the balance of plant (BoP). The PEMFC stack comprises several key components and sub-assemblies, including the membrane, catalyst layers, gas diffusion layers (GDL), bipolar plates, end plates, current collectors, gaskets, and the stack housing with compression bands. The BoP includes air, water, heat, and fuel management systems. The details of the stack components, the BoP, and their operation are provided in Chapter 2.

For the catalyst, platinum (Pt) alloys deposited on a porous carbon layer are the technology of choice for PEMFCs in FCEVs. The catalyst is modelled as a slurry composed of platinum (Pt) and cobalt (Co) deposited onto a high-surface-area carbon (HSC) support layer. For catalyst ink formation, a solution of water (37.5 wt.%), methanol (37.5 wt.%), and Nafion (10 wt.%) mixed with the PtCo/HSC powder (15 wt.%) was assumed. As for the membrane, perfluorinated polymers (e.g., Nafion) are widely used. Nafion is obtained by the copolymerization of tetrafluoroethylene (TFE) and perfluoroalkyl sulfonyl fluoride. The GDL employs graphitized carbon fibers in the form of carbon cloth, carbon felt, or carbon paper. For this study, a carbon paper GDL produced from polyacrylonitrile (PAN) is modelled, which is the most common precursor for carbon fiber. A microporous layer (MPL) on the GDL acts as an interface zone between the relatively large feature size of the GDL and the much smaller catalyst particles; it is usually made from carbon or graphite particles with polytetrafluoroethylene (PTFE) binder. The bipolar plates (BPPs) of a PEMFC are made of either high-density graphite or coated stainless steel. For automotive applications, the use of metallic BPPs is common. Gaskets are made of silicone rubber. The endplates are made of a compression-molded composite, which consists of 63% glass fiber and 37% epoxy resin. The current collectors of the system fit within the end plate and are made of a copper foil and two copper studs. For end gaskets, a resin is used for their manufacturing. Due to the lack of the same material in our database, epoxy is used as a proxy. Finally, the model accounts for the stack

compression bands, made of stainless steel, and the stack housing is modelled as a polypropylene composite.

The detailed life cycle inventory of the hydrogen storage tank, PEMFC system, and electric motor is provided in the Appendix A.

5.6.2 Results of Case Study 5

The results for the comparative life cycle environmental assessment between ICEV, BEV, and FCEV are presented in Table 5.23. The analysis covers multiple environmental impact categories, including climate change, acidification, eutrophication, energy resource use, and material resource depletion.

Impact category	Reference unit	ICEV	BEV	FCEV
Acidification	mol H ⁺ eq	0.0012	0.0011	0.0030
Climate change	kg CO ₂ -eq	0.366	0.172	0.135
Energy resources: non-renewable	MJ	4.800	2.54	1.880
Eutrophication: freshwater	kg P eq	0.00005	0.00008	0.00023
Eutrophication: marine	kg N eq	0.00031	0.00018	0.00024
Eutrophication: terrestrial	mol N eq	0.0033	0.0018	0.0029
Material resources: metals/minerals	kg Sb eq	0.000004	0.000009	0.000032

Table 5.23: Environmental impacts of ICEV, BEV, and FCEV (per km driven)

Among the three technologies, the FCEV exhibits the lowest global warming potential (0.135 kg CO₂-eq), followed by the BEV (0.172 kg CO₂-eq), while the ICEV shows the highest impact (0.366 kg CO₂-eq). However, BEV still shows slightly higher emissions than FCEV due to the electricity mix used for battery charging, which is often from fossil-based sources. The results for non-renewable energy consumption show a similar trend. The ICEV consumes the most non-renewable energy (4.80 MJ), largely due to its reliance on fossil fuels during the use phase. In contrast, the BEV and FCEV consume 2.54 MJ and 1.88 MJ, respectively.

The absolute impacts of the other impact categories, such as acidification, eutrophication, and material resource use, are very low. Relatively, acidification potential is the lowest for the ICEV and highest for the FCEV. The higher acidification potential of FCEV is primarily attributed to upstream processes, particularly electricity generation, battery, and PEMFC system manufacturing. Moreover, for eutrophication, the results reveal no single dominant technology across all subcategories. Regarding material resource depletion, FCEV demonstrates higher impacts than both BEV

and ICEV. This reflects the substantial use of several critical raw materials in the manufacturing of the glider, powertrain, and fuel cell systems.

The comparison between the BEV and FCEV is not entirely fair, as the BEV relies on grid-mixed electricity while the hydrogen used in the FCEV is produced from wind power. To ensure a fair comparison between BEVs and FCEVs, an additional analysis is conducted in which both technologies operate using the same electricity source (wind power). Results are presented in Table 5.24.

Impact category	Reference unit	BEV	FCEV
Acidification	mol H ⁺ eq	0.0009	0.0030
Climate change	kg CO ₂ -eq	0.108	0.135
Energy resources: non-renewable	MJ	1.45	1.880
Eutrophication: freshwater	kg P eq	0.00007	0.00023
Eutrophication: marine	kg N eq	0.00015	0.00024
Eutrophication: terrestrial	mol N eq	0.0014	0.0029
Material resources: metals/minerals	kg Sb eq	0.000009	0.000032

Table 5.24: Environmental impacts of BEV and FCEV when powered by wind (per km driven)

The results clearly show that, when both systems rely on renewable electricity, the BEV performs better than the FCEV across all environmental impact categories. In terms of climate change, the BEV generates 0.10886 kg CO₂-eq, noticeably lower than the 0.13558 kg CO₂-eq associated with the FCEV. A similar trend appears for energy resource use, where the BEV requires 1.45 MJ of non-renewable energy compared to 1.88 MJ for the FCEV. Unlike BEV, the FCEV, relies on hydrogen production, compression, and fuel-cell conversion, multiple steps that each introduce energy losses and increase resource consumption. As a result, even when both technologies use clean wind power, the BEV ultimately delivers lower environmental impacts per kilometer driven.

To assess the environmental hotspots in the life cycles of FCEV, a contribution analysis was performed for four key impact categories: acidification, climate change, energy resource depletion, and material resource depletion. Figure 5.10 presents the relative contributions of major FCEV components and life cycle stages. The bar graph highlights that the manufacturing phase of the FCEV is the primary contributor to its environmental impacts, in contrast to the relatively smaller contribution from vehicle operation. Manufacturing processes account for approximately 75% impacts associated with climate change and non-renewable energy use, and exceed 90% in acidification and material resource depletion. In comparison, the operational hydrogen use contributes only 6–24% of the total impacts across these categories.

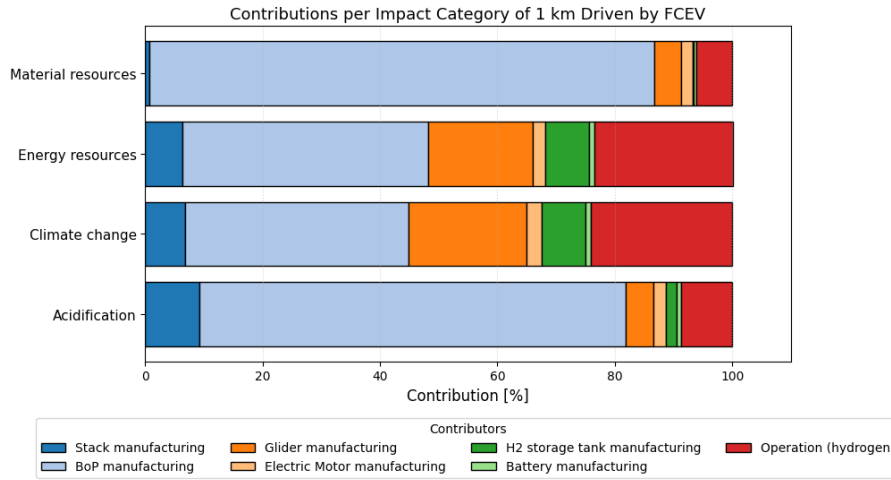


Figure 5.10: Contribution of life cycle stages to environmental impacts of a Fuel Cell Electric Vehicle (FCEV) across four categories (per km)

Among all the manufacturing stages, the Balance of Plant (BoP) in the PEM fuel cell system is realized as the most significant contributor to environmental impacts across all categories. This is mainly due to the high quantity of copper cables and related components used in the system. The BoP alone contributes around 38–41% to the impacts related to climate change and non-renewable energy use, and between 72–86% to acidification and material resource depletion. In comparison, glider manufacturing plays a smaller role in acidification and material use (around 4–5%), but shows a notable share (17–20%) in climate change and energy resource use, primarily due to the energy required for producing the vehicle body and structural materials. The remaining components, including the fuel cell stack, electric motor, battery, and hydrogen storage tank, make relatively minor contributions, together accounting for only 3–17% across all categories.

The contribution of operational hydrogen is relatively low in acidification (around 8%) and material resource depletion (approximately 6%); however, it accounts for a notable share of about 24% in both climate change and non-renewable energy resource use. This indicates that while hydrogen production and use have limited effects on acidifying and resource depletion impacts, they play a more significant role in the overall energy and carbon footprint of FCEVs due to the electricity demand for hydrogen production, even if it is renewable.

Overall, the comparative LCA study concludes that FCEV offers clear environmental advantages over ICEVs and shows comparable or even lower impacts than BEVs in several categories, particularly in climate change and non-renewable energy use. However, unlike BEVs, the manufacturing phase, particularly the balance of plant (BOP) and other material-intensive components, remains a significant challenge for FCEVs due to the use of critical raw materials such as copper and platinum.

5.7 Case Study 6: Comparative LCA of Heavy-duty Vehicle Technologies

5.7.1 Case Study Description

This study presents a comparative life cycle assessment (LCA) of two heavy-duty technologies: the conventional diesel-powered truck and a fuel cell-based hydrogen-powered truck. This study aims to evaluate and compare the environmental performance of emerging low-emission truck technologies and diesel-based conventional trucks to identify the most sustainable solution for long-haul freight operations.

The functional unit is defined as “1 tonne-kilometre (tkm) of freight transported by a heavy-duty truck.” The system boundary follows a cradle-to-gate approach, encompassing all life cycle stages from raw material extraction and component manufacturing to fuel/energy supply and vehicle operation. Similar to previous case studies, the end-of-life stage is excluded from the analysis due to data limitations and variability in recycling processes. Moreover, on-site hydrogen production at HRS is considered, and therefore, the need for hydrogen transportation is eliminated.

For the diesel truck, data are obtained from the Ecoinvent v3.11 database using the process “transport, freight, lorry, >32 metric ton, diesel, EURO 6.” This dataset represents the service of transport in a lorry of the size class >32 metric tons gross vehicle weight (GVW) and Euro VI emissions class. Fuel consumption and emissions are for average European journeys. The transport datasets encompass the complete life cycle of freight transportation, including vehicle construction, operation, maintenance, and the associated road infrastructure. The main characteristics of a diesel-fueled truck are shown in Table 5.25.

Parameter	Unit	FCEV
Gross weight	ton	40
Payload capacity	ton	>32
Diesel	kg/tkm	0.0192
Lifetime	km	540000

Table 5.25: Main characteristics of a Euro 6 truck

The fuel cell electric truck (FCET) modelled in this study includes a compressed hydrogen tank system, battery, electric motors, fuel cell system, and glider (the vehicle without a powertrain). For the operation of the FCEV, hydrogen produced on-site (through PEMWE) at the HRS is compressed and dispensed at 350 bar for use as fuel. The Life Cycle Inventory (LCI) data is sourced from multiple literature sources, particularly from [110, 111, 113]. The main technical characteristics of the FCET considered in this study are provided in Table 5.26.

Parameter	Unit	FCET
H2 consumption	kg/km	0.08
Gross weight	ton	40
Payload	ton	25
Glider	kg	5,296
Vehicle lifetime	km	1,000,000
Electric motors	pieces	2
Electric motor power (each)	kW	230
Storage tanks	pieces	5
Storage pressure	bar	350
Hydrogen stored	kg	80
Li-ion battery	kWh	93.2
PEMFC system	kW	300

Table 5.26: Main technical characteristics of the FCET

The fuel cell truck is assumed to have a technical lifetime of 10 years, corresponding to a total of 20,000 operating hours. A lithium–nickel–manganese–cobalt (NMC) battery with a capacity of 93.2 kWh and a mass of 760 kg is used in the FCET. The hydrogen tank system consists of five compressed hydrogen cylindrical Type IV tanks and a supporting structure. The tank system has a total weight of 1.04 t. The lifetime of the tank system is 15 years, which exceeds the lifetime of the fuel cell truck by 5 years. Moreover, the two electric motors, each capable of 230 kW continuous output, are modelled. The fuel cell truck also has a fuel cell system, operating with a proton exchange membrane fuel cell (PEMFC). The fuel cell system consists of two fuel cell modules, each with a rated power of 150 kW.

One of the key challenges in performing an LCA for fuel cell-powered heavy-duty trucks is the limited availability of reliable and detailed inventory data. In particular, data for PEM fuel cell systems specifically designed for heavy-duty applications are scarce. Therefore, in this study, the inventory of the PEMFC system used for passenger vehicles (from the previous case study) is adopted as a reference and scaled up linearly from 80 kW to 150 kW to represent the higher power demand of a heavy-duty truck configuration. The same approximation has been made for the electric motor as well.

5.7.2 Results of Case Study 6

The comparative life cycle environmental impacts of the diesel and fuel cell (FC) heavy-duty trucks are summarized in Table 5.27. The analysis evaluates several impact

categories, including climate change, acidification, eutrophication, non-renewable energy resource use, and material resource depletion.

Impact category	Reference unit	Diesel truck	FC truck
Acidification	mol H ⁺ eq	0.0003	0.0002
Climate change	kg CO ₂ -eq	0.102	0.016
Energy resources: non-renewable	MJ	1.544	0.210
Eutrophication: freshwater	kg P eq	0.000007	0.000016
Eutrophication: marine	kg N eq	0.00007	0.00002
Eutrophication: terrestrial	mol N eq	0.00070	0.00023
Material resources: metals/minerals	kg Sb eq	0.0000003	0.000002

Table 5.27: Environmental impacts of diesel and fuel cell heavy-duty trucks (per tonne-kilometer)

The results clearly indicate that the fuel cell truck results significantly better than a diesel truck in most environmental impact categories. In particular, the climate change impact of the FCET is reduced by nearly 85%, decreasing from 0.102 kg CO₂-eq for the diesel truck to 0.016 kg CO₂-eq per tonne-kilometer. This substantial drop is mainly attributed to the use of green hydrogen and the absence of fossil fuel combustion during operation. Similarly, the non-renewable energy consumption follows the same trend with an 85% reduction, reflecting the shift from fossil-based energy use toward renewable electricity for hydrogen production.

The other impact categories (acidification, eutrophication, and material resource use) show very low impacts in absolute terms. The acidification potential is relatively slightly lower for the FCET as compared to the diesel truck, primarily due to the elimination of sulfur and nitrogen oxide emissions from diesel combustion. The freshwater eutrophication potential of the fuel cell truck is approximately twice that of the diesel truck. This increase is largely dependent on upstream activities in hydrogen production and the manufacturing of key components such as the PEM fuel cell stack and battery system, which involve material and energy-intensive processes. The material resource depletion of the FCET (2E-6 kg Sb-eq) is also higher than that of the diesel truck (3E-7 kg Sb-eq), reflecting the greater use of critical materials such as copper, platinum, nickel, etc., in the fuel cell and upstream hydrogen production systems.

To better understand the key environmental hotspots in the life cycle of the fuel cell truck, a contribution analysis was conducted for different key impact categories. Figure 5.11 presents the relative contributions of various vehicle components and life cycle stages to these impact categories. The bar graph clearly shows that the operation phase, which includes hydrogen production and use, accounts for the majority of the

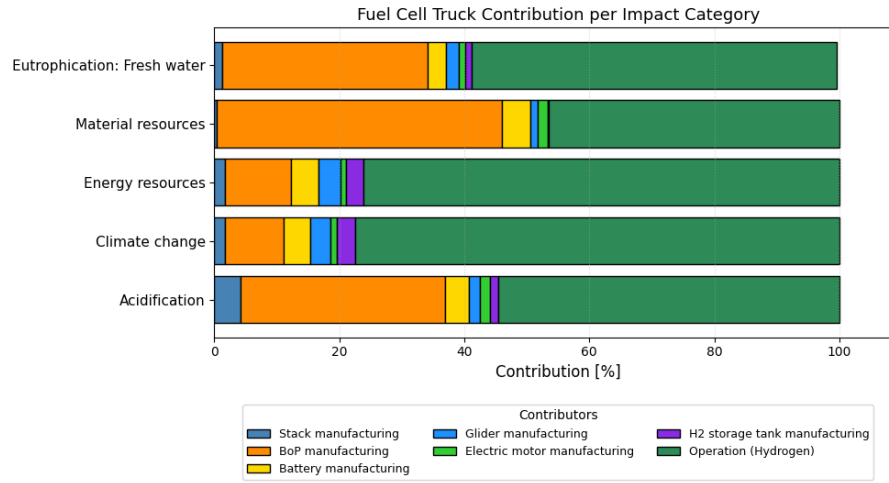


Figure 5.11: Contribution of life cycle stages to environmental impacts of a Fuel Cell Truck (per tonne-kilometer)

overall environmental impacts of the FCT. It contributes approximately 75–77% to climate change and energy resource depletion, and around 55–58% to acidification and freshwater eutrophication. This highlights the significant influence of the hydrogen production process, even when renewable electricity sources are considered, due to its high energy demand.

Among the manufacturing stages, the Balance of Plant (BoP) within the PEM fuel cell system is identified as a major hotspot. It contributes notably across all categories, at around 33% in acidification, 9–11% in climate change and energy resource use, and nearly 46% in material resource depletion, primarily due to the extensive use of copper and other metallic components. Other components, such as the battery, glider, stack, electric motor, and hydrogen storage tank, show comparatively minor contributions, each accounting for less than 5% in most categories.

5.8 Case Study 7: Comparative LCA of Steel Production Routes

5.8.1 Case Study Description

This case study compares the environmental performance of two distinct steel production routes: the conventional Blast Furnace/Basic Oxygen Furnace (BF/BOF) route and the emerging Hydrogen-based Direct Reduced Iron/Electric Arc Furnace (H_2 -DRI/EAF) route. This study aims to analyze the potential environmental benefits of replacing fossil-based reducing agents (coal and coke) with hydrogen in the steelmaking process.

The key differentiator between hydrogen-based solutions lies in how hydrogen is produced. Either through electrolysis powered by renewable electricity (green hydrogen) or via steam methane reforming of natural gas (grey hydrogen). To assess the broader environmental implications, both hydrogen production scenarios are considered and compared with the conventional steelmaking process.

The cradle-to-gate system boundary encompasses upstream processes, including raw material extraction, transportation to the site, and their transformation to feedstock ready for ironmaking (BF or DRI) and subsequent steelmaking (BOF or EAF). It also encompasses downstream processes, including casting, reheating, and hot rolling. The main product selected is Hot Rolled Coil (HRC), and the functional unit for this analysis is defined as “1 tonne of Hot Rolled Coil produced”.

The detailed process description for both steelmaking routes is provided in Chapter 2. It is assumed that the steel mill is located in Italy. Foreground LCI data were collected from various literature sources, particularly from [70, 114], while background data were sourced from Ecoinvent v3.11. The complete LCI datasets for both ironmaking and steelmaking stages are provided in the Appendix A.

The summary of energy and resource demands for the ironmaking and steelmaking processes is given in Table 5.28.

Parameter	BF	BOF	H ₂ -DRI	Electric Arc Furnace
Iron ore demand	487 kg iron ore, 1110 kg sinter	5.50 kg iron ore, 974 kg pig iron	1502.28 kg as iron pellets	64.80 kg iron scrap, 1090.8 kg sponge iron
Fossil fuel demand	367 kg coke, 164 kg hard coal	None	44.06 m ³ natural gas	2.94 m ³ natural gas, 10.15 kg hard coal
Flux demand	13.3 kg limestone	11 kg dolomite, 70 kg lime	None	27 kg quicklime
Oxygen demand	68 kg	79 kg	None	14.58 kg
Water demand	0.87 m ³	0.42 m ³	683.42 m ³	1.06 m ³
Electricity demand	102.90 kWh	21.60 kWh	3780 kWh	818.64 kWh

Table 5.28: Summary of input parameters for steelmaking processes (per tonne of HRC) [70]

5.8.2 Results of Case Study 7

Table 5.29 presents the life cycle environmental impacts for conventional BF/BOF steelmaking and hydrogen-based DRI/EAF routes using both green (electricity from renewables) and grey (SMR) hydrogen. The results indicate that both hydrogen-based steelmaking routes significantly reduce the environmental impacts compared to the conventional BF/BOF process.

In the climate change category, the BF/BOF route exhibits the highest emissions, amounting to 2,282.93 kg CO_2 -eq per tonne of hot-rolled coil (approximately 2.28 kg CO_2 -eq per kg of hot-rolled coil). Green H_2 -DRI routes result in the lowest emissions (984.83 kg CO_2 -eq per tonne of HRC), whereas the grey H_2 -DRI route achieves intermediate results of around 1397.57 kg CO_2 per tonne of HRC. For energy resource use, a similar trend is observed, with the BF/BOF process consuming the most non-renewable energy (20,800 MJ) and green H_2 -DRI consuming the least (12,880 MJ). The grey-DRI consumes as much non-renewable energy as the conventional route due to the energy intensity of hydrogen production from natural gas.

Impact category	Reference unit	BF/BOF	Green H_2 -DRI	Grey H_2 -DRI
Acidification	mol H^+ eq	4.990	4.646	2.940
Climate change	kg CO_2 -eq	2282.93	984.83	1397.57
Energy resources: non-renewable	MJ	20800	12880	20500
Eutrophication: freshwater	kg P eq	0.960	0.250	0.143
Eutrophication: marine	kg N eq	1.649	0.782	0.703
Eutrophication: terrestrial	mol N eq	17.280	8.356	7.463
Material resources: metals/minerals	kg Sb eq	0.0006	0.0134	0.0021

Table 5.29: Environmental impacts of three steelmaking processes (per tonne of HRC)

In other categories, such as acidification and eutrophication, hydrogen-based routes generally show lower impacts. The acidification impact of the green hydrogen-based route is higher than that of the grey hydrogen-based route, primarily due to the upstream processes associated with hydrogen production, such as renewable electricity generation and electrolyzer manufacturing. Eutrophication potentials (freshwater, marine, terrestrial) are also lower for both H_2 -DRI routes, reflecting reduced emissions of nitrogen and phosphorus compounds during steel-making and upstream processes.

Interestingly, material resource use is higher for green H_2 -DRI (0.0134 kg Sb eq) compared to both BF/BOF and grey H_2 -DRI processes. This is due to the additional infrastructure and materials required for electrolysis units and renewable energy supply.

To illustrate relative environmental performance, figure 5.12 presents the life cycle environmental impacts of green and grey H_2 -DRI/EAF steelmaking processes normalized against the conventional BF/BOF route, which is set as a baseline at 100%.

The graph shows that green H_2 -DRI results in the largest reductions, with GHG emissions and energy consumption dropping by more than 50% as compared to BF/BOF, reflecting the use of renewable hydrogen and electricity. The grey H_2 -DRI route also reduces impacts compared to BF/BOF, but to a lesser extent, due to CO_2 emissions associated with hydrogen production via steam methane reforming. The acidification and eutrophication show moderate reduction for both hydrogen-based routes.

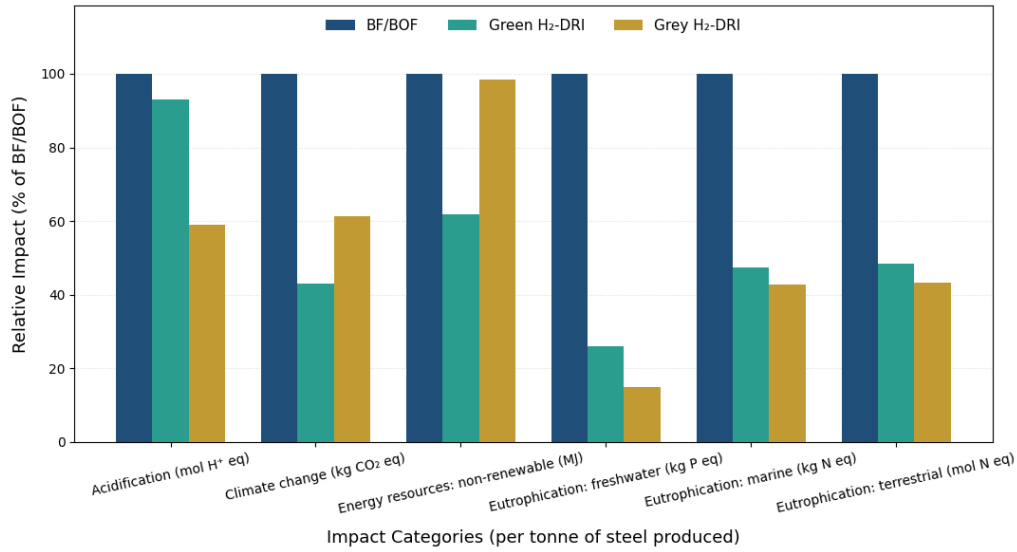


Figure 5.12: Comparative environmental impacts of BF/BOF and hydrogen-based DRI/EAF steelmaking routes (BF/BOF = 100%)

To further understand the key contributing processes behind the overall impacts, a contribution analysis was carried out for three major impact categories: acidification, climate change, and non-renewable energy resource use (Figure 5.13 and 5.14).

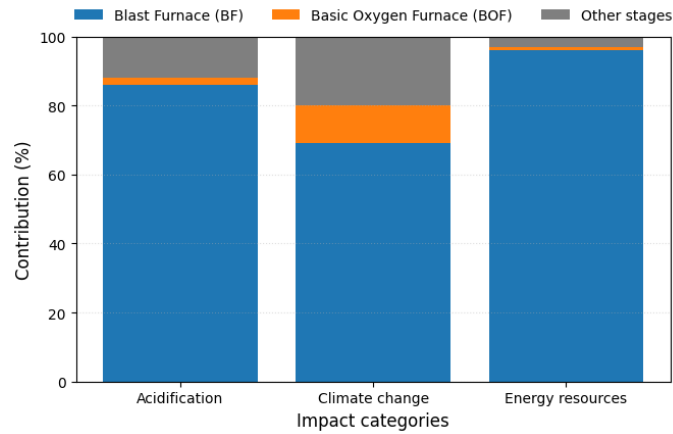


Figure 5.13: Contribution analysis of major life cycle processes in BF/BOF steelmaking process across the impact categories of acidification, climate change, and non-renewable energy resource use

The contribution analysis clearly highlights the differences in process dominance between the conventional and the hydrogen-based steelmaking routes. In the BF/BOF process, the blast furnace stage significantly dominates all impact categories, contributing around 70-95%. This dominance is due to heavy reliance on hard coal,

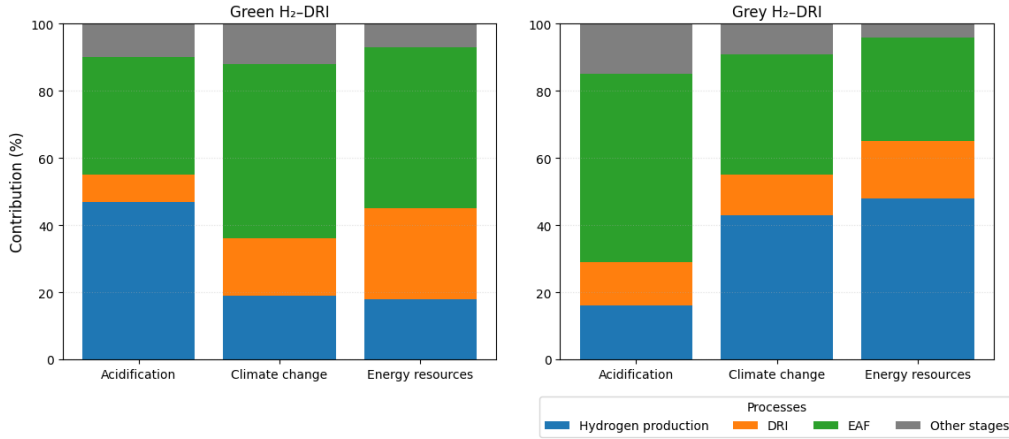


Figure 5.14: Contribution analysis of major life cycle processes green H₂-DRI/EAF, and grey H₂-DRI/EAF steelmaking processes across the impact categories of acidification, climate change, and non-renewable energy resource use

sintering, and coke combustion for Iron reduction, which results in substantial CO_2 , SO_2 , and NO_x emissions along with high fossil energy consumption. The basic oxygen furnace and other downstream processes contribute only marginally in comparison.

On the other hand, the environmental burdens are more distributed among several stages for hydrogen-based DRI routes. In the green H_2 -DRI route, hydrogen production via electrolysis contributes the most to acidification (47%), but its contribution is less to climate change and energy resource use (18-19%). This reduction is primarily due to the use of renewable electricity for hydrogen production, which significantly decreases CO_2 emissions and the fossil energy demand. The SMR-based H_2 -DRI route highlights that hydrogen production through steam methane reforming is the largest contributor to both climate change and non-renewable energy consumption because of its direct CO_2 emissions and dependence on natural gas. The EAF stage also remains a consistent contributor in all hydrogen-based routes due to its high-power requirement for melting and refining.

Overall, the results indicate that hydrogen-based steel production significantly reduces environmental impacts compared to the conventional BF/BOF route, particularly in climate change and energy resource impact categories. The green hydrogen DRI-EAF route performs best due to the use of renewable electricity for hydrogen production. Moreover, the grey hydrogen route still outperforms BF/BOF, but with higher emissions from natural gas reforming.

5.9 Case Study 8: Comparative LCA of Ammonia Production Routes

5.9.1 Case Study Description

This case study evaluates and compares the environmental impacts of conventional natural gas-based (grey) ammonia production and renewable hydrogen-based (green) ammonia production. The primary objective of this analysis is to assess the impact on overall life cycle impact categories when transitioning from fossil-based hydrogen to green hydrogen for ammonia synthesis.

The system boundary covers all stages from raw material extraction to ammonia production (cradle-to-gate). The downstream process related to ammonia usage is not included. For grey ammonia, hydrogen is produced via the steam methane reforming process using natural gas as both feedstock and energy source, followed by the Haber-Bosch synthesis process. On the other hand, green hydrogen is produced via PEM water electrolysis powered by renewable electricity (wind), followed by hydrogen storage. In both methods, nitrogen is commonly obtained from air using a cryogenic distillation process in an air separation unit (ASU) and introduced in the Haber-Bosch reactor, where it reacts with hydrogen in the presence of an iron-based catalyst.

The functional unit is defined as “1 kg of ammonia (NH_3) produced”. Foreground lifecycle inventory data are sourced from literature, particularly from [115, 68], while the background processes are modeled using the Ecoinvent v3.11 database. The complete LCI datasets for both methods are provided in the Appendix A.

The parameters and specifications of hydrogen production (via electrolysis) and storage are the same as those considered in the previous case studies. While the process for producing ammonia using hydrogen produced through the SMR process is taken from the Ecoinvent v3.11 database for comparison. The design parameters of the green ammonia production facility are provided in Table 5.30.

Table 5.30: Design parameters of the green ammonia production plant [68]

Process	Parameter	Value	Unit
Air separation unit	Design power demand	6.8	MW
	Specific energy consumption	0.243	kWh/(kg · N ₂)
	Capacity factor	0.82	–
	Energy consumption per year	60	GWh/a
	Annual production	242000	(t · N ₂)/a
	Capacity	294000	(t · N ₂)/a
Ammonia plant	Design power demand	15.57	MW
	Specific energy consumption	0.44	kWh/(kg · NH ₃)
	Annual production	280000	(t · NH ₃)/a
	Annual capacity factor	0.95	–
	Energy consumption per year	123.3	GWh/a

5.9.2 Results of Case Study 8

The results for the key important categories are presented in Table 5.31.

The comparison between grey and green ammonia production reveals a significant reduction in greenhouse gas emissions and fossil energy consumption when renewable hydrogen is used. The climate change impact decreases from 2.62 kg CO₂ eq in the grey ammonia production route to 0.83 kg CO₂ eq in the green route, primarily because the green pathway eliminates CO₂ emissions from steam methane reforming. Similarly, non-renewable energy consumption drops from 40 MJ to 12.39 MJ, reflecting the shift from natural gas to renewable electricity for hydrogen production.

Table 5.31: Environmental impacts of two ammonia production processes (per kg of NH₃ produced)

Impact category	Reference unit	Grey ammonia	Green ammonia
Acidification	mol H ⁺ eq	0.0037	0.0072
Climate change	kg CO ₂ -eq	2.622	0.828
Energy resources: non-renewable	MJ	40.050	12.387
Eutrophication: fresh- water	kg P eq	0.0002	0.0007
Eutrophication: ma- rine	kg N eq	0.0009	0.0009
Eutrophication: ter- restrial	mol N eq	0.0099	0.0099
Material resources: metals/minerals	kg Sb eq	0.00001	0.00005

The other impacts, such as acidification, eutrophication, and material resource use, remain relatively low overall; however, the green ammonia route shows slightly higher values mainly due to the upstream processes related to renewable electricity generation and electrolyzer manufacturing.

To better visualize the differences between the two ammonia production routes, a relative comparison was performed with grey ammonia set as a benchmark (100%). The environmental impacts of green ammonia are expressed relative to the grey route (Figure 5.15).

The graph highlights that green ammonia achieves a significant reduction in climate change and non-renewable energy use, with a 70% reduction in each, reflecting the shift from fossil-based hydrogen to renewable hydrogen. Moreover, eutrophication (marine and terrestrial) values are almost identical for both processes. Conversely, acidification, eutrophication (freshwater), and material resources are higher for the green route, ranging from 1.5 to 5 times the grey ammonia values. This increase, as explained earlier, is primarily driven by the electricity-intensive electrolysis process and the additional material demands for electrolyzer manufacturing.

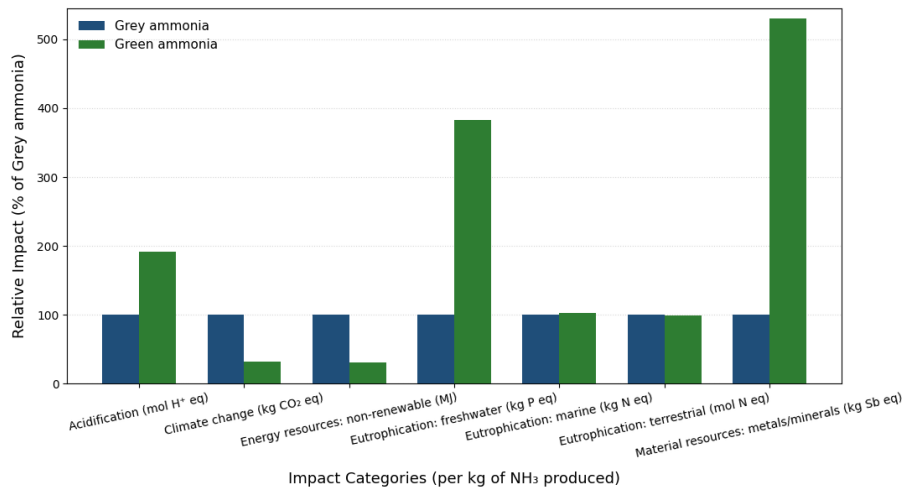


Figure 5.15: Environmental impacts of green ammonia relative to grey ammonia

To identify the main sources of greenhouse gas emissions within each ammonia production route, a contribution analysis was performed for the climate change impact category. Figure 5.16 illustrates the relative contributions of key processes to the total CO₂-equivalent emissions for grey ammonia and green ammonia.

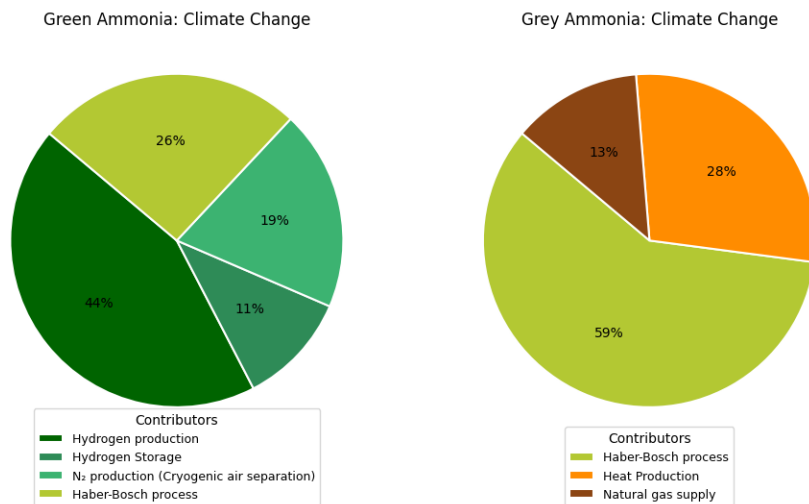


Figure 5.16: Contribution of different processes to climate change. Green ammonia (left), Grey ammonia (right)

For green ammonia, the largest contributor to climate change is hydrogen production and storage, accounting for approximately 65% combined. This contribution is mainly due to the electricity demand for electrolysis, compression, and storage. Nitrogen production via cryogenic air separation contributes about 19.5%, while the Haber–Bosch synthesis process accounts for 25.9% of total emissions. This indicates

that although the green ammonia substantially reduces CO_2 emissions, hydrogen production remains the main emissions hotspot within the system.

In contrast, the Haber-Bosch process in grey ammonia production contributes to approximately 60% of the total emissions. Heat production contributes 28.4% primarily due to the use of natural gas as a fuel, while the upstream natural gas production process accounts for 12.6%. This indicates the strong dependence of grey ammonia on fossil fuels, with most climate impacts arising from the use of natural gas both as a feedstock and an energy source.

To conclude, producing ammonia using green hydrogen offers a clear reduction in GHG emissions and also reduces reliance on fossil fuels compared to the conventional grey route. While some impact categories, such as acidification, freshwater eutrophication, and material use, are slightly higher in the green route, this is mainly due to the energy required for electrolysis and the production of electrolyzer components. The contribution analysis indicates that hydrogen production is the main source of emissions in the green pathway; however, the grey route is dominated by the Haber-Bosch process and natural gas use. These findings highlight the environmental benefits of switching to renewable hydrogen for ammonia production, while also indicating areas where efficiency improvements and material optimization could further reduce impacts.

Chapter 6

Discussion

This chapter provides a detailed discussion and interpretation of results from the eight LCA case studies analyzed in Chapter 5, which encompass hydrogen production, distribution, and utilization in both mobility and industrial applications.

The first section of the chapter summarizes the most important insights and trends observed in all case studies. The second section highlights the processes and stages that contribute the most to environmental impacts, helping to figure out areas for improvement. The third section reflects on the assumptions, data gaps, and methodological constraints encountered, providing context for interpreting the results.

6.1 Main Outcomes and Interpretation

Figures 6.1 and 6.2 present a summary of main findings from case studies.

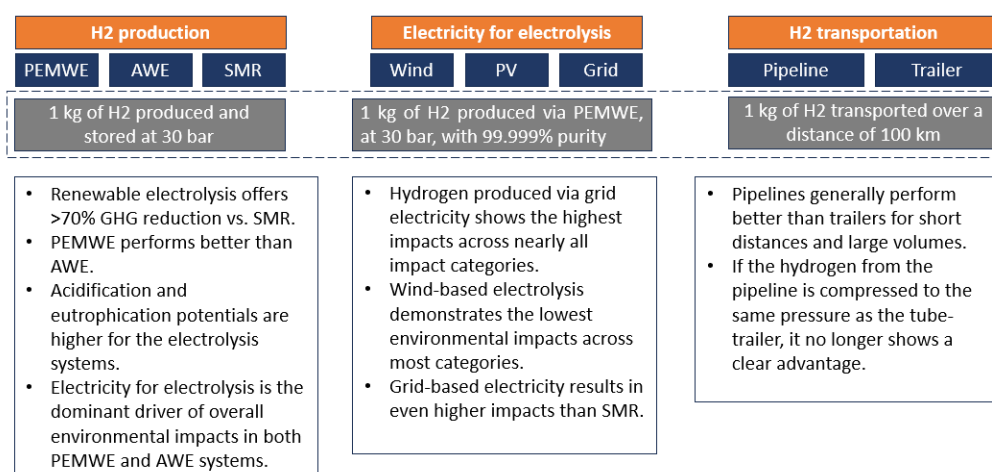


Figure 6.1: Summary of main findings across hydrogen supply chain

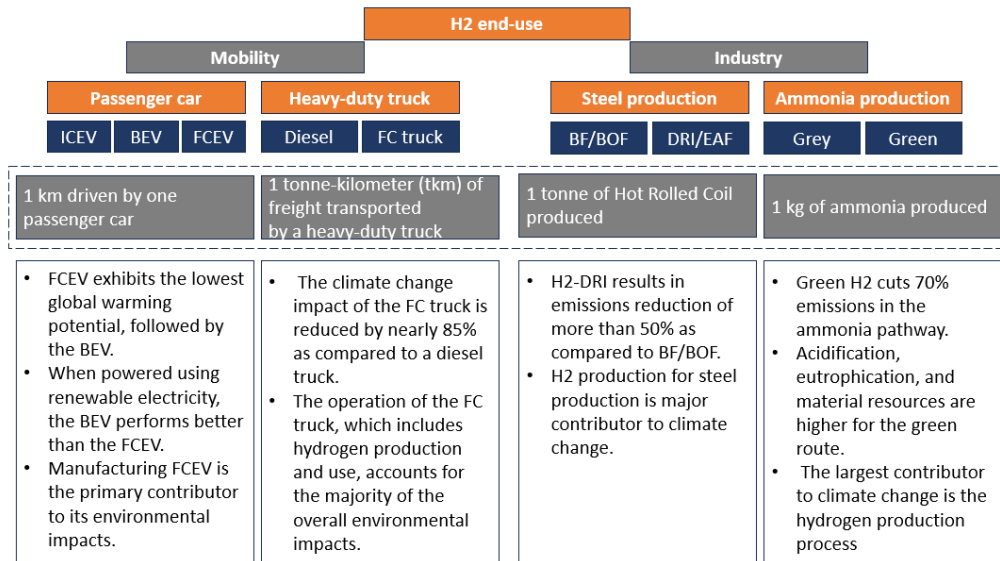


Figure 6.2: Summary of main findings across hydrogen end-use applications

The overall analysis of the case studies reveals several important findings about the environmental performance of hydrogen-related technologies. Across the studies, it is evident that the source of electricity used for the hydrogen production dominates in assessing the greenhouse gas emissions and non-renewable energy resource use. Hydrogen produced via renewable-powered electrolysis consistently results in lower climate change impacts compared to fossil-based routes.

For example, the first two case studies indicate that PEM electrolysis powered by wind or solar energy reduces CO_2 emissions significantly as compared to fossil resource-based hydrogen production routes such as steam methane reforming. The climate change impact of SMR is 11.35 kg CO_2 -eq/kg H_2 , which is significantly higher than both electrolytic pathways. PEMWE and AWE, with impacts of 2.38 kg CO_2 -eq/kg H_2 and 3.433 kg CO_2 -eq/kg H_2 , achieve reductions of nearly 80% and 70%, respectively. The results all reveal that the water electrolysis process for hydrogen production can achieve near-zero carbon emissions when powered by renewable electricity; however, if fossil-based electricity is used, the resulting emissions can exceed those of the conventional SMR process. In these scenarios, manufacturing stages contribute less to overall life cycle impacts, even though platinum used as a catalyst in the PEM electrolyzers stands out as a comparatively significant contributor. These studies also show that the manufacturing of PV modules is more energy- and material-intensive compared to wind turbines, which explains why PV-powered electrolysis results in relatively higher environmental impacts. Moreover, among two mature electrolysis technologies, alkaline water electrolysis outperforms PEM water electrolysis, primarily due to its high energy efficiency. When comparing only the manufacturing stages of both, alkaline indicates low emissions as compared

to PEM because alkaline systems use cheaper and more abundant materials (nickel, stainless steel), unlike PEM, which relies on high-impact and precious materials such as platinum and titanium.

Among two transportation modes, i.e., pipeline and tube-trailers, pipelines generally perform better than trailers for short distances and large volumes, as they require less energy per kilogram of hydrogen transported. Hydrogen is delivered through pipelines at roughly 70 bar, requiring an initial compression from 30 bar to 70 bar, which consumes about 0.4 kWh per kilogram of H_2 , while when transported by tube-trailer, hydrogen is compressed to around 500 bar, and the compression from 30 bar to this pressure requires approximately 2.1 kWh per kilogram of H_2 . Moreover, trailer transport is more energy-intensive since it requires high-pressure storage. However, if hydrogen is compressed from a pipeline to the same pressure as a tube-trailer, it no longer shows a clear advantage. The on-site hydrogen production at the usage site eliminates these transport-related emissions, resulting in lower environmental impacts. Also, repurposing already existing natural gas pipelines for hydrogen usage could reduce the overall environmental impacts. Electricity consumption during hydrogen operation emerges as a dominant contributor to GHG emissions, overshadowing the impacts from the manufacturing of transport infrastructure. The construction of both pipelines and trailers contributes relatively little to the overall life cycle impacts. Steel production imposes the main manufacturing burden for pipelines; however, for tube trailers, most of the environmental impact arises from producing high-pressure CFRP-based hydrogen storage tanks.

Based on findings from case studies, it is apparent that when hydrogen is produced using renewable electricity, it can play an important role in decarbonizing various sectors. In mobility sector, for example, FCEVs and hydrogen-powered heavy-duty trucks demonstrate lower global warming potential and reduced non-renewable energy consumption compared to conventional ICEVs and diesel trucks. However, unlike the operational hydrogen production stage, the manufacturing phases of these vehicles impose a major portion of the total environmental impact. In FCEV passenger cars, the production of major parts like the fuel cell, battery pack, hydrogen storage tank, etc., contributes more substantially to the overall environmental footprint than the hydrogen used during vehicle operation. Similarly, the LCA results indicate that in the industrial sector, processes such as steel and ammonia production can achieve substantial environmental benefits if green hydrogen is used instead of conventional fossil-based methods, with greenhouse gas emissions reduced by more than 50%.

Other life cycle impact categories, like acidification, eutrophication, and material resource use, show relatively minor contributions as compared to climate change and non-renewable energy resource use across hydrogen value chain. However, hydrogen-based pathways tend to exhibit slightly higher impacts in acidification and material resource use than conventional fossil-based alternatives, largely because producing electrolyzers and renewable energy systems requires substantial materials and energy.

From a system perspective, the case studies illustrate how the “pieces” of the

hydrogen value chain (production, storage, distribution, and end-use) can be integrated to assess the environmental performance of a complete Hydrogen Valley. For instance, by combining the results of on-site against off-site production, different transport modes, and multiple end-use applications, it becomes possible to map the cumulative impacts of a scaled Hydrogen Valley scenario.

6.2 Environmental Hotspots in Hydrogen Value Chain

The analysis across all case studies highlights several recurring environmental hotspots within the hydrogen value chain. The most dominant contributor to GHG emissions and non-renewable energy use is the electricity for hydrogen production, regardless of whether the hydrogen is used for industrial processes or for fueling vehicles. Even when powered by renewable sources, the substantial energy demand for electrolysis, compression, and storage continues to make this stage the main contributor to overall climate impacts.

Transportation of hydrogen also emerges as a secondary hotspot in off-site production scenarios. Pipeline transport requires recompression stations and energy-intensive operation, while truck transport requires high compression for on-board hydrogen storage, along with fuel consumption.

Another key area of focus is hydrogen storage and compression, particularly in on-site refueling systems and fuel cell vehicles. The electricity consumption for hydrogen compression makes a major contribution to overall environmental impacts. The use of high-pressure storage tanks, particularly Type IV cylinders, requires large amounts of carbon fiber and composite materials, resulting in notable material resource depletion and energy consumption during their manufacture. Similarly, components within the fuel cell balance of the plant, such as copper wiring, pumps, and electronic controls, add considerably to acidification and resource-related impacts.

Lastly, production of advanced components, like electrolyzers, fuel cells, and batteries, appears repeatedly as a key area of focus. The use of platinum and titanium in PEM electrolyzers and steel and nickel in alkaline electrolyzers is mostly responsible for GHG emissions during stack manufacturing. These technologies contribute to environmental impacts across categories like acidification, eutrophication, and material resource consumption. This highlights the importance of improving material efficiency, enhancing recyclability, and optimizing production technologies to lower the environmental impacts associated with an expanding hydrogen economy.

Chapter 7

Conclusions and Directions for Future Research

7.1 Concluding remarks

This research has expanded understanding of the environmental impacts associated with a range of hydrogen technologies and applications, encompassing the full hydrogen value chain from production and transportation to end-use in transport and industrial sectors. Eight case studies were analyzed to assess the environmental significance of various technological configurations.

In hydrogen production, water electrolysis using renewable electricity, particularly wind power, was identified as the most sustainable pathway compared to conventional steam methane reforming (SMR). However, the study also showed that the environmental impacts of electrolysis are strongly influenced by the source of electricity used. When powered by fossil-based grids, electrolysis can even exceed SMR in CO_2 emissions. Among the two mature electrolysis technologies, Alkaline water electrolysis (AWE) shows slightly higher impacts than PEM electrolysis.

In hydrogen transportation, the study revealed that pipelines generally perform better than tube trailers in terms of overall environmental impact. The pipeline system benefits from lower operational energy demand per kilogram of hydrogen delivered, whereas tube trailers require high compression pressures. Nevertheless, both options highlighted that electricity use during operation remains the dominant contributor to climate change impacts.

The mobility sector analysis revealed that FCEVs and hydrogen-fueled heavy-duty trucks can substantially lower emissions when compared with conventional diesel or other internal combustion engine vehicles, particularly when green hydrogen is utilized. However, for these technologies, the manufacturing stages of the fuel cell system, battery, and high-pressure hydrogen storage components remain major contributors to overall environmental burdens.

In industrial applications, the shift to hydrogen-based processes demonstrated

substantial environmental benefits. Hydrogen-based direct reduced iron (H_2 -DRI) route in steelmaking achieved over a 50% reduction in CO_2 emissions compared to the conventional blast furnace/basic oxygen furnace (BF/BOF) route, particularly when powered by green hydrogen. Similarly, shifting from grey to green hydrogen in ammonia production greatly reduced greenhouse gas emissions and the reliance on fossil energy. These findings confirm hydrogen's transformative potential in decarbonizing industrial sectors such as steelmaking and fertilizer production, provided that hydrogen is produced sustainably.

Across all case studies, electricity consumption consistently emerged as the most influential factor affecting environmental performance overall. While renewable electricity can drastically reduce impacts, its generation and infrastructure still induce non-negligible burdens, particularly in material resource use and water demand. Moreover, the production of photovoltaic panels was found to be more energy- and material-intensive as compared to wind turbines, leading to slightly higher emissions.

Overall, the study confirms that hydrogen can play a crucial role in the energy transition; however, its environmental performance strongly depends on the energy source, technological configuration, and material intensity of its production and utilization stages. Continued innovation in electrolyzer efficiency, materials recycling, and renewable power integration is essential for realizing hydrogen's full sustainability potential.

7.2 Insights and Recommendations

In view of the findings of this research, a few recommendations can be proposed to encourage the sustainable deployment of hydrogen technologies.

- The results clearly highlight the importance of using low-carbon electricity for hydrogen production, since the electricity source remains a major contributor to environmental impacts, especially for electrolysis. Policymakers should therefore prioritize the expansion of renewable energy capacity and ensure that electrolyzers are operated with low-carbon or renewable electricity wherever possible.
- Policy frameworks that encourage recycling and material recovery, especially for critical materials such as platinum, iridium, nickel, lithium, and carbon fibers, can help reduce the upstream burden associated with component manufacturing.
- Establishing clear guidelines for hydrogen transport, compression, and storage with particular attention to minimizing losses and improving efficiency would further strengthen the environmental performance of future hydrogen systems.
- From an industrial perspective, companies developing hydrogen infrastructure should place greater emphasis on optimizing each step of the hydrogen value

chain. The findings show that electrolyzer technology choice, type of storage, efficiency of compressors, and the selected transport mode all influence environmental outcomes.

- Beyond evaluating economic viability, future hydrogen initiatives should incorporate environmental, economic, and social considerations in a coordinated manner.

7.3 Research Limitations

Although this study offers a detailed and comprehensive life cycle assessment of various hydrogen technologies and industrial processes, few limitations must be taken into account.

- All case studies use a cradle-to-gate system boundary, meaning that end-of-life processing and component recycling are not considered in the assessment. Consequently, potential environmental benefits of recovering and reusing energy-intensive and valuable materials such as carbon fiber from high-pressure storage tanks, platinum and iridium from electrolyzers and fuel cells, or lithium and nickel from batteries are not considered. This could underestimate the long-term sustainability potential of hydrogen technologies, especially as advancements in material recycling and circular economy strategies continue to evolve. The same applies to BEVs; leaving out battery recycling overlooks the significant reductions in raw material extraction and manufacturing impacts that could be achieved when critical minerals are recovered and reused.
- Data availability and quality constraints pose constraints. Since there are not many LCA studies already performed on hydrogen integration in emerging technologies such as heavy-duty fuel cell trucks and hydrogen-based steel production, certain assumptions and scaling approaches are introduced, which may affect the precision of results. For example, in heavy-duty trucks, the PEM fuel cell stack and hydrogen storage tank are linearly scaled up from a passenger vehicle to meet higher power and range requirements. Moreover, this study focused exclusively on compressed hydrogen for storage and transport, as it is currently the most widely used form.
- Some technological processes, such as PEM fuel cell manufacturing or electrolysis systems, rely on proxies and literature-based datasets that may not fully reflect future industrial-scale operations. For instance, because of limited data availability for iridium, platinum was used as a proxy material in the assessment.
- The scope of this work is restricted to examining the environmental impacts of hydrogen technologies, without considering the economic or social dimensions. As the study concentrated exclusively on environmental performance throughout

the hydrogen value chain, aspects like cost competitiveness, market feasibility, and social acceptance were not evaluated. Economic factors like investment costs, operational expenses, energy prices, and market competitiveness play a crucial role in determining whether hydrogen systems can be realistically deployed at scale. Even if a technology performs well environmentally, high costs or uncertain financial viability can delay or limit adoption. Social aspects are equally important, as public acceptance of hydrogen infrastructure, safety perceptions, community impacts, job creation, and workforce requirements all influence whether the technology can be integrated smoothly into society.

Despite these limitations, the study provides valuable comparative insights and identifies key environmental hotspots that can guide policymakers, industry stakeholders, and researchers in advancing sustainable hydrogen and low-carbon technologies.

7.4 Future Works

Although this study provides important insights into the environmental aspects of hydrogen technologies, there are still several areas that remain open for future research, especially to overcome the limitations and gaps identified in this work.

- The current LCA analysis was carried out using a cradle-to-gate boundary, emphasizing production and use phases but not considering disposal or recycling stages. Integrating end-of-life management and material recovery in future assessments would better capture the circular potential of advanced materials such as carbon fibers, platinum, iridium, etc. This is especially relevant as recycling of platinum-group metals and composite materials could substantially lower environmental burdens.
- Future studies could expand the scope by including additional hydrogen technologies and pathways for comparison. For example, Solid Oxide Fuel Cells (SOFCs) could also be assessed in hydrogen production. Similarly, liquefied hydrogen and hydrogen carriers like ammonia and methanol could be assessed alongside compressed hydrogen. Moreover, hydrogen transport via ships and its application in the power sector for energy storage and grid balancing options should also be explored.
- Future studies should incorporate techno-economic and social assessments alongside environmental LCA to offer a broader perspective on the sustainability of hydrogen. Economic feasibility, infrastructure costs, job creation potential, and social acceptance are all crucial in assessing the scalability of hydrogen technologies.
- Further work is needed to improve data accuracy and representativeness, particularly for emerging components such as high-pressure hydrogen tanks, electrolyzers, and fuel cell systems. Many of the datasets used in this study rely

on assumptions or proxies, which introduce uncertainty. Developing updated, open-access inventories for hydrogen technologies would significantly enhance the robustness of LCA studies.

- The dynamic evolution of energy systems should be considered. This study relies on Italy's 2021 grid mix data; however, as power grids continue to decarbonize with rising renewable energy integration, the life cycle environmental impacts of electrolysis-based hydrogen will change over time.

Bibliography

- [1] IPCC. *Climate Change 2021: The Physical Science Basis. Contribution of Working Group I to the Sixth Assessment Report of the Intergovernmental Panel on Climate Change*. Cambridge, United Kingdom and New York, NY, USA: Cambridge University Press, 2021 (cit. on p. 1).
- [2] European Environment Agency (EEA). *Trends and Projections in Europe*. European Environment Agency, 2024. DOI: 10.2800/7574066. URL: <https://doi.org/10.2800/7574066> (cit. on p. 1).
- [3] United Nations. *Paris Agreement*. https://unfccc.int/sites/default/files/english_paris_agreement.pdf. Retrieved from the United Nations Framework Convention on Climate Change (UNFCCC). 2015 (cit. on p. 1).
- [4] S. Algburi, O. Al-Dulaimi, H. F. Fakhruldeen, D. H. Khalaf, R. N. Hanoon, F. I. Jabbar, Q. Hassan, A. K. Al-Jiboory, and S. Kiconco. «The Green Hydrogen Role in the Global Energy Transformations». In: *Renewable and Sustainable Energy Transition* 8 (2025). DOI: 10.1016/j.rset.2025.100118. URL: <https://doi.org/10.1016/j.rset.2025.100118> (cit. on p. 1).
- [5] European Commission. *The European Green Deal*. Tech. rep. COM(2019) 640 final. European Commission, 2019. URL: <https://eur-lex.europa.eu/legal-content/EN/TXT/?uri=CELEX:52019DC0640> (cit. on p. 1).
- [6] Clean Hydrogen Partnership. *REPowering the EU with Hydrogen Valleys: Clean Hydrogen Partnership invests EUR 105.4 million for funding 9 Hydrogen Valleys across Europe*. https://www.clean-hydrogen.europa.eu/media/news/repowering-eu-hydrogen-valleys-clean-hydrogen-partnership-invests-eur-1054-million-funding-9-2023-01-31_en. Retrieved from the Clean Hydrogen Partnership website. Jan. 2023 (cit. on p. 2).
- [7] Clean Hydrogen Partnership. *Hydrogen Valleys*. https://www.clean-hydrogen.europa.eu/hydrogen-valleys-0_en. Retrieved from the Clean Hydrogen Partnership website. n.d. (Cit. on pp. 2, 3).
- [8] HEAVENN Project. *Hydrogen Energy Applications in Valley Environments for Northern Netherlands (HEAVENN)*. <https://www.heavenn.org/>. Retrieved from the HEAVENN Project website. n.d. (Cit. on p. 2).

- [9] HEAVENN Project. *Hydrogen Energy Applications in Valley Environments for Northern Netherlands (HEAVENN)*. <https://h2v.eu/hydrogen-valleys/heavenn-0>. Retrieved from the HEAVENN Project website. n.d. (Cit. on p. 2).
- [10] Clean Hydrogen Partnership. *North Adriatic Hydrogen Valley (NAHV) – Project Summary*. Accessed: 2025-11-07. 2023. URL: https://www.clean-hydrogen.europa.eu/projects-dashboard/projects-repository/nahv_en (cit. on p. 3).
- [11] Clean Hydrogen Partnership. *North Adriatic Hydrogen Valley (NAHV) – Project Summary*. Accessed: 2025-11-07. 2025. URL: https://www.clean-hydrogen.europa.eu/document/download/d5e3a8b9-00a6-459b-9be5-161767e4c193_en?filename=NAHV-2025.pdf (cit. on p. 3).
- [12] Clean Hydrogen Partnership. *GREEN HYSLAND – Deployment of a H₂ Ecosystem on the Island of Mallorca*. Accessed: 2025-11-07. 2023. URL: https://www.clean-hydrogen.europa.eu/projects-dashboard/projects-repository/green-hysland_en (cit. on p. 3).
- [13] GREEN HYSLAND. *GREEN HYSLAND – Project Overview*. Accessed: 2025-11-07. n.d. URL: <https://greenhysland.eu> (cit. on p. 3).
- [14] Mohsen Salimi, Morteza Hosseinpour, and Tohid N.Borhani. «The Role of Clean Hydrogen Value Chain in a Successful Energy Transition of Japan». In: *Energies* 15 (Aug. 2022), p. 6064. DOI: 10.3390/en15166064 (cit. on p. 4).
- [15] J. M. M. Arcos and D. M. F. Santos. «The Hydrogen Color Spectrum: Techno-Economic Analysis of the Available Technologies for Hydrogen Production». In: *Gases* 3.1 (2023), pp. 25–46. DOI: 10.3390/gases3010002. URL: <https://doi.org/10.3390/gases3010002> (cit. on p. 7).
- [16] Hydrogen Portal. *Hydrogen from Ammonia by Photocatalysis at Ambient Temperature*. Retrieved October 5, 2025, from <https://hydrogen-portal.com/hydrogen-from-ammonia-by-photocatalysis-at-ambient-temperature/>. n.d. (Cit. on p. 7).
- [17] M. Bampaou and K. D. Panopoulos. «An overview of hydrogen valleys: Current status, challenges and their role in increased renewable energy penetration». In: *Renewable and Sustainable Energy Reviews* 207 (2025). DOI: 10.1016/j.rser.2024.114923. URL: <https://doi.org/10.1016/j.rser.2024.114923> (cit. on p. 8).
- [18] N. Shaya and S. Glöser-Chahoud. «A Review of Life Cycle Assessment (LCA) Studies for Hydrogen Production Technologies through Water Electrolysis: Recent Advances». In: *Energies* 17.16 (2024). DOI: 10.3390/en17163968. URL: <https://doi.org/10.3390/en17163968> (cit. on p. 8).

- [19] I. Dincer, M. A. Rosen, and M. Al-Zareer. «Chemical Energy Production». In: *Comprehensive Energy Systems*. Ed. by I. Dincer. Elsevier, 2018, pp. 470–520. DOI: 10.1016/B978-0-12-809597-3.00326-6. URL: <https://doi.org/10.1016/B978-0-12-809597-3.00326-6> (cit. on pp. 9, 10).
- [20] M. Katebah, M. Al-Rawashdeh, and P. Linke. «Analysis of hydrogen production costs in Steam-Methane Reforming considering integration with electrolysis and CO₂ capture». In: *Cleaner Engineering and Technology* 10 (2022), p. 100552. DOI: 10.1016/j.clet.2022.100552. URL: <https://doi.org/10.1016/j.clet.2022.100552> (cit. on p. 9).
- [21] S. Shiva Kumar and H. Lim. «An overview of water electrolysis technologies for green hydrogen production». In: *Energy Reports* 8 (2022), pp. 13793–13813. DOI: 10.1016/j.egy.2022.10.127. URL: <https://doi.org/10.1016/j.egy.2022.10.127> (cit. on p. 10).
- [22] IEA. *Global Hydrogen Review*. Retrieved from <https://iea.blob.core.windows.net/assets/c5bc75b1-9e4d-460d-9056-6e8e626a11c4/GlobalHydrogenReview2022.pdf>. 2022 (cit. on p. 10).
- [23] S. Shiva Kumar and V. Himabindu. «Hydrogen production by PEM water electrolysis – A review». In: *Materials Science for Energy Technologies* 2.3 (2019), pp. 442–454. DOI: 10.1016/j.mset.2019.03.002. URL: <https://doi.org/10.1016/j.mset.2019.03.002> (cit. on pp. 10, 11).
- [24] N. Sezer, S. Bayhan, U. Fesli, and A. Sanfilippo. «A comprehensive review of the state-of-the-art of proton exchange membrane water electrolysis». In: *Materials Science for Energy Technologies* 8 (2025), pp. 44–65. DOI: 10.1016/j.mset.2024.07.006. URL: <https://doi.org/10.1016/j.mset.2024.07.006> (cit. on p. 11).
- [25] J. Gerhardt-Mörsdorf, F. Peterssen, P. Burfeind, M. Benecke, B. Bensmann, R. Hanke-Rauschenbach, and C. Minke. «Life Cycle Assessment of a 5 MW Polymer Exchange Membrane Water Electrolysis Plant». In: *Advanced Energy and Sustainability Research* 5.4 (2024). DOI: 10.1002/aesr.202300135. URL: <https://doi.org/10.1002/aesr.202300135> (cit. on pp. 12, 45–47).
- [26] G. Zhao, M. R. Kraglund, H. L. Frandsen, A. C. Wulff, S. H. Jensen, M. Chen, and C. R. Graves. «Life cycle assessment of H₂O electrolysis technologies». In: *International Journal of Hydrogen Energy* 45.43 (2020), pp. 23765–23781. DOI: 10.1016/j.ijhydene.2020.05.282. URL: <https://doi.org/10.1016/j.ijhydene.2020.05.282> (cit. on pp. 12, 49).
- [27] M. El-Shafie. «Hydrogen production by water electrolysis technologies: A review». In: *Results in Engineering* 20 (2023), p. 101426. DOI: 10.1016/j.rineng.2023.101426. URL: <https://doi.org/10.1016/j.rineng.2023.101426> (cit. on p. 12).

- [28] A. Keçebaş, M. Kayfeci, and M. Bayat. «Electrochemical hydrogen generation». In: *Solar Hydrogen Production*. Ed. by F. Calise, M. D. D’Accadia, M. Santarelli, A. Lanzini, and D. Ferrero. Academic Press, 2019, pp. 299–317. DOI: 10.1016/B978-0-12-814853-2.00009-6. URL: <https://doi.org/10.1016/B978-0-12-814853-2.00009-6> (cit. on p. 13).
- [29] S. Krishnan, B. Corona, G. J. Kramer, M. Junginger, and V. Koning. «Prospective LCA of alkaline and PEM electrolyser systems». In: *International Journal of Hydrogen Energy* 55 (2024), pp. 26–41. DOI: 10.1016/j.ijhydene.2023.10.192. URL: <https://doi.org/10.1016/j.ijhydene.2023.10.192> (cit. on pp. 13, 48).
- [30] FinH2. *Electrolyser technologies*. Retrieved October 5, 2025, from <https://www.finh2.fi/electrolyser-technologies/>. n.d. (Cit. on p. 13).
- [31] SynerHy. *Balance of Plant (BoP) of an Electrolyser*. Retrieved from <https://synerhy.com/en/2022/02/balance-of-plant-bop-of-an-electrolyser/>. 2022 (cit. on p. 14).
- [32] Francesco Currenti. *Techno-Economic Evaluation of Alkaline Electrolyzers for Green H2 Production from Seawater*. Master’s thesis, Politecnico di Torino. Retrieved from <https://webthesis.biblio.polito.it/26113/1/tesi.pdf>. 2023 (cit. on p. 14).
- [33] A. Midilli, H. Kucuk, M. E. Topal, U. Akbulut, and I. Dincer. «A comprehensive review on hydrogen production from coal gasification: Challenges and Opportunities». In: *International Journal of Hydrogen Energy* 46.50 (2021), pp. 25385–25412. DOI: 10.1016/j.ijhydene.2021.05.088. URL: <https://doi.org/10.1016/j.ijhydene.2021.05.088> (cit. on p. 14).
- [34] R. Rodrigues. *Coal gasification technologies to power generation in Brazil*. Retrieved from <https://doi.org/10.13140/RG.2.1.1336.2165>. 2016 (cit. on p. 15).
- [35] F. Safari and I. Dincer. «A review and comparative evaluation of thermochemical water splitting cycles for hydrogen production». In: *Energy Conversion and Management* 205 (2020), p. 112182. DOI: 10.1016/j.enconman.2019.112182. URL: <https://doi.org/10.1016/j.enconman.2019.112182> (cit. on p. 15).
- [36] IEA Bioenergy. *Biomass gasification for hydrogen production*. Retrieved from https://www.ieabioenergy.com/wp-content/uploads/2025/03/IEA-Bioenergy_T33_Bio-H2_Final_v2.pdf. 2025 (cit. on p. 16).
- [37] A. Ratoi, C. Munteanu, and D. Eliezer. «Maximizing Onboard Hydrogen Storage Capacity by Exploring High-Strength Novel Materials Using a Mathematical Approach». In: *Materials* 17.17 (2024). DOI: 10.3390/ma17174288. URL: <https://doi.org/10.3390/ma17174288> (cit. on p. 16).

- [38] H. Barthelemy, M. Weber, and F. Barbier. «Hydrogen storage: Recent improvements and industrial perspectives». In: *International Journal of Hydrogen Energy* 42.11 (2017), pp. 7254–7262. DOI: 10.1016/j.ijhydene.2016.03.178. URL: <https://doi.org/10.1016/j.ijhydene.2016.03.178> (cit. on p. 17).
- [39] X. Hong, V. B. Thaore, I. A. Karimi, S. Farooq, X. Wang, A. K. Usadi, B. R. Chapman, and R. A. Johnson. «Techno-enviro-economic analyses of hydrogen supply chains with an ASEAN case study». In: *International Journal of Hydrogen Energy* 46.65 (2021), pp. 32914–32928. DOI: 10.1016/j.ijhydene.2021.07.138. URL: <https://doi.org/10.1016/j.ijhydene.2021.07.138> (cit. on pp. 17, 63).
- [40] L. Ye and L. Lu. «Environmental and economic evaluation of the high-pressured and cryogenic vessels for hydrogen storage on the sedan». In: *International Journal of Low-Carbon Technologies* 18 (2023), pp. 144–149. DOI: 10.1093/ijlct/ctac126. URL: <https://doi.org/10.1093/ijlct/ctac126> (cit. on p. 17).
- [41] Argonne National Laboratory (ANL). *Technical Assessment of Compressed Hydrogen Storage Tank Systems for Automotive Applications*. Tech. rep. Argonne National Laboratory, 2011 (cit. on p. 17).
- [42] E. Weiszflog and M. Abbas. *Life Cycle Assessment of Hydrogen Storage Systems for Trucks: An assessment of environmental impacts and recycling flows of carbon fiber*. Unpublished report or online document. n.d. (Cit. on p. 18).
- [43] Z. Abdin and K. R. Khalilpour. «Single and Polystorage Technologies for Renewable-Based Hybrid Energy Systems». In: *Polygeneration with Polystorage for Chemical and Energy Hubs*. Ed. by K. R. Khalilpour. Academic Press, 2019, pp. 77–131. DOI: 10.1016/B978-0-12-813306-4.00004-5. URL: <https://doi.org/10.1016/B978-0-12-813306-4.00004-5> (cit. on p. 18).
- [44] Z. Yanxing, G. Maoqiong, Z. Yuan, D. Xueqiang, and S. Jun. «Thermodynamics analysis of hydrogen storage based on compressed gaseous hydrogen, liquid hydrogen and cryo-compressed hydrogen». In: *International Journal of Hydrogen Energy* 44.31 (2019), pp. 16833–16840. DOI: 10.1016/j.ijhydene.2019.04.207. URL: <https://doi.org/10.1016/j.ijhydene.2019.04.207> (cit. on p. 18).
- [45] M. W. Davids, M. Lototsky, M. Malinowski, D. van Schalkwyk, A. Parsons, S. Pasupathi, D. Swanepoel, and T. van Niekerk. «Metal hydride hydrogen storage tank for light fuel cell vehicle». In: *International Journal of Hydrogen Energy* 44.55 (2019), pp. 29263–29272. DOI: 10.1016/j.ijhydene.2019.01.227. URL: <https://doi.org/10.1016/j.ijhydene.2019.01.227> (cit. on p. 18).

- [46] L. J. Murray, M. Dincă, and J. R. Long. «Hydrogen storage in metal–organic frameworks». In: *Chemical Society Reviews* 38.5 (2009), pp. 1294–1314. DOI: 10.1039/B802256A. URL: <https://doi.org/10.1039/B802256A> (cit. on p. 18).
- [47] H. Yang et al. «Recent advances in kinetic and thermodynamic regulation of magnesium hydride for hydrogen storage». In: *Rare Metals* 42.9 (2023), pp. 2906–2927. DOI: 10.1007/s12598-023-02306-z. URL: <https://doi.org/10.1007/s12598-023-02306-z> (cit. on p. 18).
- [48] M. Reuß, T. Grube, M. Robinius, P. Preuster, P. Wasserscheid, and D. Stolten. «Seasonal storage and alternative carriers: A flexible hydrogen supply chain model». In: *Applied Energy* 200 (2017), pp. 290–302. DOI: 10.1016/j.apenergy.2017.05.050. URL: <https://doi.org/10.1016/j.apenergy.2017.05.050> (cit. on p. 19).
- [49] H2 Tools. *Hydrogen Pipelines September 2016*. Retrieved from <https://h2tools.org/hyarc/hydrogen-data/hydrogen-pipelines>. 2016 (cit. on p. 19).
- [50] C. Tsiklios, M. Hermesmann, and T. E. Müller. «Hydrogen transport in large-scale transmission pipeline networks: Thermodynamic and environmental assessment of repurposed and new pipeline configurations». In: *Applied Energy* 327 (2022), p. 120097. DOI: 10.1016/j.apenergy.2022.120097. URL: <https://doi.org/10.1016/j.apenergy.2022.120097> (cit. on pp. 19, 57, 58, 112).
- [51] Anthony Wang, Kees van der Leun, and Daan Peters. *European Hydrogen Backbone: How a Dedicated Hydrogen Infrastructure Can Be Created*. Retrieved from <https://transparency.entsog.eu/>. 2020 (cit. on p. 19).
- [52] Jens Mischner. *On the flow velocities in gas pipelines*. gwf Gas+Energy, 63. Retrieved from https://gwf-gas.de/wp-content/uploads/2021/05/GE_05_2021_fb_Mischner.pdf. 2021 (cit. on p. 19).
- [53] S. K. Sharma and S. Maheshwari. «A review on welding of high strength oil and gas pipeline steels». In: *Journal of Natural Gas Science and Engineering* 38 (2017), pp. 203–217. DOI: 10.1016/j.jngse.2016.12.039. URL: <https://doi.org/10.1016/j.jngse.2016.12.039> (cit. on p. 19).
- [54] D. Li, R. P. Gangloff, and J. R. Scully. «Hydrogen trap states in ultrahigh-strength AERMET 100 steel». In: *Metallurgical and Materials Transactions A* 35.3 (2004), pp. 849–864. DOI: 10.1007/s11661-004-0011-1. URL: <https://doi.org/10.1007/s11661-004-0011-1> (cit. on p. 20).
- [55] I. A. Gondal. «Hydrogen transportation by pipelines». In: *Compendium of Hydrogen Energy*. Ed. by R. B. Gupta, A. Basile, and T. N. Veziroğlu. Woodhead Publishing, 2016, pp. 301–322. DOI: 10.1016/B978-1-78242-362-1.00012-2. URL: <https://doi.org/10.1016/B978-1-78242-362-1.00012-2> (cit. on p. 20).

- [56] J. P. Kopasz. «Fuel cells and odorants for hydrogen». In: *International Journal of Hydrogen Energy* 32.13 (2007), pp. 2527–2531. DOI: 10.1016/j.ijhydene.2006.11.001. URL: <https://doi.org/10.1016/j.ijhydene.2006.11.001> (cit. on p. 20).
- [57] R. Cussons and S. Renewables. *RHyMES Renewable Hydrogen Models for Energy Storage Feasibility Study Final Report*. Retrieved from <https://www.researchgate.net/publication/329270083>. 2019 (cit. on p. 20).
- [58] Christina Wulf, Markus Reuß, Thomas Grube, Petra Zapp, Martin Robinius, Jürgen-Friedrich Hake, and Detlef Stolten. «Life Cycle Assessment of hydrogen transport and distribution options». In: *Journal of cleaner production* 199 (2018), pp. 431–443 (cit. on pp. 21, 58, 62, 63).
- [59] Krishna Reddi, Amgad Elgowainy, Neha Rustagi, and Erika Gupta. «Techno-economic analysis of conventional and advanced high-pressure tube trailer configurations for compressed hydrogen gas transportation and refueling». In: *International Journal of Hydrogen Energy* 43.9 (2018), pp. 4428–4438. ISSN: 0360-3199. DOI: <https://doi.org/10.1016/j.ijhydene.2018.01.049>. URL: <https://www.sciencedirect.com/science/article/pii/S0360319918300843> (cit. on p. 21).
- [60] R. Lan, J. T. S. Irvine, and S. Tao. «Ammonia and related chemicals as potential indirect hydrogen storage materials». In: *International Journal of Hydrogen Energy* 37.2 (2012), pp. 1482–1494. DOI: 10.1016/j.ijhydene.2011.10.004. URL: <https://doi.org/10.1016/j.ijhydene.2011.10.004> (cit. on p. 21).
- [61] IRENA. *Geopolitics of the energy transformation: the hydrogen factor*. 2022 (cit. on p. 21).
- [62] G. Song, Q. Zhao, B. Shao, H. Zhao, H. Wang, and W. Tan. «Life Cycle Assessment of Greenhouse Gas (GHG) and NO_x Emissions of Power-to-H₂-to-Power Technology Integrated with Hydrogen-Fueled Gas Turbine». In: *Energies* 16.2 (2023). DOI: 10.3390/en16020977. URL: <https://doi.org/10.3390/en16020977> (cit. on pp. 21, 22).
- [63] Siemens Energy. *Hydrogen Power Plants*. Retrieved October 3, 2025, from <https://www.siemens-energy.com/global/en/home/products-services/product/hydrogen-power-plants.html>. n.d. (Cit. on p. 21).
- [64] International Energy Agency. *Global Hydrogen Review 2023*. 2023 (cit. on p. 22).
- [65] I. Rossetti. «Reactor Design, Modelling and Process Intensification for Ammonia Synthesis». In: *Sustainable Ammonia Production*. Ed. by Inamuddin, R. Boddula, and A. M. Asiri. Springer International Publishing, 2020, pp. 17–48. DOI: 10.1007/978-3-030-35106-9_2. URL: https://doi.org/10.1007/978-3-030-35106-9_2 (cit. on p. 22).

- [66] I. Dincer and Y. Bicer. «Chapter 2.1 Ammonia». In: *Comprehensive Energy Systems*. Ed. by I. Dincer. Elsevier, 2018, pp. 1–39. DOI: 10.1016/B978-0-12-809597-3.00201-7. URL: <https://doi.org/10.1016/B978-0-12-809597-3.00201-7> (cit. on p. 22).
- [67] I. Dincer and Y. Bicer. «Chapter 3.2 Ammonia Production». In: *Comprehensive Energy Systems*. Ed. by I. Dincer. Elsevier, 2018, pp. 41–94. DOI: 10.1016/B978-0-12-809597-3.00305-9. URL: <https://doi.org/10.1016/B978-0-12-809597-3.00305-9> (cit. on p. 22).
- [68] W. H. L. Stafford, K. J. Chaba, V. Russo, T. Goga, T. H. Roos, M. Sharp, and A. Nahman. «Life cycle assessment of green ammonia production at a coastal facility in South Africa». In: *Frontiers in Energy* (2025). DOI: 10.1007/s11708-025-1013-5 (cit. on pp. 22, 81, 82, 113).
- [69] D. A. Chisalita, L. Petrescu, and C. C. Cormos. «Environmental evaluation of European ammonia production considering various hydrogen supply chains». In: *Renewable and Sustainable Energy Reviews* 130 (2020), p. 109964. DOI: 10.1016/j.rser.2020.109964. URL: <https://doi.org/10.1016/j.rser.2020.109964> (cit. on p. 23).
- [70] A. Azimi and M. van der Spek. «Prospective Life Cycle Assessment Suggests Direct Reduced Iron Is the Most Sustainable Pathway to Net-Zero Steel-making». In: *Industrial and Engineering Chemistry Research* 64.7 (2025), pp. 3871–3885. DOI: 10.1021/acs.iecr.4c03321. URL: <https://doi.org/10.1021/acs.iecr.4c03321> (cit. on pp. 23–25, 76, 77).
- [71] S. Mekhilef, R. Saidur, and A. Safari. «Comparative study of different fuel cell technologies». In: *Renewable and Sustainable Energy Reviews* 16.1 (2012), pp. 981–989. DOI: 10.1016/j.rser.2011.09.020. URL: <https://doi.org/10.1016/j.rser.2011.09.020> (cit. on p. 25).
- [72] International Energy Agency (IEA). *Fuel cell electric vehicle (FCEV) stock by region and by mode, 2022*. Retrieved from <https://www.iea.org/data-and-statistics/charts/fuel-cell-electric-vehicle-fcev-stock-by-region-and-by-mode-2022>. 2022 (cit. on p. 25).
- [73] M. A. Elazab, A. T. Elgohr, M. Bassyouni, A. E. Kabeel, M. E. H. Attia, M. K. Elshaarawy, A. K. Hamed, and H. A. H. Alzahrani. «Green Hydrogen: Unleashing the Potential for Sustainable Energy Generation». In: *Results in Engineering* 27 (2025), p. 106031. DOI: 10.1016/j.rineng.2025.106031. URL: <https://doi.org/10.1016/j.rineng.2025.106031> (cit. on p. 26).
- [74] A. Lubecki, J. Szczurowski, and K. Zarębska. «A comparative environmental Life Cycle Assessment study of hydrogen fuel, electricity and diesel fuel for public buses». In: *Applied Energy* 350 (2023), p. 121766. DOI: 10.1016/j.apenergy.2023.121766. URL: <https://doi.org/10.1016/j.apenergy.2023.121766> (cit. on p. 26).

- [75] D. Burchart and I. Przytuła. «Review of Environmental Life Cycle Assessment for Fuel Cell Electric Vehicles in Road Transport». In: *Energies* 18.5 (2025). DOI: 10.3390/en18051229. URL: <https://doi.org/10.3390/en18051229> (cit. on pp. 26, 27).
- [76] Toyota Motor Corporation. *Toyota Mirai Technical Specifications*. Accessed: 2025-10-21. 2021. URL: https://www.toyota.com/content/dam/toyota/brochures/pdf/2021/mirai_ebrochure.pdf (cit. on p. 27).
- [77] T. Yoshida and K. Kojima. «Toyota MIRAI Fuel Cell Vehicle and Progress Toward a Future Hydrogen Society». In: *The Electrochemical Society Interface* 24.2 (2015). Accessed: 2025-10-21, p. 45. DOI: 10.1149/2.F03152if. URL: <https://doi.org/10.1149/2.F03152if> (cit. on p. 27).
- [78] M. M. Tellez-Cruz, J. Escorihuela, O. Solorza-Feria, and V. Compañ. «Proton Exchange Membrane Fuel Cells (PEMFCs): Advances and Challenges». In: *Polymers* 13.18 (2021). DOI: 10.3390/polym13183064. URL: <https://doi.org/10.3390/polym13183064> (cit. on p. 28).
- [79] S. T. Thompson, B. D. James, J. M. Huya-Kouadio, C. Houchins, D. A. DeSantis, R. Ahluwalia, A. R. Wilson, G. Kleen, and D. Papageorgopoulos. «Direct hydrogen fuel cell electric vehicle cost analysis: System and high-volume manufacturing description, validation, and outlook». In: *Journal of Power Sources* 399 (2018), pp. 304–313. DOI: 10.1016/j.jpowsour.2018.07.100. URL: <https://doi.org/10.1016/j.jpowsour.2018.07.100> (cit. on p. 28).
- [80] *ISO 14040: Environmental Management — Life Cycle Assessment — Principles and Framework*. Geneva, Switzerland, 2006 (cit. on p. 30).
- [81] *ISO 14044: Environmental Management — Life Cycle Assessment — Requirements and Guidelines*. Geneva, Switzerland, 2006 (cit. on p. 30).
- [82] European Commission Joint Research Centre (JRC). *International Reference Life Cycle Data System (ILCD) Handbook — General Guide for Life Cycle Assessment — Detailed Guidance*. Luxembourg: Publications Office of the European Union, 2010 (cit. on p. 30).
- [83] SH2E Consortium. *SH2E Project Guidelines: Harmonised and Performance-Based Sustainability Assessment of Hydrogen Systems*. <https://www.sh2e.eu>. 2023 (cit. on p. 30).
- [84] P. Masoni and A. Zamagni. *Guidance Document for Performing LCAs on Fuel Cells and Hydrogen Technologies (FC-HyGuide)*. Technical Report. Fuel Cells and Hydrogen Joint Undertaking (FCH JU). European Commission, Joint Research Centre, 2011 (cit. on pp. 30, 35, 38).

- [85] E. Bargiacchi, G. Puig-Samper, F. Campos-Carriedo, D. Iribarren, and J. Dufour. *SUSTAINABILITY ASSESSMENT OF HARMONISED HYDROGEN ENERGY SYSTEMS D2.2 Definition of FCH-LCA guidelines WP2 Reformulation of current guidelines for Life Cycle Assessment DELIVERABLE LEADERS*. Accessed: 2025-10-23. n.d. (Cit. on pp. 32, 35).
- [86] Daniele Melideo, Rafael Ortiz Cebolla, and Eveline Weidner. *Life Cycle Assessment of Hydrogen and Fuel Cell Technologies: Inventory of Work Performed by Projects Funded Under FCH JU*. Publications Office of the European Union, 2020 (cit. on p. 33).
- [87] P. L. Spath and M. K. Mann. *Life Cycle Assessment of Hydrogen Production via Natural Gas Steam Reforming*. Accessed: 2025-10-23. U.S. Department of Energy, n.d. URL: <http://www.doe.gov/bridge> (cit. on p. 34).
- [88] M. P. Maniscalco, S. Longo, M. Cellura, G. Micciché, and M. Ferraro. «Critical Review of Life Cycle Assessment of Hydrogen Production Pathways». In: *Environments* 11.6 (2024). DOI: 10.3390/environments11060108. URL: <https://doi.org/10.3390/environments11060108> (cit. on p. 34).
- [89] G. Puig-Samper et al. «A Systematic Review of Life Cycle Assessment Studies on Hydrogen Production: Methodological Variability and its Impact on Reported Results». In: *Journal to be updated* (2024). The study highlights variability due to functional units, system boundaries, electricity sources, and electrolyzer efficiencies. (cit. on p. 34).
- [90] X. Wei, S. Sharma, A. Waeber, D. Wen, S. N. Sampathkumar, M. Margni, F. Maréchal, and J. Van Herle. «Comparative Life Cycle Analysis of Electrolyzer Technologies for Hydrogen Production: Manufacturing and Operations». In: *Joule* 8.12 (2024), pp. 3347–3372. DOI: 10.1016/j.joule.2024.09.007. URL: <https://doi.org/10.1016/j.joule.2024.09.007> (cit. on p. 34).
- [91] N. Shaya and S. Glöser-Chahoud. «A Review of Life Cycle Assessment (LCA) Studies for Hydrogen Production Technologies through Water Electrolysis: Recent Advances». In: *Energies* 17.16 (2024). DOI: 10.3390/en17163968. URL: <https://doi.org/10.3390/en17163968> (cit. on p. 34).
- [92] O. Kanz, K. Bittkau, K. Ding, U. Rau, and A. Reinders. «Review and Harmonization of the Life-Cycle Global Warming Impact of PV-Powered Hydrogen Production by Electrolysis». In: *Frontiers in Electronics* 2 (2021). DOI: 10.3389/felec.2021.711103. URL: <https://doi.org/10.3389/felec.2021.711103> (cit. on p. 35).
- [93] W. Ajeeb, R. Costa Neto, and P. Baptista. «Life Cycle Assessment of Green Hydrogen Production through Electrolysis: A Literature Review». In: *Sustainable Energy Technologies and Assessments* 69 (2024). DOI: 10.1016/j.seta.2024.103923. URL: <https://doi.org/10.1016/j.seta.2024.103923> (cit. on p. 35).

- [94] A. I. Osman, M. Nasr, A. R. Mohamed, A. Abdelhaleem, A. Ayati, M. Farghali, A. H. Al-Muhtaseb, A. S. Al-Fatesh, and D. W. Rooney. «Life Cycle Assessment of Hydrogen Production, Storage, and Utilization toward Sustainability». In: *Wiley Interdisciplinary Reviews: Energy and Environment* 13.3 (2024). DOI: 10.1002/wene.526. URL: <https://doi.org/10.1002/wene.526> (cit. on p. 35).
- [95] A. Moro and L. Lonza. «Electricity Carbon Intensity in European Member States: Impacts on GHG Emissions of Electric Vehicles». In: *Transportation Research Part D: Transport and Environment* 64 (2018), pp. 5–14. DOI: 10.1016/j.trd.2017.07.012. URL: <https://doi.org/10.1016/j.trd.2017.07.012> (cit. on p. 35).
- [96] M. Pehnt. «Assessing Future Energy and Transport Systems: The Case of Fuel Cells. Part I: Methodological Aspects». In: *International Journal of Life Cycle Assessment* 8 (2003), pp. 283–289. DOI: 10.1007/BF02978920. URL: <https://doi.org/10.1007/BF02978920> (cit. on p. 35).
- [97] V. Vogl, M. Åhman, and L. J. Nilsson. «Assessment of Hydrogen Direct Reduction for Fossil-Free Steelmaking». In: *Journal of Cleaner Production* 203 (2018), pp. 736–745. DOI: 10.1016/j.jclepro.2018.08.279. URL: <https://doi.org/10.1016/j.jclepro.2018.08.279> (cit. on p. 35).
- [98] B. Lee, L. R. Winter, H. Lee, D. Lim, H. Lim, and M. Elimelech. «Pathways to a Green Ammonia Future». In: *ACS Energy Letters* (2022), pp. 3032–3038. DOI: 10.1021/acsenerylett.2c01615. URL: <https://doi.org/10.1021/acsenerylett.2c01615> (cit. on p. 35).
- [99] European Commission. *Commission Recommendation (EU) 2021/2279 of 15 December 2021 on the use of the Environmental Footprint methods to measure and communicate the life cycle environmental performance of products and organisations*. <http://data.europa.eu/eli/reco/2021/2279/oj>. Accessed: October 16, 2025. 2021 (cit. on pp. 37, 42).
- [100] ecoinvent. *ecoQuery*. Retrieved October 16, 2025. 2025. URL: <https://ecoquery.ecoinvent.org/3.11/cutoff/search?query=¤tPage=1&pageSize=10&searchBy=activity> (cit. on pp. 42, 66, 67).
- [101] Nel Hydrogen. *A-Series Alkaline Electrolyser: Specification Sheet*. Accessed: 2025-02-10. 2024. URL: https://nelhydrogen.com/wp-content/uploads/2024/08/A-Series-Spec-Sheet%E2%80%9393DOC001974_03.pdf (cit. on p. 45).
- [102] S. Krishnan, V. Koning, M. Theodorus de Groot, A. de Groot, P. G. Mendoza, M. Junginger, and G. J. Kramer. «Present and future cost of alkaline and PEM electrolyser stacks». In: *International Journal of Hydrogen Energy* 48.83 (2023), pp. 32313–32330. DOI: 10.1016/j.ijhydene.2023.05.031. URL: <https://doi.org/10.1016/j.ijhydene.2023.05.031> (cit. on p. 48).

- [103] S. Yang, D. Mao, Z. Yu, W. Ma, L. Ma, X. Li, and F. Xi. «Comparison of life cycle assessment between hydrogen production from silicon waste and alkaline water electrolysis». In: *Science of the Total Environment* 920 (2024), p. 171065. DOI: 10.1016/j.scitotenv.2024.171065. URL: <https://doi.org/10.1016/j.scitotenv.2024.171065> (cit. on p. 48).
- [104] H. Lee, D. T. Dung, J. Kim, J. H. Pak, S. Kyung Kim, H. S. Cho, W. C. Cho, and C. H. Kim. «The synthesis of a Zirfon-type porous separator with reduced gas crossover for alkaline electrolyzer». In: *International Journal of Energy Research* 44.3 (2020), pp. 1875–1885. DOI: 10.1002/er.5038 (cit. on p. 49).
- [105] International Energy Agency (IEA). *Italy: Renewables*. <https://www.iea.org/countries/italy/renewables>. Accessed: 2025-11-07. 2025 (cit. on p. 53).
- [106] PVPS Task 12. *Life Cycle Inventories and Life Cycle Assessments of Photovoltaic Systems 2020 Task 12 PV Sustainability*. International Energy Agency Photovoltaic Power Systems Programme (IEA PVPS). 2020. URL: <https://www.iea-pvps.org> (cit. on p. 53).
- [107] Springer. *Transport Transitions: Advancing Sustainable and Inclusive Mobility*. Ed. by C. McNally, P. Carroll, B. Martinez-Pastor, B. Ghosh, M. Efthymiou, and N. Valantasis-Kanellos. Springer Nature Switzerland, 2025. DOI: 10.1007/978-3-031-89444-2. URL: <https://doi.org/10.1007/978-3-031-89444-2> (cit. on p. 62).
- [108] J. Burkhardt, A. Patyk, P. Tanguy, and C. Retzke. «Hydrogen mobility from wind energy – A life cycle assessment focusing on the fuel supply». In: *Applied Energy* 181 (2016), pp. 54–64. DOI: 10.1016/j.apenergy.2016.07.104. URL: <https://doi.org/10.1016/j.apenergy.2016.07.104> (cit. on p. 62).
- [109] S. Evangelisti, C. Tagliaferri, D. J. L. Brett, and P. Lettieri. «Life cycle assessment of a polymer electrolyte membrane fuel cell system for passenger vehicles». In: *Journal of Cleaner Production* 142 (2017), pp. 4339–4355. DOI: 10.1016/j.jclepro.2016.11.159. URL: <https://doi.org/10.1016/j.jclepro.2016.11.159> (cit. on p. 67).
- [110] C. Drawer, A. Rödl, and M. Kaltschmitt. «Life cycle assessment of construction and driving operation of a hydrogen-powered truck built from a used diesel truck». In: *Transportation Research Interdisciplinary Perspectives* 24 (2024), p. 101020. DOI: 10.1016/j.trip.2024.101020. URL: <https://doi.org/10.1016/j.trip.2024.101020> (cit. on pp. 67, 72).
- [111] Mercedes-Benz Trucks. *Daimler GenH2*. <https://www.daimlertruck.com/newsroom/pressemitteilung/mercedes-benz-trucks-gibt-auf-der-iaa-transportation-2022-in-hannover-einen-ausblick-auf-den-wasserstoffbasierten-genh2-truck-52032506>. Accessed: 2025-10-19. 2022 (cit. on pp. 67, 72).

- [112] L. Usai, C. R. Hung, F. Vásquez, M. Windsheimer, O. S. Burheim, and A. H. Strømman. «Life cycle assessment of fuel cell systems for light duty vehicles, current state-of-the-art and future impacts». In: *Journal of Cleaner Production* 280 (2021), p. 125086. DOI: 10.1016/j.jclepro.2020.125086. URL: <https://doi.org/10.1016/j.jclepro.2020.125086> (cit. on pp. 68, 108–111).
- [113] A. M. Syré, P. Shyposha, L. Freisem, A. Pollak, and D. Göhlich. «Comparative Life Cycle Assessment of Battery and Fuel Cell Electric Cars, Trucks, and Buses». In: *World Electric Vehicle Journal* 15.3 (2024), p. 114. DOI: 10.3390/wevj15030114. URL: <https://doi.org/10.3390/wevj15030114> (cit. on p. 72).
- [114] A. Nurdiawati, I. N. Zaini, W. Wei, R. Gyllenram, W. Yang, and P. Samuelsson. «Towards fossil-free steel: Life cycle assessment of biosyngas-based direct reduced iron (DRI) production process». In: *Journal of Cleaner Production* 393 (2023). DOI: 10.1016/j.jclepro.2023.136262. URL: <https://doi.org/10.1016/j.jclepro.2023.136262> (cit. on p. 76).
- [115] A. Arrigoni, E. Weidner, and U. Eynard. «Environmental life cycle assessment (LCA) comparison of hydrogen delivery options within Europe». In: *Publications Office of the European Union* (2024). DOI: 10.2760/5459 (cit. on p. 81).
- [116] D. Candelaresi, A. Valente, D. Iribarren, J. Dufour, and G. Spazzafumo. «Comparative life cycle assessment of hydrogen-fuelled passenger cars». In: *International Journal of Hydrogen Energy* 46.72 (2021), pp. 35961–35973. DOI: 10.1016/j.ijhydene.2021.01.034. URL: <https://doi.org/10.1016/j.ijhydene.2021.01.034> (cit. on p. 108).

Appendix A

Appendix

Table A.1: Life cycle inventory (LCI) for hydrogen storage tank system used in FCEVs [112]

Flow	Unit	Quantity
Carbon fiber	kg	62.16
Epoxy resin	kg	25.64
Foam	kg	4.30
Glass fiber	kg	4.30
High-density polyethylene	kg	7.50
Aluminum	kg	1.80
Electricity	kWh	4.50
Transport, train	tkm	66.80
Transport, lorry	tkm	11.10

Table A.2: LCI for 80 kW Electric Motor for FCEV [116]

Input	Amount	Unit
Steel, low-alloyed	39.31	kg
Ferrite	1.67	kg
Neodymium oxide	0.611	kg
Boron carbide	0.0291	kg
Copper	14.5	kg
Aluminium, production mix	20.4	kg
Polyphenylene sulphide	1.6	kg
Cable, three-conductor cable	4.54	m

Table A.3: LCI for main PEMFC Stack components (per kW) [112]

Flow	Amount	Unit	Comments
<i>Gas Diffusion Layer (GDL)</i>			
Methyl acrylate	0.01	kg	
Acrylonitrile	0.15	kg	
Heat	11.20	MJ	
Electricity	3.88	kWh	
High-density polyethylene	0.01	kg	
Carbon black	0.03	kg	
<i>Catalyst</i>			
Water	2.19E-03	kg	
Carbon black	5.49E-04	kg	
Formaldehyde	3.62E-05	kg	
Sodium hydroxide	4.82E-05	kg	
Cobalt	7.10E-05	kg	
Nitric acid	6.08E-04	kg	
Sodium nitrate	6.15E-04	kg	Platinum nitrate
Platinum	1.65E-04	kg	Chloroplatinic acid
Secondary platinum	7.06E-05	kg	Chloroplatinic acid
Hydrochloric acid	2.64E-04	kg	Chloroplatinic acid
Spent solvent mixture	1.31E-03	kg	
Wastewater	8.68E-05	kg	
Heat	7.63E-05	MJ	
Methanol	2.06E-03	kg	Catalyst ink
Tetrafluoroethylene	2.06E-03	kg	Catalyst ink
Sulfur trioxide	5.27E-04	kg	Catalyst ink
Electricity	3.24E-05	kWh	
<i>Bipolar Plates (BPPs)</i>			
Titanium	0.24	kg	
Carbon black	2.59E-06	kg	proxy
<i>Membrane</i>			
Tetrafluoroethylene	5.4E-03	kg	
Sulfur trioxide	4.32E-04	kg	
Heat	1.62E-03	MJ	
Plastic sheets extrusion	7.46E-03	kg	

Table A.4: LCI for Other PEMFC Stack Components per kW [112]

Flow	Amount	Unit
<i>Endplates</i>		
Glass fibre	0.02	kg
Epoxy resin	0.01	kg
Electricity	0.09	kWh
<i>Current Collectors</i>		
Copper	0.006	kg
Electricity	1.25E-04	kWh
<i>End Gaskets</i>		
Epoxy resin	0.0002	kg
Electricity	0.04	kWh
<i>Stack Compression Bands</i>		
Chromium steel	0.01	kg
Electricity	0.04	kWh
<i>Stack Housing</i>		
Polypropylene	0.05	kg
Electricity	0.001	kWh
<i>Membrane Electrode Assembly (MEA)</i>		
Silicone rubber	0.03	kg
Epoxy resin	0.06	kg
Electricity	0.31	kWh

Table A.5: LCI for the balance of plant (per kW) of PEMFC [112]

Flow	Amount	Unit	Comments
<i>Air Management</i>			
Chromium steel	0.02	kg	Compression/Expansion motor
Aluminium	0.04	kg	Compression/Expansion motor
Low-alloyed steel	0.01	kg	Compression/Expansion motor
Permanent magnet	0.01	kg	Compression/Expansion motor
Air filter	0.013	pc	
Tetrafluoroethylene	0.001	kg	Air ducting
Plastic pipes	0.03	kg	
Electronics	0.004	kg	Mass flow sensor
<i>Water Management</i>			
Polyphenylene sulfide	0.01	kg	Humidifier housing
Sulfur trioxide	0.00	kg	Nafion tubes
Tetrafluoroethylene	0.01	kg	Nafion tubes
Extrusion of plastic	0.01	kg	Nafion tubes
Aluminium	0.088	kg	Air precooler
Polyurethane	0.019	kg	proxy for Cordierite
Nylon 6	0.03	kg	Demister
<i>Heat Management</i>			
High-density polyethylene	0.01	kg	Fan
40W pump	3	pc	Coolant pump
Aluminium	0.01	kg	Radiators
Ethylene glycol	0.01	kg	Antifreeze
<i>Fuel Management</i>			
Low-alloyed steel	0.06	kg	Blower
Chromium steel	0.02	kg	Blower
Aluminium	0.03	kg	Blower, ejectors, pipes
<i>Other BoP</i>			
Electronics	0.03	kg	Controler
Cables	16	m	Wiring
Aluminium	0.10	kg	Mounting belly pan
Low-alloyed steel	0.013	kg	Fasteners

Table A.6: LCI for a new hydrogen transmission pipeline (per km of pipeline [50])

Process/Flow	Unit	Quantity
Output – Product		
Transmission pipeline, hydrogen	km	1.00
Inputs – Manufacture		
Building hall, steel construction	m ²	0.20
Building, multi-storey	m ³	16
Drawing of pipe, steel	kg	791,447.36
FBE powder coat, steel	m ²	3,830.23
Galvalume® coat, pieces	m ²	3,660.00
HDPE coat, extruded	kg	5,599.17
Steel, low-alloyed	kg	791,447.36
Inputs – Installation		
Excavation, hydraulic digger	m ³	1,200
Excavation, skid-steer loader	m ³	19,000
Sand	kg	2,280,000
Transport, freight train	tkm	120,171.49
Inputs – Use		
Transport, helicopter	hour	26
Transport, helicopter, LTO cycle	unit	10.4
Outputs – End-of-life		
Decommissioned pipeline	kg	395,895.24
Waste plastic, mixture	kg	2,732.40
Elementary flows – natural resources		
Land occupation, construction site	m ² · year	3,300
Land transformation, from forest to annual crop	m ²	2,000
Land transformation, from unspecified to industrial area	m ²	2.49
Water, from water	m ³	187
Elementary flows – emissions		
Water, to air	m ³	28.05
Water, to water	m ³	158.95

Table A.7: LCI for production of 1 kg of Green and Grey Ammonia [68]

Flow	Amount	Unit
<i>Green Ammonia Production</i>		
Chemical factory, organics	4E-10	p
Aluminium oxide, metallurgical	2.68E-10	kg
Hydrogen, liquid	8.94E-11	kg
Magnetite	8.58E-09	kg
Nitrogen gas	0.87	kg
Hydrogen gas	0.19	kg
Renewable electricity mix (solar and wind)	0.44	kWh
Emissions to air		
Nitrogen, atmospheric	0.04	kg
Argon-40	0.03	kg
Hydrogen	9.43E-03	kg
Steel and iron (waste treatment)	2.68E-03	kg
Copper scrap	1.10E-04	kg
Aluminium scrap	3.20E-04	kg
<i>Grey Ammonia Production</i>		
Chemical factory, organics	4E-10	p
Heat, district or industrial, natural gas	8.28	MJ
Natural gas, high pressure	0.625	m3
Nickel, class 1	3.50E-04	kg
Solvent, organic	3E-05	kg
Tap water	0.721	kg
Water, cooling, unspecified	0.14	m3
Emissions to air		
Carbon dioxide, fossil	1.44	kg
Nitrogen oxides	7E-04	kg
Water	0.0544	m3
Emissions to water		
Nitrogen	1.2E-04	kg
Water	0.0865	m3

Table A.8: LCI for Hot Rolled Coil Production (BF/BOF route)

Flow	Amount	Unit
Hot rolled coil, reheating and rolling process	1	ton
Slab cast steel production	1.05	ton
Electricity production, power plant (no CCS)	105.6	kWh
Oxygen (Air separation process)	0.00376	ton
Water, deionised	2000	kg
Air (input)	746	kg
Carbon dioxide (to air)	57.8	kg
Oxygen (to air)	65.83	kg
Water (to air)	84.13	kg
Nitrogen (to air)	575.36	kg
Sulfur trioxide (to air)	0.0064	kg
Nitrogen oxides (to air)	0.320	kg
Particulates, unspecified (to air)	0.0029	kg

Table A.9: LCI for Slab Cast Steel Production (BF/BOF route)

Flow	Amount	Unit
Slab cast steel production	1.05	ton
Refined steel, ladle metallurgy	1.09	ton
Electricity, power plant (no CCS)	10.9	kWh
Oxygen, air separation process	0.0031	ton
Water, deionised	914	kg
Carbon dioxide	0.797	kg

Table A.10: LCI for Refined Steel Production (BF/BOF route)

Flow	Amount	Unit
Refined steel, ladle metallurgy	1.09	ton
Crude steel, basic oxygen furnace	1.08	ton
Lime, lime production	0.00543	ton
Electricity, power plant (no CCS)	27.2	kWh
Oxygen, air separation process	0.00326	ton
Aluminium, primary (cast alloy slab)	1.63	ton
Ferromanganese (high coal)	11.9	ton
Carbon dioxide	0.801	kg

Table A.11: LCI for Crude Steel Production (Basic Oxygen Furnace)

Flow	Amount	Unit
Crude steel, basic oxygen furnace	1.08	ton
Lime, lime production	0.0701	ton
Hot metal, blast furnace	0.974	ton
Electricity, power plant (no CCS)	21.6	kWh
Oxygen, air separation process	0.0796	ton
Water, deionised	418	kg
Iron ore, 66.2% Fe (Brazil)	5.5	kg
Dolomite	11.9	kg
Carbon dioxide	50.2	kg
BOF slag (residual material)	32.1	kg

Table A.12: LCI for Hot Metal Production (Blast Furnace)

Flow	Amount	Unit
Hot metal, blast furnace	0.992	ton
Sinter	1.11	ton
Coke	0.367	ton
Limestone, unprocessed	13.3	kg
Hard coal	164	kg
Iron ore, 57.95% Fe (Australia)	131	kg
Iron ore, 66.2% Fe (Brazil)	356	kg
Oxygen, air separation process	0.0679	ton
Electricity, power plant (no CCS)	102.9	kWh
Water, deionised	871	kg
Carbon dioxide	435.07	kg
Oxygen (to air)	8.85	kg
Water (to air)	39.73	kg
Nitrogen (to air)	634.47	kg
Sulfur trioxide	0.0090	kg
Nitrogen oxides	0.054	kg
Particulates, unspecified	0.0040	kg
Blast furnace slag	316	kg

Table A.13: LCI for Hot Rolled Coil Production (DRI/EAF route)

Flow	Amount	Unit
Hot rolled coil, reheating and rolling process	1	ton
Slab cast steel production	1.05	ton
Electricity, medium voltage	105.6	kWh
Water, deionised	2000	kg
Carbon dioxide	57.8	kg
Oxygen	65.83	kg
Water (to air)	84.13	kg
Nitrogen	575.36	kg
Sulfur trioxide	0.0064	kg
Nitrogen oxides	0.320	kg
Particulates, unspecified	0.0029	kg

Table A.14: LCI for Slab Cast Steel Production (DRI/EAF route)

Flow	Amount	Unit
Slab cast steel production	1.05	ton
Refined steel, ladle metallurgy	1.09	ton
Electricity, medium voltage	10.9	kWh
Water, deionised	914	kg
Carbon dioxide	0.797	kg

Table A.15: LCI for Refined Steel Production (DRI/EAF route)

Flow	Amount	Unit
Refined steel, ladle metallurgy	1.09	ton
Crude steel, electric arc furnace	1.08	ton
Quicklime, in pieces, loose	0.00543	ton
Electricity, medium voltage	27.2	kWh
Carbon dioxide	0.801	kg

Table A.16: LCI for Iron Ore Pellet Production (Pelletization, DRI/EAF route)

Flow	Amount	Unit
Iron ore pellets, pelletization	1	kg
Iron ore concentrate	0.9499	kg
Hard coal	0.0077	kg
Bentonite	0.0053	kg
Dolomite	0.0068	kg
Limestone, crushed, washed	0.0025	kg
Compressed air, 1000 kPa	0.0089	m ³
Tap water	0.399	kg
Light fuel oil	0.002	kg
Electricity, medium voltage	0.0203	kWh
Carbon dioxide	0.0194	kg
Carbon monoxide	0.00001	kg
Sulfur oxides	4.84E-05	kg
Nitrogen oxides	2.87E-04	kg
Particulates, unspecified	4.85E-05	kg

Table A.17: LCI for Sponge Iron Production (H_2 -DRI)

Flow	Amount	Unit
Sponge iron, H_2 DRI	1	ton
Iron ore pellets, pelletization	1.391	ton
Water, unspecified natural origin	0.621	m ³
Water, cooling, unspecified origin	0.0118	m ³
Natural gas, high pressure	40.8	m ³
Electricity, medium voltage	3500	kWh
Carbon dioxide	40	kg

Table A.18: LCI for Crude Steel Production (Electric Arc Furnace, H₂-DRI route)

Flow	Amount	Unit
Crude steel, electric arc furnace	1	ton
Sponge iron, H ₂ DRI	1.01	ton
Quicklime, in pieces, loose	0.025	ton
Iron scrap, sorted and pressed	0.06	ton
Anode, for metal electrolysis	0.0043	ton
Hard coal	0.0094	ton
Refractory, fireclay, packed	0.007	ton
Water, deionised	977.77	kg
Natural gas, high pressure	2.725	m ³
Electricity, medium voltage	796.7	kWh
Carbon dioxide	124.98	kg
Carbon monoxide	0.008	kg
Sulfur oxides	0.19	kg
Nitrogen oxides	0.24	kg
Particulates, < 2.5 µm	0.08	kg